



HAL
open science

**Analysing red heartwood in Beech (*Fagus sylvatica* L.)
related to external tree characteristics - towards the
modelling of its occurrence and shape at the individual
tree level**

Holger Wernsdörfer

► **To cite this version:**

Holger Wernsdörfer. Analysing red heartwood in Beech (*Fagus sylvatica* L.) related to external tree characteristics - towards the modelling of its occurrence and shape at the individual tree level. Life Sciences [q-bio]. ENGREF (AgroParisTech), 2006. English. NNT: . pastel-00001965

HAL Id: pastel-00001965

<https://pastel.hal.science/pastel-00001965>

Submitted on 14 Dec 2006

HAL is a multi-disciplinary open access archive for the deposit and dissemination of scientific research documents, whether they are published or not. The documents may come from teaching and research institutions in France or abroad, or from public or private research centers.

L'archive ouverte pluridisciplinaire **HAL**, est destinée au dépôt et à la diffusion de documents scientifiques de niveau recherche, publiés ou non, émanant des établissements d'enseignement et de recherche français ou étrangers, des laboratoires publics ou privés.



Albert-Ludwigs-Universität Freiburg im Breisgau



Institut National de la Recherche Agronomique



Ecole Nationale du Génie Rural des Eaux et des Forêts

Analysing red heartwood in Beech (*Fagus sylvatica* L.)
related to external tree characteristics – towards the modelling
of its occurrence and shape at the individual tree level

Thèse / Inaugural-Dissertation
(Cotutelle)

pour l'obtention du grade de Docteur / zur Erlangung der Doktorwürde

de l'Ecole Nationale du Génie Rural des Eaux et des Forêts
et / und
der Fakultät für Forst- und Umweltwissenschaften
der Albert-Ludwigs-Universität Freiburg im Breisgau

présentée par / vorgelegt von

Holger Wernsdörfer

Nancy / Freiburg im Breisgau
2005



Institut für Forstbenutzung und Forstliche
Arbeitswissenschaft der Universität Freiburg



Laboratoire d'Etude des Ressources Forêt-Bois
Unité Mixte de Recherche INRA-ENGREF Nancy

Directeur / Direktor ENGREF: Cyrille Van Effenterre
Doyen / Dekan FFU: Prof. Dr. Ernst Hildebrand

Président du Jury / Vorsitzender
der Prüfungskommission: Prof. Dr. Dr. h.c. Gero Becker (Universität Freiburg)

Directeurs de thèse / Betreuer: Gérard Nepveu (DR INRA, Nancy)
PD Dr. Ute Seeling (Universität Freiburg)

Rapporteurs / Referenten: Dr. Bernard Thibaut (DR CNRS, Guyane)
Prof. Dr. Siegfried Fink (Universität Freiburg)

Examineurs / Prüfer: Dr. Gilles Le Moguédec (CR INRA, Nancy)
Prof. Dr. Dr. h.c. Gero Becker (Universität Freiburg)

Date et lieu de soutenance / Datum und Ort der Disputation: 18. 01. 2006, ENGREF Centre de Nancy

ENGREF: Ecole Nationale du Génie Rural des Eaux et des Forêts
FFU: Fakultät für Forst- und Umweltwissenschaften der Universität Freiburg
INRA: Institut National de la Recherche Agronomique
CNRS: Centre National de la Recherche Scientifique

Acknowledgements

The present study was performed from March 2002 to October 2005 at the Wood Quality Research Team of LERFoB (INRA-ENGREF)^I in Nancy, France, and at the Institute of Forest Utilisation and Work Science (Fobawi) of the University of Freiburg in Germany. The doctorate examination was passed jointly (as a “Cotutelle”) at the ENGREF, the French Institute of Forestry, Agricultural and Environmental Engineering, and at the Faculty of Forest and Environmental Sciences of the University of Freiburg.

I wish to thank the directors of the home/host laboratories, Prof. Dr. Dr. h.c. Gero Becker (Fobawi), Dr. Jean-François Dhôte (LERFoB) and Gérard Nepveu (DR) (Wood Quality Research Team of LERFoB) for the possibility of realising the project at their laboratories and for their support during all phases of the work. Furthermore, I am grateful for their assistance in coordinating the administrative conditions for the joint doctorate examination. For accepting the examination of the thesis, I wish to thank Prof. Dr. Siegfried Fink and Dr. Bernard Thibaut.

Special thanks are extended to my supervisors, Gérard Nepveu (DR) and PD Dr. Ute Seeling, for their support to the different tasks of the work including project elaboration and performance, and applications for funding. They gave valuable impulses and suggestions in this respect, but gave me the freedom to choose the focus and orientation of the study. In the same way, I am particularly grateful to Dr. Thiéry Constant, Dr. Gilles Le Moguédec and Dr. Frédéric Mothe. I appreciated their availability, motivation and valuable scientific advice, and the agreeable working atmosphere.

The results of this work are based on two samplings performed in 2002 and 2003. For their cooperation in the organisation of the field work, thanks are extended to Dr. Heinz-Otto Denstorf, Karl Heinz Spissinger and Gerhard Weiß (Waldgesellschaft der Riedesel Freiherren zu Eisenbach GbR, Germany). For assistance in field and laboratory measurements, I wish to thank Emmanuel Cornu, Etienne Farré, Claude Houssement, Alain Mercanti, André Perrin and Daniel Rittié (LERFoB), and Erwin Hummel, Hannes Lechner and Renato Robert (Fobawi). I appreciated their motivation and interest in the work, and their efforts to find optimum technical and operational solutions.

Performing the work jointly at institutions of two countries implied that administrative tasks were often more complicated than they usually are. For their great assistance in this respect, I wish to thank Hélène Busch, Ginette Jacquemot and Nathalie Morel (LERFoB), and Beate Albrecht and Monika Wirth-Lederer (Fobawi).

This work was funded by the European Commission (Marie Curie grant), the Ministry of Baden-Württemberg in Germany (LGFG^{II} grant) and the French National Forest Administration (ONF^{III}).

Nancy, January 2006

Holger Wernsdörfer

^I Joint Research Unit for Forest and Wood Resources (Laboratoire d’Etude des Ressources Forêt-Bois LERFoB) of the French National Institute for Agricultural Research (Institut National de la Recherche Agronomique INRA) and the French Institute of Forestry, Agricultural and Environmental Engineering (Ecole Nationale du Génie Rural des Eaux et des Forêts ENGREF)

^{II} Landesgraduiertenförderungsgesetz

^{III} Office National des Forêts

Table of contents

0	List of papers -----	1
1	Introduction -----	2
1.1	Scope -----	2
1.2	State-of-the-art -----	3
1.2.1	Types of coloured heartwood -----	3
1.2.2	Red heart formation -----	5
1.2.3	Red heart shape -----	5
1.2.4	External tree traits -----	7
1.2.5	Dendrometric variables -----	9
1.2.6	Approaches to the modelling of coloured heartwood in Beech -----	10
1.2.7	Conclusion -----	13
1.3	Objectives and structure of the study -----	14
2	Materials and variables measured -----	17
2.1	Group 1 -----	17
2.2	Group 2 -----	19
3	Analyses of red heart occurrence and shape -----	27
3.1	Explorative analysis (Paper I) -----	27
3.2	Red heart occurrence (Paper II) -----	30
3.3	Overall red heart shape (Paper III) -----	32
3.4	Local red heart shape (not yet reported in a paper) -----	37
3.4.1	Methods -----	37
3.4.2	Results and discussion -----	44
4	Synoptic discussion -----	60
4.1	Methodological developments -----	60
4.2	Interpretation of results with respect to red heart initiation and development -----	61
4.3	New approaches to the modelling of red heart occurrence and shape -----	62
5	Conclusions and perspectives -----	67
5.1	Conclusions -----	67
5.2	Perspectives -----	68
6	Summary -----	74
6.1	English summary -----	74
6.2	French summary (Résumé) -----	75
6.3	German summary (Zusammenfassung) -----	77
7	References -----	80
8	Annex -----	87
8.1	Complementary information -----	87
8.1.1	Explorative analysis (analysis I) -----	87
8.1.2	Red heart occurrence (analysis II) -----	87
8.1.3	Overall red heart shape (analysis III) -----	88
8.1.4	Local red heart shape (analysis IV) -----	88

0 List of papers

The present study is based on work reported in the following papers:

- Paper I Wernsdörfer H, Constant T, Mothe F, Badia MA, Nepveu G, Seeling U (2005) Detailed analysis of the geometric relationship between external traits and the shape of red heartwood in beech trees (*Fagus sylvatica* L.). *Trees – Structure and Function* 19:482–491
- Paper II Wernsdörfer H, Le Moguédec G, Constant T, Mothe F, Seeling U, Nepveu G (2005) Approach to the estimation of red heart occurrence in *Fagus sylvatica* based on geometric relationships between branch scar development and knot dimensions. *Scandinavian Journal of Forest Research* 20:448-455
- Paper III Wernsdörfer H, Le Moguédec G, Constant T, Mothe F, Nepveu G, Seeling U: Modelling of the shape of red heartwood in beech trees (*Fagus sylvatica* L.) based on external tree characteristics. *Annals of Forest Science* (accepted)

Further references reporting the work of the present study:

- 1 Wernsdörfer H, Constant T, Le Moguédec G, Mothe F, Nepveu G, Seeling U: Le cœur rouge du Hêtre – Peut-on prévoir sa présence depuis l'extérieur de l'arbre ? *Rendez-vous techniques* (submitted 3 December 2004; in French)
- 2 Wernsdörfer H, Seeling U, Nepveu G (2002) Glass logs – Methodische Ansätze zur Messung und Visualisierung der äußeren Merkmale und der Ausdehnung des Rotkerns im Stamm der Buche (*Fagus sylvatica* L.). *Forstwissenschaftliche Tagung*, 9-11 October 2002, Göttingen, Germany, summary (in German)
- 3 Wernsdörfer H, Constant T, Mothe F, Le Moguédec G, Nepveu G, Seeling U (2003) Analyse et modélisation intra- et interarbre de la variabilité d'extension du cœur rouge chez le Hêtre (*Fagus sylvatica* L.) – Premiers résultats d'une étude sur les extensions radiale et longitudinale du cœur rouge en liaison avec les singularités du tronc. *6^{ème} Journées Scientifiques de la Forêt et du Bois*, 3-5 June 2003, Epinal, France, summary (in French)
- 4 Wernsdörfer H, Seeling U, Le Moguédec G, Constant T, Mothe F, Nepveu G (2004) Die Ausdehnung des Rotkerns im Stamm der Buche – Ansätze zur Modellierung auf der Ebene des Einzelbaums. *Forstwissenschaftliche Tagung*, 6-8 October 2004, Freising, Germany, summary (in German)
- 5 Wernsdörfer H, Le Moguédec G, Constant T, Mothe F, Nepveu G, Seeling U (2004) Modélisation de la présence du cœur rouge chez le Hêtre (*Fagus sylvatica* L.) à partir de caractéristiques externes de l'individu. *6^{ème} Colloque Sciences et Industrie du Bois*, 2-4 November 2004, Epinal, France, summary (in French)

1 Introduction

1.1 Scope

Beech (*Fagus sylvatica* L.) is the most important broadleaf tree species in Germany where it represents 17% of the growing-stock volume¹, and the second broadleaf tree species in France (Beech: 11%, Oak: 25%)². High value utilisation of this resource on an industrial level focuses on light-coloured, white beechwood (i.e. free of coloured heartwood) of upper quality (e.g. low level of growth stresses) which can be processed for appearance products like sliced veneer and sawn timber for indoor applications (furniture, flooring, interior design). However, older trees of larger dimensions are capable of forming coloured heartwood, which is usually developed as red heart. The occurrence of larger red hearts reduces the value of beechwood considerably: red heartwood is poorly suitable to serial production of appearance products owing to its heterogeneity and instability in colour and appearance structure (Rathke 1996). Furthermore, tyloses and heartwood substances affect impregnation and drying properties [e.g. Seeling (1998)]. European Standards EN 1316-1 (CEN 1997c) for round timber grading therefore set the maximum red heart percentage³ to 20% and 30% for the better quality classes A and B, respectively.

Two complementary strategies emerge from this problem. On the one hand, forest research aims at understanding, quantifying and controlling red heart formation by silvicultural means. Based on the results, methods shall be developed to optimise the amount of white beechwood in the frame of forestry production, and downstream the forest-wood chain, in industrial processing of roundwood. On the other hand, wood research aims at characterising, treating and/or modifying red heartwood (Magel and Höll 1993; Schleier 1999; Albert et al. 2003; Koch et al. 2003; Liu et al. 2005). Using the outcomes, methods of processing and marketing shall be developed to valorise the high amount of red heartwood coming to the market each year (Schüpbach and Ruf 2000; Wagemann 2001; Verhoff and Wurster 2002). The present study comes mainly within the scope of the first strategy.

Different concepts of silviculture and forest management are analysed (Wilhelm et al. 1999; Klädtke 2001; Börner 2002; Knoke 2002; Seeling and Becker 2002; Knoke 2003a; Zell et al. 2004) to produce and select crop trees of good wood quality, containing a minimal proportion of red heartwood and providing the optimum economic benefit. However, variability of red heart occurrence and shape is high. In stem-axial direction, red heart is often spindle-shaped. The spindle can reach from the felling cut to the crown base, but it can be located somewhere in between as well. In stem radial-direction, red

¹ German Federal Forest Inventory, second survey from 2001 – 2002 (BWI 2). Retrieved 13 September 2005 from <http://www.bundeswaldinventur.de/>.

² French National Forest Inventory (IFN). Retrieved 13 September 2005 from <http://www.ifn.fr/>.

³ Ratio (%) of the diameter of the circle enclosing the red heart and the diameter of the cross-section, according to EN 1310 (CEN 1997b).

heart does usually not coincide with the annual rings, but appears cloudy and composed of several formation zones. Since knowledge and means are lacking to determine this variability on the individual tree level, it has proven difficult to estimate the quality and to control the quality development of standing trees with respect to red heart occurrence and shape, and downstream, to optimise the yield of white beechwood in industrial processing of logs. Preceding studies therefore suggest quantifying red heart occurrence and shape in more detailed analyses (Becker et al. 2005), and including the resulting models into growth simulation (Nepveu et al. 2005).

1.2 State-of-the-art

The state-of-the-art about research relevant to the present study is reported using the following structure. First, types of coloured heartwood in Beech, red heart formation, and red heart shapes in stem-axial and stem-radial direction are characterised. Second, factors being related to red heart occurrence and shape are reported and discussed, including results of statistical modelling. Furthermore, approaches to the modelling of coloured heartwood in Beech are discussed from a methodological point of view. Finally, conclusions are drawn from the literature review, to introduce the objectives and research questions of the present study.

1.2.1 *Types of coloured heartwood*

While tree species like Oak always (obligatory) form coloured heartwood, the formation of coloured heartwood in Beech is facultative (Bosshard 1967); Beech is capable of forming coloured heartwood under certain conditions. Four types of coloured heartwood in Beech are distinguished by their appearance (Figure 1), and by possible causes and formation processes. They are red heartwood (synonyms: red heart, red core), wounded heartwood, splashing heartwood (synonym: dotty red heart) and abnormal heartwood (Sachsse 1991). Regarding cross-sections of stems, red heartwood has round borders, partly a cloudy appearance, and usually the outer red heart border does not coincide with the annual rings. The reddish-brown colour of red heartwood results from an oxidation process (described in more detail in section 1.2.2 below) accompanied by plugging of vessels with tyloses at the heartwood margins. The formation of wounded heartwood has its origin in a wound to the cambium, but cytological and biochemical processes are similar to that of red heart formation. However, wounded heartwood has a small spatial extent of about 25 cm to 75 cm above a wound (Sachsse 1991)⁴, and it is usually located at the stem periphery. The other heartwood types can reach from the stem base to the crown base, and they are located in the stem centre. Splashing heartwood shows jagged borders on the cross-section, and its maximum extent is usually located at the stem base

⁴ Results are based on artificial wounds at the stem base (Sachsse and Simonsen 1981), so that the extent of wounded heartwood below a wound was not determined.

(Walter and Kucera 1991). The formation process of splashing heartwood seems complex and caused by several factors, which are not well known up to now. An effect of fungi was reported by Necessary (1960; 1969), and intensive tyloses formation at the heartwood margins is a further characteristic of this type (Seeling 1998). Abnormal heartwood can have jagged borders similar to splashing heartwood, but as a characteristic the margins of abnormal heartwood appear black and are attacked by bacteria. The hypothesis that abnormal heartwood formation is related to forest decline has not been verified (Seeling 1991). Both splashing and abnormal heartwood can develop around a central red heart. While in red heartwood the moisture content is lower than in sapwood, in abnormal heartwood it is higher (Seeling 1991).

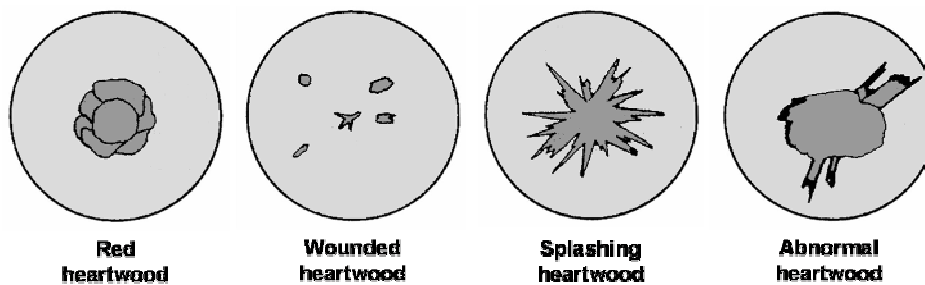


Figure 1. Characteristic appearance in cross-section of the four types of coloured heartwood in Beech according to Sachsse (1991); illustrations adopted from Seeling (1998).

In the present study, only red heartwood was analysed. This choice was made since red heartwood usually occurs most frequently, and the formations and related factors of splashing and abnormal heartwood seem lesser known. Wounded heartwood was also excluded because of its small spatial extent. The literature review was therefore focused on red heartwood. In recent studies, the classification by Sachsse (1991) was adopted by many authors. However, other classifications of coloured heartwood (Mahler and Höwecke 1991; Walter and Kucera 1991) are used in some references and, especially in many older studies, different types of coloured heartwood are not clearly distinguished. Therefore, in the present study the general term “coloured heartwood” is used where most likely types other than red heart are included in the analyses cited, hypothesising that their results apply to red heart to a large extent.

For example, in the study by von Büren (2002), 1017 (78%) out of 1305 observations of coloured heartwood are reported to show round or cloudy shape in cross-section. They correspond most likely to red heart according to Sachsse (1991). Compared with this, there are 201 observations (15%) of coloured heartwood with splashing appearance in the study by this author. These observations are assumingly splashing or abnormal heartwood according to Sachsse (1991). Another 87 observations (7%) of coloured heartwood with irregular shape (Büren von 2002) are difficult to match with the classification by Sachsse (1991).

1.2.2 Red heart formation

Heartwood formation in general is associated with breaking down of the water transport system and decreasing vitality of the parenchyma tissue (Necesany 1966); radial transport processes (assimilate- and ion-shifting), decrease of various physiological performances (Ziegler 1968), and decomposition of soluble carbohydrates (Dietrichs 1964) occur; storage substances are degraded or transformed into heartwood substances (Bosshard 1974). The theory of red heart formation in Beech is based on research by Zycha (1948). According to Zycha (1948), red heart formation is initiated when oxygenous air can penetrate through dead branches or other entrances into the stem core of older trees, where water content is low and vitality of parenchyma cells is reduced. The oxygen causes transformation of soluble carbohydrates and starch into coloured phenol substances in the still-living parenchyma tissue (Bauch and Koch 2001). Additionally, the relatively vital parenchyma cells near the margin to the sapwood react by plugging vessels with tyloses (Necesany 1966). Since necrobiosis of parenchyma is slow, but heartwood substances polymerise rapidly, the substances are not deposited in the cell walls (Bosshard 1974). As a consequence, durability of red heartwood is low compared to that of tree species with obligatory heartwood formation. Nevertheless, resistance to fungi can be greater than in sapwood (Gäumann 1946; Baum 2000; Baum et al. 2000; Baum and Bariska 2002). The process of red heart formation is assumed to develop in successive phases, leading to a cloudy appearance of several formation zones on the cross-section (Zycha 1948; Sachsse 1991).

Reduced water content in the inner stem parts, being replaced by gas, seems an important condition of red heart formation. Gas occurring in the stem is rich in carbon dioxide and low in oxygen, which results in an oxygen gradient between air outside and gas inside the stem; Bosshard (1967; 1974) explains oxygen penetration as cause of the so-called mosaic heartwood in Beech by this phenomenon. Zycha (1948) assumes that a suction of oxygenous air towards the stem centre develops when water tension in the sapwood increases and storage water is towed towards the stem periphery. Furthermore, “most likely (...) an indirect relation exists between the water/gas ratio (...) near the heartwood-boundary and the vitality of parenchymatic cells” (Sachsse 1967). Torelli (1979) distinguishes a dehydration phase, and a subsequent discolouration phase initiated by oxygen penetration.

1.2.3 Red heart shape

Some authors make assumptions about the development of red heartwood, which may lead to characteristic red heart shapes in stem-axial direction. According to Zycha (1948), red heart starts at a middle stem height and develops towards the stem base and about up to the crown base. Keller (1961) states that coloured heartwood develops in the stem either downwards, mostly in the case of forks at a relatively low stem height, or upwards, mostly in the case of coppice shoots. Walter and Kucera

(1991) report that red heart⁵ starts mostly from dead branches and wounds, and becomes smaller towards the stem base. Correspondingly, red heart is reported to be spindle- or cone-shaped (Seeling 1998; Frommhold 2001; Lux 2001). With respect to the spindle shape, the frequency of red heart⁶ occurrence is low at the stem base, increases rapidly within the first few meters of stem height and is highest between 2 m and 10 m of stem height (Höwecke et al. 1991). Several authors analyse the maximum size of coloured heartwood in stem-axial direction using different variables: the maximum diameter of coloured heartwood⁷ with spindle shape is reported at 4 m of stem height (Rácz 1961), the maximum diameter and area at approximately 4 – 5 m of stem height (Krempf and Mark 1962), and the maximum volume percentage at 4 – 8 m (Vasiljevic 1974) of stem height. According to Sachsse (1991), red heart reaches its maximum diameter at 30 – 50% of stem height. In addition to a diameter maximum occurring at 1 – 4 m from the bottom end of logs, Tomaševski (1958) reports a second culmination point at 8 m. However, a second culmination in the upper stem part occurs very seldom according to the study by Krempf and Mark (1962). At the stump zone coloured heartwood can sharply increase in size, and it ends at the zone of the crown base (Krempf and Mark 1962). On butt-logs⁸ the red heart diameter is reported to be bigger at the top end than at the bottom end, with a maximum in-between (Seeling and Becker 2002). Distinguishing up to three stem sections per tree, Zell (2002) and Zell et al. (2004) estimate for each stem section the probability that the diameter percentage of coloured heartwood exceeds 30%. According to the authors, the results indicate that coloured heartwood has the shape of a spindle.

The red heart shape in stem-radial direction is described as round, cloudy or irregular with round borders (section 1.2.1). Bulging of coloured heartwood towards external wounds, rotten branches and the ramification zones of forks is observed on cross-sections by Krempf and Mark (1962). Similar observations are reported by Groß (1992) for dead branches and branch scars/buckles.

The previous paragraphs provide background information about the characteristics of red heartwood in comparison with other types of coloured heartwood, about the red heart formation process, and about the possible development and characteristics of red heart shape. Starting from this background, factors being related to red heart occurrence and shape are discussed in the following: tree external traits like dead branches are assumed to be pathways through which oxygenous air can penetrate into the stem and initiate red heart formation; dendrometric characteristics like an elevated tree age are reported to

⁵ Coloured heartwood with round appearance on cross-sections according to the classification by Walter and Kucera (1991), which corresponds most likely to red heart according to the classification by Sachsse (1991).

⁶ Coloured heartwood with round or cloudy appearance on cross-sections according to the classification by Höwecke et al. (1991), which corresponds most likely to red heart according to the classification by Sachsse (1991).

⁷ Apart from Sachsse (1991), the authors cited do not distinguish between red heart and other types of coloured heartwood.

⁸ Log between the felling cut and the first cross-cut.

make trees susceptible to red heart formation. Site characteristics are discussed in less detail in this literature review, since they were not analysed explicitly in the present study.

1.2.4 External tree traits

Relationships between external tree traits and red heart formation are reported in several studies (given in the following), while others do not confirm such results (Hupfeld et al. 1997; Börner 2002; Denstorf 2004; Ebert and Amann 2004). In this respect, the following traits seem most important: dead branches/branch scars, forks, wounds, cracks and dead roots. Their possible effect on red heart formation is discussed in the following.

Dead branches/branch scars and forks: in the course of natural pruning of younger branches, hardwoods form in the branch basis a protection zone of tyloses and inclusions (Mayer-Wegelin 1929; Trendelenburg and Mayer-Wegelin 1955). Torelli (1984) assumes broken branches with no previously formed protection zone to be most susceptible to oxygen penetration while, according to Zycha (1948), oxygenous air may pass the protection zone driven by suction (section 1.2.2). Similarly, red heart formation zones are assumed to develop if oxygenous air can pass the tyloses margin of a previous red heart zone (Zycha 1948), or to originate from a larger dead branch each (Jaroschenko 1935). The formation of such protection zone seems similar to heartwood formation and requires vital parenchyma cells; in older and larger branches the protection zone is incomplete and limited to the sapwood (Aufsess von 1975; Aufsess von 1984). For this reason, larger branches may have been found more susceptible to rot (Mayer-Wegelin 1929; Erteld and Achterberg 1954); through rotten branches oxygenous air may enter the stem (Keller 1961). Furthermore, larger branches are exposed for a longer time to exterior influences, as the duration between branch necrosis and occlusion approximately increases with branch diameter (Volkert 1953). For artificially pruned branches this relationship is stronger, and it is shown that the duration of occlusion decreases with increasing annual ring width (Mayer-Wegelin 1930; Volkert 1953). Similar to larger branches, more inclined branches are reported to be more susceptible to rot (Mayer-Wegelin 1929; Erteld and Achterberg 1954). Steep-angled branches and V-shaped forks with bulging ramification zones are assumed to be oxygen entrances owing to cracking by freezing of accumulated water or by wind-stress (Amann 2003; Knoke 2003a), and owing to rot resulting from water accumulation in the ramification zone. Furthermore, relationships between knot discolouration and fungi development are analysed by Volkert (1953) and Buchholz (1958).

Results of statistical modelling also suggest an effect on red heart formation by larger dead branches/branch scars and forks. Distinguishing trees with coarse, medium and fine knottiness (visual assessment), von Büren (1998; 2002) reports that the probability of occurrence of coloured heartwood increases with the presence of larger branch scars. In a multiple regression analysis for estimating the red heart diameter, Knoke and Schulz Wenderoth (2001) report a significant effect of the number of

dead branches and branch scars/knobs with minimum sizes of 6 cm (dead branches) and 9 cm (scars/knobs); including smaller traits into the analyses has led to less exact estimation results. Using the same criteria, a significant effect is reported of the number of dead branches and knobs/scars on the probability of red heart occurrence (Knoke 2003b). The probability of occurrence of coloured heartwood also depends on the occurrence of forks (Büren von 2002); the effect of forks seems stronger in younger trees (Knoke 2003a; Knoke 2003b).

Wounds and cracks: embolism originating from wounds to the bark provokes a process of discolouration and tyloses formation similar to the process of red heart formation. The resulting wounded heartwood usually has a small spatial extent and is located at the stem periphery (section 1.2.1). Sachsse and Simonsen (1981) report wounded heartwood to be formed one year after the cutting of felling notches in 75 – 90 year old trees. During this period, the moisture content does not decrease to the low levels reported by other authors (Zycha 1948; Bauch and Koch 2001) to be characteristic for red heart formation. However, development from wounded heartwood to red heartwood may occur gradually (Sachsse and Simonsen 1981). Furthermore, observations on log cross-sections about a coloured zone between wounds and coloured heartwood in the stem centre (Krempf and Mark 1962) may indicate wounds to be initiation points of red heart formation. Between trees with external traits (frost cracks and bars, extended and deep wounds to the cambium, rotten branches, dryness of tree top) and trees with no such traits, a significant difference (t-test) in the size of coloured heartwood (percentage of tree and stem volume) is reported (Krempf and Mark 1962). Moreover, a significant effect of larger damage areas on the probability of occurrence of coloured heartwood is reported by von Büren (1998; 2002), who concludes that larger damage areas are effective entrances for air. Very small “hairline” cracks can lead to the so-called mosaic heartwood in Beech (Bosshard 1967), which is a small T-shape discolouration being also referred to as T-disease.

Dead roots: Jaroschenko (1935), Paclt (1953) and Raunecker (1953) report dead roots to be possible initiation points for the formation of coloured heartwood. However, Zycha (1948) states that red heart formation starts at a middle stem height. Walter and Kucera (1991) differentiate between coloured heartwood with splashing appearance, having its maximum extent at the stem base and starting assumingly from the roots, and coloured heartwood with round or irregular appearance, which would often start from dead branches and wounds. [To match with the classification by Sachsse (1991): coloured heartwood with splashing appearance according to Walter and Kucera (1991) corresponds most likely to splashing or abnormal heartwood according to Sachsse (1991), and coloured heartwood with round appearance to red heart.]

Altogether, there are indications in literature that relationships between external tree traits and red heart formation may depend on type (e.g. wound) and size (e.g. larger branch scars) of external traits.

However, differentiation between these characteristics is rather difficult; it is not clear which traits most likely have an effect on the red heart, and how traits visible on the stem surface are related to the red heart inside the stem.

1.2.5 Dendrometric variables

With respect to the effect of dendrometric variables it is reported that dehydration of the inner stem parts is related to radial and height growth and simultaneous reduction of the crown (Torelli 1985). In forest stands, the occurrence of coloured heartwood is low before beech trees reach an age of approximately 80 years (Rácz et al. 1961; Vasiljevic 1974; Pichery 2000). Below this age, water content in the inner stem parts is usually still high, and larger dead branches, which could be oxygen entrances, rarely occur (Zycha 1948).

In general, the frequency of coloured heartwood increases with tree age (Rácz 1961; Rácz et al. 1961; Krempf and Mark 1962; Lanier and Le Tacon 1981; Mahler and Höwecke 1991; Walter and Kucera 1991). Noticeable increase is reported at ages of 100 – 120 years (Krempf and Mark 1962), 120 – 150 years (Lanier and Le Tacon 1981), and 150 years (Redde 1998)⁹. The diameter (Rácz et al. 1961; Kotar 1994) and volume percentage (Krempf and Mark 1962) of coloured heartwood increase with tree age, also. However, according to Walter and Kucera (1991), the increase in diameter of coloured heartwood stagnates at an age of about 120 years. With increasing stem diameter, the occurrence and size of coloured heartwood increase as well (Rácz 1961; Rácz et al. 1961; Höwecke et al. 1991; Mahler and Höwecke 1991). The effect of diameter was stronger than the effect of age in the studies by Rácz et al. (1961) and Mahler and Höwecke (1991). Considering the interaction of both variables, the mean diameter increase, fast grown trees seem to show less frequent and less severe formation of coloured heartwood (Vasiljevic 1974; Knoke and Schulz Wenderoth 2001; Seeling and Becker 2002). These results are reflected in statistical modelling as follows. The probability of occurrence of coloured heartwood increases with tree age (Büren von 2002; Knoke 2003a; Knoke 2003b). Trees with high mean diameter increase are reported to contain less likely red heartwood (Knoke and Schulz Wenderoth 2001); the effect of diameter at breast height on red heart occurrence is stronger in younger stands than in older ones (Knoke 2003a; Knoke 2003b). Mavric (2003) and Schmidt (2004) estimate the probability of occurrence of red heartwood, splashing heartwood and no coloured heartwood based on the diameter at breast height. Börner (1998) and Zell et al. (2004) use the diameter at breast height to estimate the probability that coloured heartwood exceeds 30% of the cross-section diameter. An effect of stem diameter or stem radius, on the size (radius, radius percentage, diameter or diameter percentage) of coloured heartwood is reported in several studies (Torelli 1985; Höwecke et al. 1991; Börner 1998; Knoke and Schulz Wenderoth 2001; Börner 2002; Mavric 2003; Knoke 2003a; Schmidt

⁹ The results of Redde (1998) were obtained at the felling cut. At the zone of the stem base coloured heartwood can sharply increase towards the tree top (Krempf and Mark 1962), so that it cannot always be detected at the felling cut. Considering this, Redde (1998) might have underestimated the frequency of coloured heartwood.

2004). Few studies (Torelli 1985; Kotar 1994; Büren von 2002) also report an effect of age on this variable.

Furthermore, the radius of coloured heartwood at one fifth of tree height is reported to be related to its distance to the crown base, and the radius percentage of coloured heartwood to the relative crown length (Torelli 1984; Torelli 1985). According to von Büren (2002), the diameter percentage of coloured heartwood increases with tree height class (5 m-classes) up to the class 20–25 m, and it is almost constant between this class and the higher classes. Also, an effect of the ratio of tree height and diameter at breast height (hd-ratio) on the occurrence of coloured heartwood is reported by this author.

Height at an age of 100 years and top height are used as measures of site class in the studies by Torelli (1985) and Kotar (1994), and positive relationship with red heart radius and with red heart volume percentage in stands is reported, respectively. Also, an effect of mean stand height on the probability of occurrence of more than 30% of red heart (diameter percentage) is reported (Zell et al. 2004). However, according to von Büren (2002), the frequency of coloured heartwood is higher on sites with unfavourable nutrient supply. Kotar (1994) reports that the relationship between red heart diameter and tree age differs with site unit. Compared with this, tree age has the greatest effect on red heart probability in the model by Knoke (2003a; 2003b). However, in this model and in the model of red heart size by Knoke (2003a), variables of site characteristics (growing area, site unit and relief) were partly significant, but had little effect upon the estimation results. Altogether, it appears difficult to specify the effect and interaction of different site characteristics in relationship to red heart formation. Similarly, other authors conclude from literature review that different results are reported about the influence of site characteristics on red heart formation (Seeling et al. 1999; Günsche 2000). Also, Stuber et al. (2002) state that no clear relationship between site characteristics and red heart formation is reported in literature. They assume that there may be overlaying by other factors.

1.2.6 Approaches to the modelling of coloured heartwood in Beech

As reported in sections 1.2.4 and 1.2.5, external traits and dendrometric variables are included as explanatory variables into approaches to the modelling of coloured heartwood in Beech. These approaches are discussed in the following from a methodological point of view. Referring to the characteristics of coloured heartwood reported in sections 1.2.1, 1.2.2 and 1.2.3, important considerations in modelling of coloured heartwood in Beech seem to be:

- (1) there are beech trees with and with no coloured heartwood (*occurrence*);
- (2) different *types* of coloured heartwood occur in Beech; the types are of different origins;
- (3) occurrence, type and size of coloured heartwood vary with stem height (*shape in stem-axial direction*);
- (4) the *shape* of coloured heartwood varies *in stem-radial direction*.

An overview of approaches to the modelling of coloured heartwood is provided in Table 1. In this table, the following characteristics are listed: model author, total number of sample trees, model type, target variable of coloured heartwood, differentiation by type of coloured heartwood and number of observations of coloured heartwood per tree/differentiation by stem height.

Table 1. Overview of approaches to the modelling of coloured heartwood in Beech.

Author	Total number of trees (a)	Model type	Target variable of coloured heartwood	Differentiation by type of coloured heartwood	Number of observations of coloured heartwood per tree/ differentiation by stem height
Torelli (1979; 1984; 1985)	100	Multiple linear regression	Radius, radius percentage	–	1/ 20% of tree height
Höwecke et al. (1991)	3961	Simple linear regression	Diameter, diameter percentage	Round, cloudy, splashing, 3 types of irregular (b)	2/ 1 st stem cross-section and 2 nd –4 th stem cross-section
Kotar (1994) (c)	3634	Simple linear regression	Diameter	–	1/ 1.3 m
Knoke and Schulz Wenderoth (2001)	195	Probit analysis	Occurrence, diameter \geq 33% (both dichotomy)	Exclusively red heartwood (d)	2/ Height as continuous variable (e)
		Multiple linear regression	Diameter, diameter percentage	Exclusively red heartwood (d)	2/ Height as continuous variable (e)
Knoke (2003a; 2003b)	392	Logistic regression	Occurrence (dichotomy)	Exclusively red heartwood (f)	2/ Height as continuous variable
Knoke (2003a)	392	Multiple linear regression	Diameter, diameter percentage	Exclusively red heartwood (f)	2/ Height as continuous variable
von Büren (2002) (g)	610	Logistic regression	Occurrence (dichotomy)	–	1/ –
		Multiple regression	Diameter percentage	–	1/ –
Börner (1998; 2002)	146	Hyperbolic	Diameter \geq 30%	Mainly red heartwood (h)	2/ Maximum at 1.3 m or 7 m
		Simple linear regression	Diameter percentage	Mainly red heartwood (h)	2/ Maximum at 1.3 m or 7 m
Mavric (2003)	1385	Multi-nominal logit	Occurrence (3 categories)	Red heartwood, splashing heartwood	2/ Log bottom and top ends
		Non-linear regression	Diameter percentage	Red heartwood, splashing heartwood	2/ Log bottom and top ends
Schmidt (2004)	1252	Multi-nominal regression	Occurrence (3 categories)	Red heartwood, splashing heartwood	2/ Log bottom and top ends
		Non-linear regression	Diameter percentage	Red heartwood, splashing heartwood	2/ Log bottom and top ends
Zell (2002); Zell et al. (2004) (i)	535	Logistic regression	Diameter \geq 30% (dichotomy)	–	up to 3/ Stem-section as dummy variable

(a) Total number of trees in the study. Depending on the analysis, the number of trees included in models can be smaller (e.g. exclusion of outliers, of observations with no coloured heartwood, etc.).

(b) Red, brown/black and marbled/grey.

(c) Kotar (1994) also reports analyses of the volume percentage of coloured heartwood on the stand level. They are not given in this table, since the present study focused on red heart occurrence and shape on the tree level.

(d) Cracked heart according to Klemmt (1996) considered as no coloured heartwood (“white”).

(e) Relative height of the cross-section in the zone of the branch-free bole.

(f) Cracked heart according to Klemmt (1996) included.

(g) Von Büren (2002) reports analyses of 2402 trees with respect to site characteristics and of a sub-group of 610 trees with respect to tree morphological characteristics.

(h) Including 3 trees with splashing heartwood out of 146 trees.

(i) Zell (2002) and Zell et al. (2004) use an unpublished model of Kügler (1999).

The *occurrence* (point 1) or minimum size (e.g. 30%) of coloured heartwood, being dichotomy variables, are estimated by generalised linear models (probit or logistic regression models) (Knoke and Schulz Wenderoth 2001; Büren von 2002; Zell 2002; Knoke 2003a; Knoke 2003b; Zell et al. 2004). Börner (1998) uses a hyperbolic model to estimate the probability that the diameter percentage of coloured heartwood exceeds 30%. Three categories (no coloured heartwood, red heartwood and splashing heartwood) are distinguished in the multi-nominal models by Mavric (2003) and Schmidt (2004).

Types of coloured heartwood (point 2) other than red heart are excluded explicitly in the models of Knoke and Schulz Wendroth (2001) and Knoke (2003a; 2003b) for estimating red heart occurrence and size¹⁰. Börner (1998) includes red heartwood and splashing heartwood into the same sample, as very few trees show splashing heartwood. Separate models for the diameter and diameter percentage of six types of coloured heartwood are given by Höwecke et al. (1991). Mavric (2003) and Schmidt (2004) distinguish between red heartwood and splashing heartwood in their models of occurrence and size of coloured heartwood. However, possible differences between the formation of the two types of coloured heartwood are taken into account by one explanatory variable only (diameter at breast height; section 1.2.5).

The size (diameter percentage) of coloured heartwood based on one observation per tree is estimated by von Büren (2002) using a multiple regression model. To take account of the *shape* of coloured heartwood *in stem-axial direction* (point 3), cross-sections at one fifth of tree height are analysed by Torelli (1979; 1984; 1985), hypothesising that the maximum size of coloured heartwood is located there. Börner (1998; 2002) analyses the larger percentage of coloured heartwood occurring at either 1.3 m or 7 m of stem height. Further models based on one observation of coloured heartwood per tree are given by Kotar (1994). Descriptive models (not given in Table 1) show linear relationships between the diameter of coloured heartwood at 0.3 m and 1.3 m of tree height (Kotar 1994), and at 1.3 m and 7 m of tree height (Börner 1998; Börner 2002); similar relationships are reported for the diameter percentage of coloured heartwood. Coming back to the predictive models given in Table 1, Zell (2002) and Zell et al. (2004) use up to three stem sections (logs) per tree, and the larger percentage of coloured heartwood at the ends of each section; stem sections are distinguished by dummy variables. Knoke and Schulz Wendroth (2001), and Knoke (2003a; 2003b) use two cross-sections per tree and take account of their height in the stem. In the models by these authors, the probability of coloured heartwood is estimated individually for each log (Zell 2002; Zell et al. 2004) and cross-section (Knoke and Schulz Wenderoth 2001; 2003a; 2003b), respectively. Also, Mavric (2003) estimates the occurrence of red heartwood, splashing heartwood and no coloured heartwood at the bottom and top ends of logs separately. However, for obtaining a good prognosis at the bottom

¹⁰ According to Knoke (2003a), a plausible model could not be developed for splashing and abnormal heartwood, since they represent only 8% of the cross-sections observed in this study.

end, the heartwood type at the top end has to be included into the model as a dummy variable. Schmidt (2004) stresses correlation of the occurrence, type and size of coloured heartwood between cross-sections of the same tree. Analysing the bottom and top ends of butt-logs, this author proposes a multinomial regression model distinguishing nine combinations of red heartwood, splashing heartwood, and no coloured heartwood. The size (diameter percentage) of coloured heartwood is described by non-linear regression models. However, the distance between cross-sections is not taken into account in the study by this author.

To take the spindle shape of red heart into account as parabola, Knoke and Schulz Wendroth (2001), and Knoke (2003a; 2003b) include the height of the observed cross-sections (two per tree) and its square into their models of red heart occurrence and size (diameter, diameter percentage). With respect to sampling, a similar approach is used by these authors for modelling, and by older studies (Rácz 1961; Höwecke et al. 1991) for describing the shape of coloured heartwood in stem-axial direction: the red heart size is measured on bottom and top ends of logs of different length and diameter. These are butt-logs and also logs from higher stem zones in the studies by Rácz (1961) and Höwecke et al. (1991), and butt-logs in the studies by Knoke and Schulz Wenderoth (2001) and Knoke (2003a). This way, observations of many trees and at various tree heights are obtained. However, the shape of coloured heartwood of each individual tree is only represented by few observations along the stem axis. Furthermore, observations come from trees with different ages and dimensions, and trees are taken from different stands. In this respect, Rácz (1961) comments on the issue of sampling optimisation: a high total number of stems could only be analysed within the framework of conditions in practice; but determining coloured heartwood systematically at constant intervals in all trees would be more exact from the point of view of natural science.

Models quantifying the *shape* of coloured heartwood *in different stem-radial directions* (point 4), were not found in the literature review.

1.2.7 Conclusion

In conclusion, coloured heartwood in Beech can be of different origins (types). Normal red heartwood is formed in older trees when oxygenous air can penetrate into the stem centre. This process may start and develop at various stem heights, which may lead to characteristic red heart shapes. Different tree external traits may be red heart initiation points, and certain dendrometric tree characteristics like tree age and diameter are related to red heart formation. Using these relationships, statistical models are developed to estimate red heart occurrence and size. While the models are based on rather high numbers of sample trees, few observations of coloured heartwood per tree are analysed. Thus, the variability of red heart occurrence and shape within trees is poorly taken into account. Considering that tree external traits may indicate initiation points of red heart formation, the position (height and azimuth) of traits on the stem surface may be related to the red heart shape inside the stem. Differences between traits and their probable relationship to the red heart may depend on trait type

(e.g. dead branch) and dimensions (e.g. branch diameter). Furthermore, dendrometric variables (e.g. crown base height, diameter at breast height) may be related to the red heart shape in stem-axial and stem-radial direction.

1.3 Objectives and structure of the study

Referring to section 1.2, many scientific works indicate a high variability of red heart occurrence between trees and of red heart shape between and within trees. However, knowledge and means are lacking to determine this variability from tree morphological (macroscopic) and dendrometric characteristics. The overall objective of the present study therefore is to quantify relationships, and to develop a hypothesis about basic “mechanisms” between external and dendrometric tree characteristics on the one hand, and red heart occurrence and shape in stem-axial and stem-radial direction on the other hand. Owing to the high variability within trees, in the present study an approach of more detailed analyses at the intra-tree level (higher resolution of red heart shape and external trait measurements) based on a smaller number of sample trees was chosen (35 trees in total) in comparison with existing approaches to the modelling of coloured heartwood in Beech (section 1.2). This way, basic and complementary knowledge, and approaches to quantify the red heart occurrence and shape on the individual tree level should be provided, to be used and further developed in modelling on a larger and more general scale.

To reach the overall objective, the following research questions were deduced from the state-of-the-art (section 1.2), which were analysed in the present study:

- Q1: Which external traits can be related to the red heart inside the stem?*
- Q2: How are these external traits related to the red heart inside the stem?*
- Q3: How can this relationship (Q2) be used to estimate the occurrence (initiation) of red heart?*
- Q4: How can this relationship (Q2) be used to estimate the overall¹¹ shape of red heart along the stem axis (e.g. spindle shape)?*
- Q5: How can relationships between dendrometric variables and red heart be used to estimate the overall shape of red heart?*
- Q6: How does the overall red heart shape vary close¹² to external traits?*

¹¹ Overall red heart shape: longitudinal red heart shape between the felling cut and the crown base (rotation symmetry); local red heart shape: deviation from the overall red heart shape close to (near/at the location of) external traits.

¹² i.e. near/at the location of external traits.

Referring to Figure 2, the analyses were structured as follows:

I. first, an explorative analysis (analysis I) of 4 red heart trees (group 1) was performed with the aim of *identifying and characterising possible relationships between tree external traits and the red heart within the tree* (Q1 and Q2). Therefore, complete mapping of traits (dead branches, branch scars, wounds, cracks and fork) on the stem surface was performed as well as a very *detailed description*¹³ *of the red heart shape*. This description made it possible to characterise both the overall red heart shape along the stem axis and the local¹⁴ red heart shape close to external traits.

The subsequent analyses focused on particular aspects based on results of analysis I. Also, the results of analysis I made it possible to perform selective measurement and sampling of traits (dead branches/branch scars) and red heart (overall red heart shape based on discs; local red heart shape based on boards including knots) on a second group (group 2) of 17 red heart trees and 14 trees with no coloured heartwood (later referred to as white trees). Using the trees of group 2, the red heart was studied within and between trees as well:

II. using results of analysis I about relationships between external traits and red heart, the aim of analysis II was *to estimate the probability that red heart occurs (does not occur) in individual standing trees* (Q3). A type logistic regression model was developed based on the 17 red heart trees and the 14 white trees of group 2;

III. using the description of the *overall red heart shape* (analysis I), the aim of analysis III was to develop a statistical modelling approach *to estimate this shape in standing trees between the felling cut and the crown base* (Q4 and Q5). The approach was developed on 16 red heart trees¹⁵ of group 2, and it was applied to the 4 red heart trees of group 1 to test its suitability for an independent sample;

IV. finally, using the 16 red heart trees of group 2, *the local red heart shape close to external traits was analysed* with the following aims. In analysis I, deviation of the local red heart shape around knots from the overall red heart shape was observed. In this respect, the first aim of analysis IV was to quantify this deviation in stem-axial direction by means of descriptive statistics (Q6). Also, geometric relationships between branch scars, knots and red heart were developed in analysis I. In this respect, the second aim of analysis IV was to test the validity of the geometric relationships between branch scars and knots. Furthermore, a model should be developed to estimate the link between knot and red heart based on both knot variables and branch scars (Q2).

¹³ Measurement step of red heart description: 50 cm in stem-axial direction, 1° in stem-radial direction.

¹⁴ See footnote 11.

¹⁵ One tree of group 2 was excluded owing to a very special red heart shape: there were two red heart zones separated by an inter-section of white wood.

In summary, based on intensive measurements of external traits and red heart shape on 4 trees (analysis I), hypotheses were deduced to develop models of red heart occurrence and shape. Based on the hypotheses, three analyses were performed: modelling of red heart occurrence (analysis II; 31 trees), modelling of the overall red heart shape (analysis III; 16 trees) and description and estimation of the local red heart shape (analysis IV; 58 boards of 16 trees).

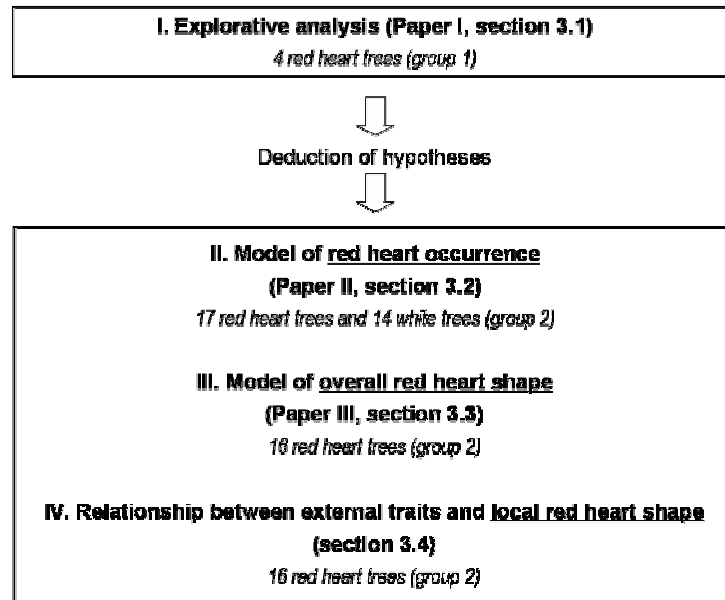


Figure 2. Structure of the analyses of red heart occurrence and shape (reported in sections 3.1, 3.2, 3.3 and 3.4).

Referring to Figure 2, each analysis was based on trees of either group 1 or group 2, but results were also tested on trees of the respective other group (see above). Furthermore, samples and data of each group were used in several analyses. Therefore, at first an overview about materials and variables measured on the trees of groups 1 and 2 is provided to the reader in section 2. Methods of data analysis, results and discussion of analyses I–III are reported in detail in Papers I–III (section 0); they are summarised in sections 3.1, 3.2 and 3.3 below, respectively. Additionally, in sections 3.2 and 3.3 complementary analyses are presented which have not been described already in Papers II and III, respectively. Analysis IV was not submitted for publication yet. It is described in detail in section 3.4, including methods, results and discussion of results. In section 4, the outcomes of this study are discussed in a synoptic manner, including methodological developments, interpretation of results with respect to red heart initiation and development, and new approaches to the modelling of red heart occurrence and shape. Finally, conclusions are drawn, and perspectives in the short term and in the medium and long term are discussed (section 5).

2 Materials and variables measured

2.1 Group 1

Group 1 consisted of 4 trees (*Fagus sylvatica* L.) with red heart (numbered B01, B08, C04 and C06). The trees were selected to represent various types of external traits (dead branch, branch scar, wound, crack and fork), and spindle- and cone-shaped red hearts (Paper I). They were taken in March 2002 from two high-forest stands (B and C), located in the German federal state of Hesse; trees B01 and B08 came from stand B, trees C04 and C06 from stand C. Stand B was located at about 500 m of altitude on a medium dry, eutrophic site. Stand age amounted to approximately 140 years. Stand C was located at an altitude of about 340 m on a fresh, eutrophic site. Its age was approximately 160 years. A dendrometric description of the sample trees is given in Table 2.

Table 2. Dendrometric description of the sample trees of group 1. All trees contained red heart.

Tree number	dbh (cm)	age (years)	mi _{dbh} (cm/year)	h _{tot} (m)	h _{cb} (m)	h _{cbrel} (1)	cl (m)	cl _{rel} (1)	hd (m/cm)	Fork
B01	58	95	0.61	33.7	15.5	0.46	18.2	0.54	0.58	No
B08	48	104	0.46	34.3	21.6	0.63	12.7	0.37	0.71	Yes
C04	62	170	0.36	30.9	14.5	0.47	16.4	0.53	0.50	No
C06	61	154	0.40	35.4	19.3	0.55	16.1	0.45	0.58	No

dbh: diameter at breast height (over bark; crosswise calliper measurement)

age: single tree age (number of annual rings at tree height 0.5 – 0.8 m)

mi_{dbh}: mean increase of diameter at breast height (dbh / age)

h_{tot}: total tree height (measured on standing tree by VERTEX device)

h_{cb}: height of crown base (defined as the lowest living primary branch; measured on standing tree by VERTEX device)

h_{cbrel}: relative height of crown base (h_{cb} / h_{tot})

cl: crown length (h_{tot} – h_{cb})

cl_{rel}: relative crown length (cl / h_{tot})

hd: hd-ratio (h_{tot} / dbh)

Fork: forked stem below the crown base

(1): no unit

An original method was developed and applied to observe and analyse relationships between external traits on the stem surface and the shape of the red heart in the stem, as reported in Paper I. Three reference levels were distinguished as illustrated in Figure 3: (1) the stem of each sample tree where the position of logs was recorded, (2) the log (length \approx 2 m) where the log surface and the external traits (dead branches, branch scars, wounds and cracks; N = 1091 traits in total) were mapped by laser scanning, and (3) the disc (inter-disc distance \approx 50 cm) where the red heart shape was measured by digital image analysis¹⁶. The method, which was based on Constant et al. (2003), made it possible to reconstruct and visualise the stem surface with the external traits and the intra-tree shape of red heart in three dimensions, based on the measurements at each reference level.

¹⁶ Some discs were cut additionally for more detailed observation, but they were not measured.

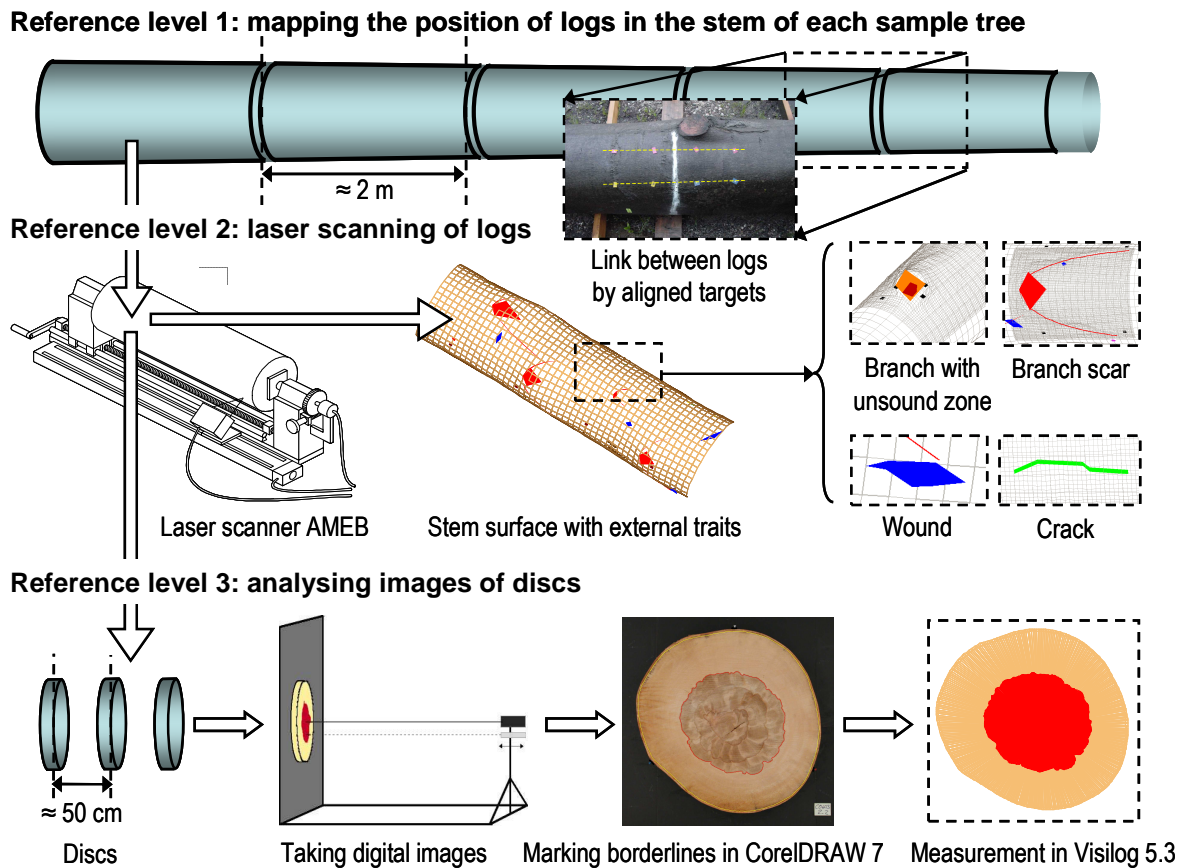


Figure 3. Sequence of measurements of trees in group 1. Details about the method of measurement are given in Paper I.

Laser scanning of logs (reference level 2) was done using the prototype apparatus of the LERFoB-laboratory in Nancy called *Appareil de Mesure de l'Enveloppe des Billons* (AMEB). The following variables of external traits were calculated from the scanning data:

- diameter db (mm) of dead branches¹⁷;
 - seal length ls (mm),
 - seal width ws (mm) and
 - moustache length lm (mm)
- of branch scars¹⁸; branch scar variables are illustrated in Figure 4.

¹⁷ Diameter in tangential and axial direction, based on 4 measurement points as illustrated in Figure 2 of Paper I.

¹⁸ In forestry practice, and in accordance with European Standards EN 844-8 (CEN 1997a), the term Chinese moustache is used instead of branch scar.

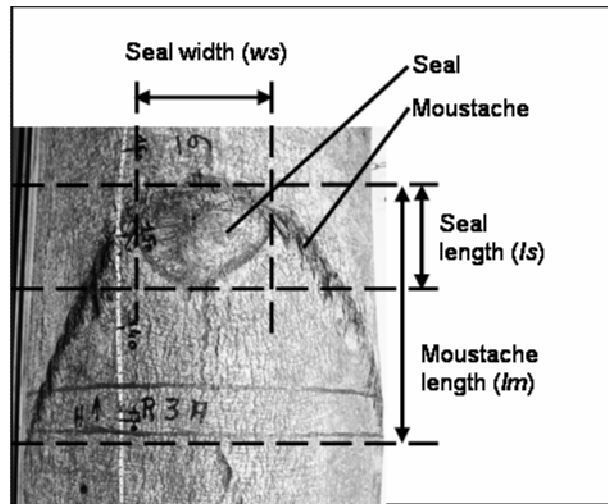


Figure 4. Branch scar consisting of the “seal” and “moustache”, measured variables (Figure adopted from Paper II).

Digital images of discs (reference level 3) were taken using equipment of the Fobawi-institute in Freiburg including a Nikon Coolpix 990 camera (Wernsdörfer et al. 2004). In the images, the outer red heart border and the disc border (under bark) were marked manually in CorelDRAW 7 (Corel Corporation, Ottawa, Canada)¹⁹. Using automated detection of the borderlines in Visilog 5.3 (NOESIS, Les Ulis, France) and a calibration step, the following variables were calculated:

- mean red heart radius r_{mean} (mm),
- standard deviation of the red heart radius r_{std} (mm) and
- mean disc radius r_{discMean} (mm under bark);

the variables were calculated from 360 radii per disc (inter-measurement angle 1°).

For visualisation purposes the software Bil3d, developed in LERFoB, was used. Bil3d makes it possible to display, rotate and zoom the objects measured which are partly rendered with polygonal facets.

2.2 Group 2

Group 2 consisted of 31 trees (*Fagus sylvatica* L.), of which 17 were red heart trees and 14 were white trees. All trees of group 2 were selected (according to criteria given in Paper II) in February/March 2003 from one high-forest stand in the German federal state of Hesse (stand D). Sampling in the single stand situation was chosen to focus on the effect of external tree characteristics on red heart occurrence, and to limit the range of tree age and diameter and possible influences of site characteristics. The stand was located at about 520 m of altitude on a fresh, eutrophic site. Stand age

¹⁹ The software PHOTO-PAINT 7 of the CorelDRAW 7 suite was used.

amounted to approximately 120 years. A dendrometric description of the sample trees is given in Table 3.

Table 3. Dendrometric description of the sample trees of group 2: 17 red heart trees and 14 white trees.

	Tree number	dbh (cm)	age (years)	mi_{dbh} (cm/year)	h_{tot} (m)	h_{cb} (m)	h_{cbrel} (1)	cl (m)	cl_{rel} (1)	hd (m/cm)	Fork
Red heart trees	1	57	147	0.39	28.5	12.2	0.43	16.4	0.57	0.50	Yes
	2	43	108	0.40	27.5	12.1	0.44	15.5	0.56	0.64	No
	4	44	111	0.40	32.3	14.6	0.45	17.7	0.55	0.73	Yes
	15	50	117	0.43	30.2	13.1	0.43	17.1	0.57	0.60	Yes
	21	49.5	108	0.46	25.4	10.0	0.39	15.4	0.61	0.51	No
	22	49	120	0.41	32.6	13.3	0.41	19.4	0.59	0.67	No
	24	46.5	110	0.42	33.1	16.2	0.49	16.9	0.51	0.71	Yes
	29	49.5	107	0.46	28.3	10.2	0.36	18.1	0.64	0.57	No
	31	42	111	0.38	32.3	17.9	0.55	14.4	0.45	0.77	No
	35	44.5	106	0.42	27.8	10.8	0.39	17.1	0.61	0.62	Yes
	39	53.5	101	0.53	25.6	8.4	0.33	17.2	0.67	0.48	No
	41	49	109	0.45	34.1	16.9	0.50	17.2	0.50	0.70	No
	42	47	111	0.42	30.5	10.8	0.35	19.8	0.65	0.65	No
	43	56.5	117	0.48	30.2	13.5	0.45	16.7	0.55	0.53	Yes
	45	44	117	0.38	30.6	19.4	0.63	11.3	0.37	0.70	No
	47	49.5	115	0.43	35.3	16.7	0.47	18.6	0.53	0.71	No
	50	48.5	116	0.42	33.1	18.2	0.55	14.9	0.45	0.68	No
White trees	7	42	109	0.39	31.6	12.7	0.40	18.9	0.60	0.75	No
	8	42.5	104	0.41	27.9	10.7	0.38	17.2	0.62	0.66	No
	9	42	107	0.39	31.4	12.7	0.41	18.7	0.59	0.75	No
	11	53.5	107	0.50	31.7	13.0	0.41	18.7	0.59	0.59	No
	13	41	117	0.35	32.7	16.2	0.50	16.5	0.50	0.80	No
	17	43	107	0.40	29.8	17.3	0.58	12.6	0.42	0.69	No
	19	51.5	106	0.49	28.1	10.0	0.36	18.1	0.64	0.55	No
	25	47.5	108	0.44	33.9	15.8	0.47	18.1	0.53	0.71	No
	28	40.5	108	0.38	26.9	10.3	0.38	16.6	0.62	0.66	No
	30	46.5	110	0.42	30.2	12.7	0.42	17.6	0.58	0.65	No
	44	46.5	107	0.43	31.6	14.0	0.44	17.6	0.56	0.68	No
	52	47.5	110	0.43	31.1	16.6	0.53	14.5	0.47	0.65	Yes
	55	42.5	104	0.41	31.1	16.5	0.53	14.6	0.47	0.73	No
	56	41	104	0.39	28.1	15.3	0.54	12.8	0.46	0.69	No

dbh: diameter at breast height (over bark; crosswise calliper measurement)

age: single tree age (number of annual rings at tree height 0.3 m)

mi_{dbh}: mean increase of diameter at breast height (dbh / age)

h_{tot}: total tree height (measured on standing tree by VERTEX device)

h_{cb}: height of crown base (defined as the lowest living primary branch; the height of the lower ends of the moustache (Figure 4) of this branch was measured after felling)

h_{cbrel}: relative height of crown base (h_{cb} / h_{tot})

cl: crown length (h_{tot} - h_{cb})

cl_{rel}: relative crown length (cl / h_{tot})

hd: hd-ratio (h_{tot} / dbh)

Fork: forked stem below the crown base

(1): no unit

For measurements and sampling the stem between the felling cut and the crown base was used; the crown base was defined as the lowest living primary branch.

The following variables were determined on the outside of the 31 trees:

- stem diameter sd (mm): starting at 1.3 m of tree height, the stem diameter was measured every 2 m. The highest diameter measurement was performed just above the crown base (crosswise calliper measurement).

All dead branches ($N = 49$), and those branch scars corresponding to threshold values derived from

results of Paper I/group 1 ($ls \geq 50$ mm and $\frac{ws}{ls} \leq 2.3$; $N = 616$), were listed for each 2 m-section:

- branch inclination α ($^\circ$): the angle α' ($^\circ$) between the axes of stem and branch was estimated using a protractor. The branch inclination relative to the cross-sectional (horizontal) plane was calculated as $\alpha = 90^\circ - \alpha'$;
- branch diameter db (mm): the branch diameter was measured close to the stem and in stem-tangential direction, using callipers. For partly occluded branches, the mean of the length and width of the non-occluded area was calculated;
- seal length ls (mm),
- seal width ws (mm) and
- moustache length lm (mm) of branch scars (Figure 4).

From 16 red heart trees²⁰ discs and short logs were sampled as illustrated in Figure 5: discs were taken at the felling cut, at 1.3 m of tree height, and above 1.3 m about every 2 m; the highest disc was taken just above the crown base. The discs had to be located in between external traits; if an external trait occurred at a foreseen disc height, the disc height was slightly changed. Furthermore, at least 4 logs per tree (mean length ≈ 50 cm) were sampled which included dead branches or branch scars²¹. The logs were selected from various tree heights; preferably, only one trait should occur per log; small, medium-sized, and large traits had to be represented; branch scars had to correspond to the threshold values given above. The height in the tree was recorded for the upper side of each disc, and for the lower and upper ends of each log.

²⁰ Referring to footnote 15, tree number 1 of group 2 (Table 3) was excluded.

²¹ Additionally, 4 stem sections including the ramification zone of forks were sampled, but they were not subjected to the present study.

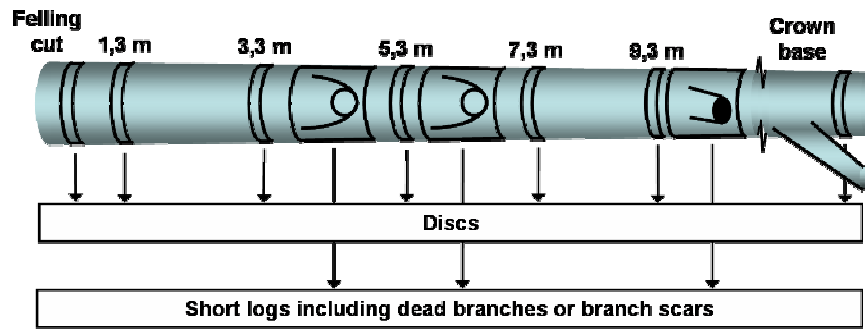


Figure 5. Sampling of discs between the felling cut and the crown base at about every 2 m of tree height; sampling of short logs (at least 4 logs per tree, mean length \approx 50 cm) including dead branches or branch scars.

In the laboratory, the variables describing dead branches (α , db) and branch scars (ls, ws and lm) were measured manually on the outside of the logs, as described above. Each log was cut in a stem-axial direction, passing through the pith at both log ends and through the midpoint of the external trait to be analysed (Figure 6). The midpoint of dead branches was defined as the pith on the branch cross-section, the midpoint of branch scars was located at half of the seal width²². A second cut was made to obtain one board per log (mean board thickness \approx 30 mm)²³.

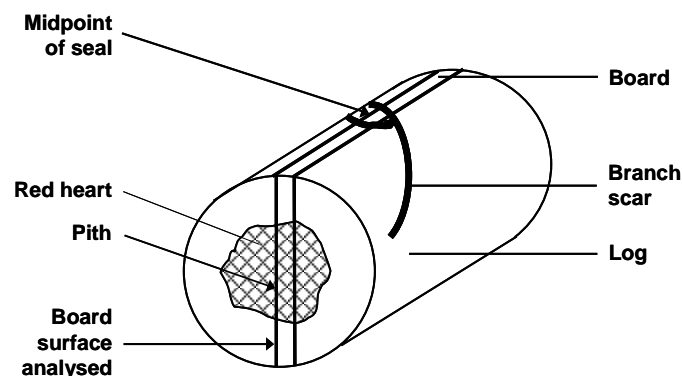


Figure 6. Cutting pattern of logs: the board surface to be analysed passes through the pith at both log ends and through the midpoint of the branch scar (or dead branch, not illustrated) to be analysed. Mean board thickness \approx 30 mm.

²² Similarly, in the case of forks (footnote 21) the cutting plane passed through the pith at the lower log end, and through the piths of the fork branches at the upper end.

²³ Two boards per log were cut additionally, but they were not included in the present study.

Digital images were taken of the discs and boards, using the same method as for group 1 (section 2.1, Figure 3, Paper I; in the case of boards the camera lens was positioned on a perpendicular to the board surface passing through the midpoint between the pith locations at both board ends). For each disc the following variables were obtained from image analysis in CorelDRAW 7 and Visilog 5.3:

- mean red heart radius r_{mean} (mm) and
- mean disc radius r_{discMean} (mm under bark),
calculated from the measured areas of red heart and disc using the formula for circular areas;
- red heart radius r_a (mm) and
- disc radius r_{disc_a} (mm under bark)
with $a = 1$ to 360; 360 radii per disc with an inter-measurement angle of 1° .

The images of the boards were aligned such that the course of the bark was approximately in parallel to the abscissa axis of the image coordinate system. The course of the pith, the red heart borders and the white wood borders (the interior borders of the bark) were marked manually in CorelDRAW 7 (Figure 7). Subsequently, the borderlines were detected and measured automatically in Visilog 5.3, including a calibration step. An algorithm was developed specifically to measure each borderline as a series of points with an inter-point distance of 4 mm in parallel to the abscissa axis.

In stem-axial direction, three red heart zones were distinguished as illustrated in Figure 7: the knot zone was the zone from the junction of the piths of knot and stem to the point where the border of the central red heart crosses the upper side of the knot. Within the red heart below and above the knot zone, two zones of equal length (l_{z_b}) were defined, which were called the lower zone and the upper zone. The upper limit of the lower zone was the junction of the pith of knot and stem, the lower limit of the upper zone was the zone of branch excision and occlusion; regarding the stem from outside, the lower zone and the upper zone represented the red heart just below and above the branch scar, respectively. For each board (b), the length (l_{z_b}) was given by the shorter one of both zones, to make it possible to compare the lower zone and the upper zone within boards, and to use from each board as much information as possible.

In stem-radial direction, the knot side and the opposite knot side were separated by the pith. On the knot side, the image coordinates of a straight line between the ends of the knot zone were calculated (red heart border excluding knot, illustrated as dashed line in Figure 7), in order to separate the central red heart from the red heart in the knot.

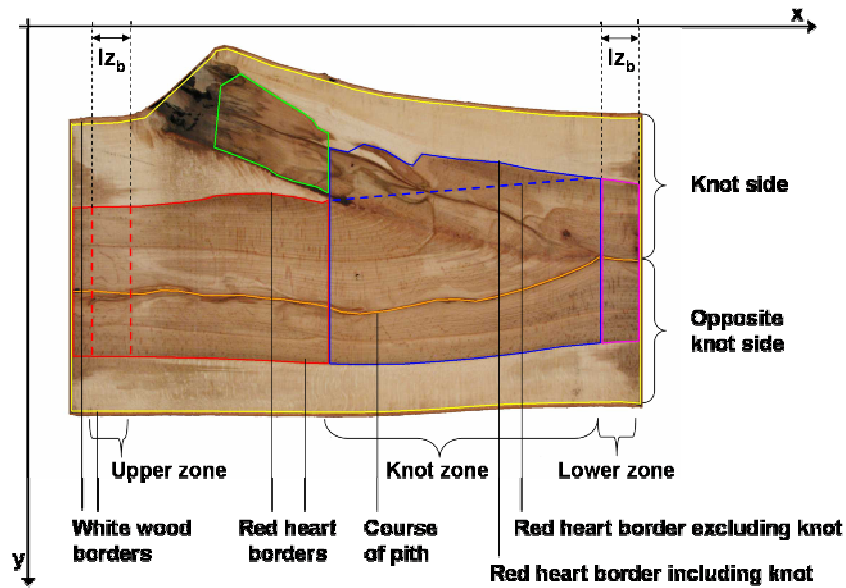


Figure 7. Digital image analysis of boards: three red heart zones and two board sides were distinguished; the course of the pith and the borders of red heart and white wood were marked manually in CorelDRAW 7, and detected and measured automatically in Visilog 5.3.

From the image coordinates of the borderlines measured in Visilog 5.3 the following variables of board zones were calculated²⁴:

- mean red heart radius of the lower zone, including both knot sides²⁵ $r_{\text{lowerZone}}$ (mm);
- mean red heart radius of the knot zone, including both knot sides and the red heart in the knot $r_{\text{knotZoneIncl}}$ (mm);
- mean red heart radius of the knot zone, including both knot sides, but excluding the red heart in the knot $r_{\text{knotZoneExcl}}$ (mm);
- mean red heart radius of the upper zone, including both knot sides $r_{\text{upperZone}}$ (mm);
- mean board radius of the lower zone, including both knot sides $r_{\text{boardLowerZone}}$ (mm under bark);
- mean board radius of the knot zone, including both knot sides $r_{\text{boardKnotZone}}$ (mm under bark);
- mean board radius of the upper zone, including both knot sides $r_{\text{boardUpperZone}}$ (mm under bark);
- mean height (in the tree) of the lower zone $h_{\text{lowerZone}}$ (m);
- mean height of the knot zone h_{knotZone} (m);
- mean height of the upper zone $h_{\text{upperZone}}$ (m);
- mean height of the three zones $h_{\text{moyZone}} = \text{mean}(h_{\text{lowerZone}}, h_{\text{knotZone}}, h_{\text{upperZone}})$ (m);
- mean height of the three zones related to the height of the upper red heart end $h_{\text{moyZoneRel}}$ (1),

²⁴ Preliminary analyses of the red heart shape on boards did not suggest analysis of the knot side and the opposite knot side separately, since results were highly influenced by the curved course of the pith (e.g. Figure 7).

²⁵ Some boards had no lower zone. In these cases the mean of two radii (one at each side) was calculated, which were located at the lower limit of the knot zone/at the junction of the piths of knot and stem. Correspondingly, the mean of two radii was calculated for the upper zone (lz_b equalled zero in this case, Figure 7).

where the height of the upper end of the red heart was the height of the lowest “white” disc without red heart²⁶, and (1) stands for no unit.

For analysing the red heart zones on boards related to the nearest discs, angular disc sections were defined both on the knot side and on the opposite knot side (Figure 8). Referring to the radial orientation (azimuth) of the cutting plane (surface) of the board, the angular sections had a width of $\pm 15^\circ$ on each side. This way, in total 60 out of the 360 radii per disc (r_a , r_{disc_a}) were selected, and the mean radius was calculated

- for the red heart of the disc below the board r_{below} (mm),
- for the red heart of the disc above the board r_{above} (mm),
- for the disc below the board $r_{discBelow}$ (mm under bark) and
- for the disc above the board $r_{discAbove}$ (mm under bark);

the abbreviations of the corresponding disc heights were

- h_{below} (m) and
- h_{above} (m),

respectively.

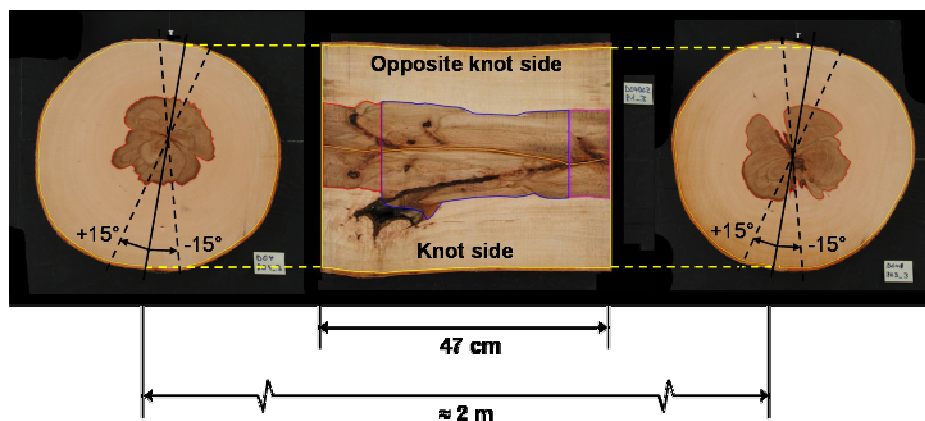


Figure 8. Red heart shape on boards related to the nearest discs (inter-disc distance ≈ 2 m): on the discs the mean red heart radius of angular sections was calculated, having a width of $\pm 15^\circ$ both on the knot side and on the opposite knot side.

Furthermore, knot variables were measured manually in Visilog 5.3 as distances between specific pixel positions in the Cartesian coordinate system of each image (Figure 9). The following variables were measured²⁷:

²⁶ Tree number 47 had a second small red heart above the upper red heart end.

²⁷ Explanation of variable abbreviations: inclination and diameter of dead branches measured on the outside of the stem were abbreviated as α and db, respectively (see above). Inclination and diameter of knots measured on boards were abbreviated as β_m and dk_m , respectively; the index “m” indicates measured variable values to be distinguished from corresponding knot variables (β and dk) estimated from branch scars. Estimation of knot variables is described in Paper I and in section 3.4.1.2.1 below.

- knot inclination β_m (rad),
- knot diameter dk_m (mm),
- buckle thickness bt_m (mm over bark),
- stem radius at the point in time of branch excision, called the knot radius rk_m (mm),
- stem radius observed ro_m (mm over bark) and
- stem diameter observed do_m (mm over bark).

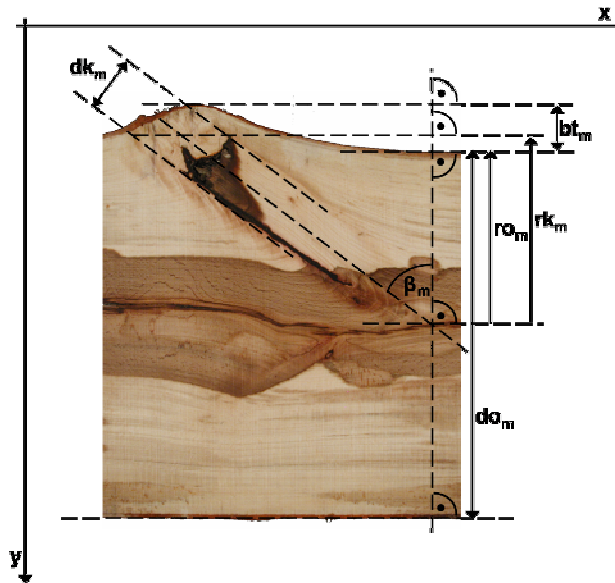


Figure 9. Knot variables measured manually on board images as distances between specific pixel positions in the image coordinate system: knot inclination (β_m), knot diameter (dk_m), buckle thickness (bt_m), knot radius (rk_m), observed radius (ro_m), observed diameter (do_m); the index “m” of variable abbreviations indicates measured variable values.

Boards were eliminated if the knot to be analysed was completely included in the central red heart, or if more than one larger knot occurred on the same board (the larger knots had a minimum seal length of 50 mm, see above). Additional knots which were very small were accepted, since they hardly seemed to influence the shape of the red heart around the (larger) knot to be analysed. Furthermore, the junction of the piths of knot and stem had to be located on the board. Additionally, boards were eliminated if red heart borders were not clearly enough visible owing to discolorations developed during storage of short logs. However, certain uncertainty in red heart identification was accepted in order to keep a sufficient number of samples. In total $N = 60$ boards were included in the analyses, the 16 red heart trees of group 2 were represented by 2 – 5 boards each.

3 Analyses of red heart occurrence and shape

3.1 Explorative analysis (Paper I)

The aim of analysis I (Paper I) was to identify and characterise possible relationships between tree external traits and the red heart within the tree.

Based on the measurements of group 1 (section 2.1, Figure 3), trees B01, B08, C04 and C06 were reconstructed and visualised in three dimensions. A visual assessment was carried out to identify systematically traits which were clearly linked to the red heart.

The links appeared in the visualisation software Bil3d as local, one-sided bulges of the red heart towards some traits as illustrated in Figure 10. Figure 11 shows on disc images the development of two bulges. The bulges appear related to one knot each: regarding in sequence discs b, c, d and e, the red heart bulge on the left side of disc e appears to originate from knot 1, the bulge on the right side from knot 2.

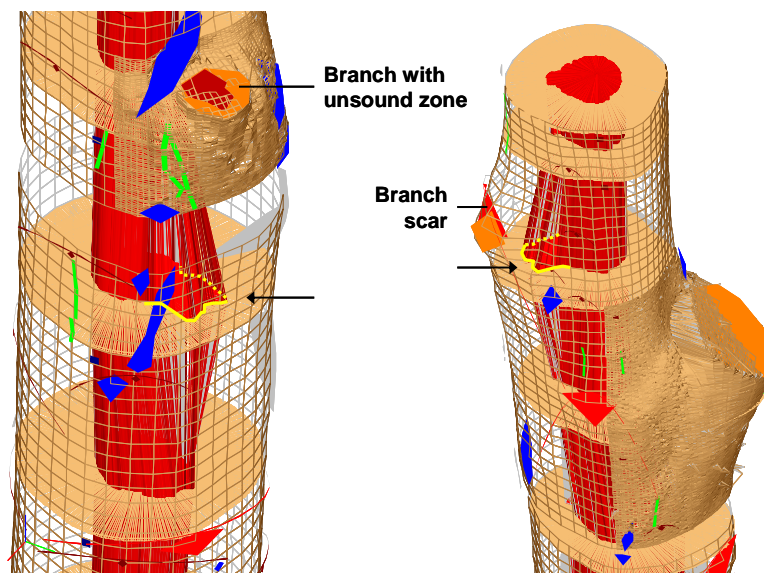


Figure 10. Bulging of the red heart (arrows) towards a dead branch (on the left; tree B01) and a branch scar (on the right; tree C06).

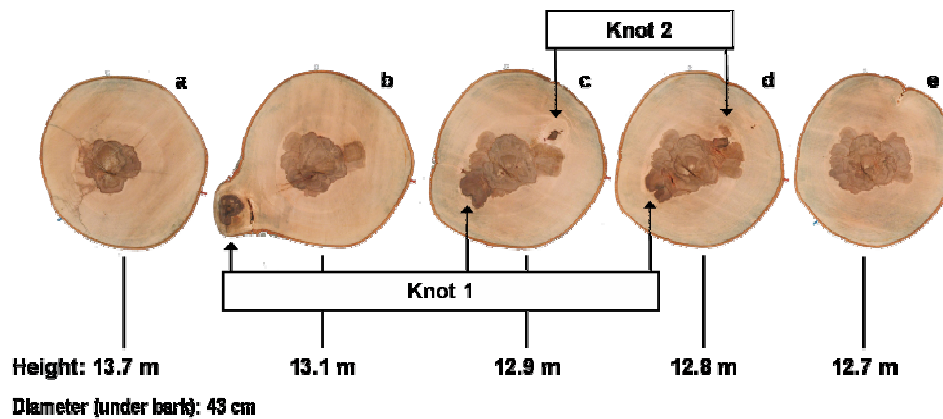


Figure 11. Development of two bulges of the red heart (from disc a to disc e), which appear related to one knot each (tree C04).

The results of Figure 10 and Figure 11 were in accordance with observations by Krempf and Mark (1962) (section 1.2), who concluded that an objective, quantitative acquisition of tree traits, and an identification of traits influencing the size of coloured heartwood would be necessary. This was done in the present analysis: a complete map of traits on the stem surface was available, and bulging of the red heart was observed for 4 out of 5 dead branches and 27 out of 344 branch scars, while no clear relationships were observed for wounds and cracks. However, these results were based on visual assessment focusing on clearly evolved bulges of the outer red heart surface; there might have been other traits linked to the red heart which could not be identified by visual assessment, because bulges might have been overlaid in the course of the evolution of red heart extent with time, for instance.

The knots corresponding to the branch scars which were found to be linked to the red heart (later referred to as the selected branch scars) had a knot inclination of $\beta \geq 30^\circ$ (with one exception) and were situated close to the bark (knot depth $kd \leq 1.3$)²⁸. Furthermore, all selected branch scars had a seal length of $ls \geq 55$ mm; the seal length is approximately related to the knot diameter (Erteld and Achterberg 1954). Most of the selected branch scars (93%) corresponded simultaneously to the criteria of β , kd and ls . However, within the bounds given by the criteria, there were still 61% of non-selected branch scars.

Referring to the research questions asked in section 1.3, the results of Paper I contribute to answer questions *Q1* and *Q2*.

Q1: Which external traits can be related to the red heart inside the stem?

Q2: How are these external traits related to the red heart inside the stem?

In response to *Q1* one may say that some dead branches and branch scars/knots were related to the red heart inside the stem. Also, in the case of sample tree B08, relationship between the ramification zone

²⁸ The calculation method of β and kd are given in Paper I.

of the fork and red heart was observed (Figure 7 of Paper I). However, the hypothesis of relationship between red heart and wounds or cracks could not be verified by the present analysis.

The relationship between dead branches/knots and red heart seemed to depend on the geometry of the dead branch/knot (Q_2): using geometric relationships between branch scars, knots and red heart (Paper I), particularly larger knots, more inclined knots and knots located close to the bark were found to be linked to the red heart.

In addition to the local red heart shape (bulges towards external traits), the overall red heart shape along the stem axis was described in Paper I as the mean red heart radius versus tree height. The red heart shape of trees B01 and C04 was that of a spindle; the red heart below the fork of tree B08 tapered towards the stem bottom; the red heart of tree C06 tapered towards the stem top almost in parallel to the bark. Using the observations on trees B01, C04 and C06, a simple hypothesis about the development of the overall red heart shape was derived as described in the following²⁹. According to Zycha (1948) red heart starts at a middle stem height and develops towards the stem base and about up to the crown base. The red heart shapes of trees B01, C04 and C06 may represent stages of this development as illustrated in Figure 12: the spindle-shaped red heart of tree B01 just reaches the felling cut, and it ends below the crown base ($h_{cb} = 15.5$ m, Table 2). A later stage of development may be represented by tree C04, where, in stem-axial direction, the red heart reaches from the felling cut to the crown base ($h_{cb} = 14.5$ m, Table 2), and the red heart extent in stem-radial direction is systematically larger. Assuming that the red heart shape continues to increase in stem-axial and stem-radial direction, at an even later stage it may run almost in parallel to the bark (tree C06). To generalise these observations one may hypothesise that in all stages of development the overall red heart shape is that of a spindle; in earlier stages the spindle is included to a large extent in the stem between the felling cut and the crown base (tree B01), and in later stages the spindle has increased in stem-axial and stem-radial direction, so that the stem between the felling cut and the crown base includes a section of the spindle only (trees C04 and C06).

Using this hypothesis, an approach to describe the overall red heart shape mathematically, and to relate this shape to tree external and dendrometric characteristics is presented in section 3.3 below and in Paper III. The approach was based on 16 red heart trees of group 2, and it was tested on the 4 trees of group 1.

²⁹ The red heart shape of the forked tree B08 was not taken into account at first, but is discussed in section 3.3 below.

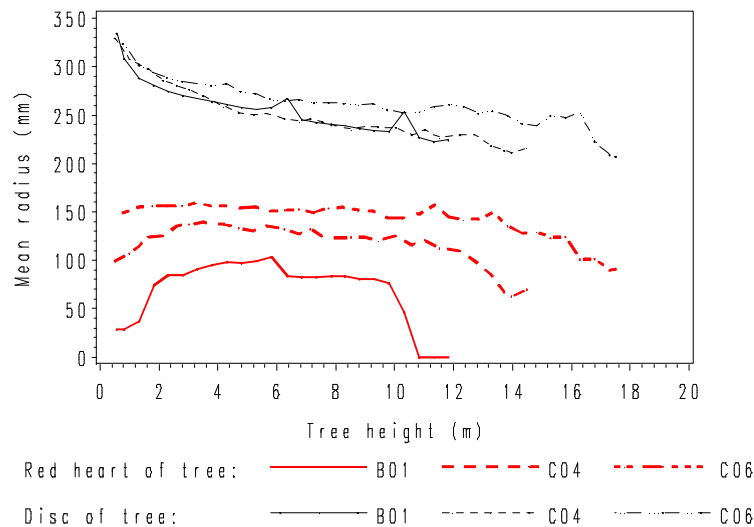


Figure 12. Hypothesised stages of development of the overall red heart shape (mean red heart radius versus tree height) observed on sample trees B01, C04 and C06. Mean disc radius under bark.

3.2 Red heart occurrence (Paper II)

The aim of analysis II was to estimate the probability that red heart occurs (does not occur) in individual standing trees, based on relationships between external traits and red heart. Given the results of the explorative analysis (section 3.1), it was hypothesised that the probability of red heart occurrence changes with the inclination, diameter and/or depth of a dead branch/knot.

Paper II describes a type logistic regression model based on the 17 red heart trees and the 14 white trees of group 2 (section 2.2). The model estimates the probability for each tree of its being a white tree as the product of individual probabilities of branch scars and a probability at the dendrometric level. The probability of each branch scar not to initiate red heart formation was estimated from three so-called “mechanistic” variables, which reflected the hypothesised effect of dead branches/knots on red heart occurrence stated above. At the dendrometric level, a significant effect of dbh was found on the probability that red heart does not occur. Using this model, 27 of 31 trees were correctly classified, and the two groups of red heart trees and white trees were clearly distinguished by probabilities below 0.25 and above 0.85 (with one exception).

Based on Paper II, in the following a complementary analysis is presented to better understand the effect on the tree level, which was included in the model as effect on the dendrometric level. Referring to Table 3, possible effects of h_{tot} , h_{cb} , h_{cbrel} , cl , cl_{rel} and hd were tested (dbh , age , mi_{dbh} and $Fork$ were already tested in Paper II). Comparing the two groups by a t-test, a difference at the significance level of 10% was only found for hd ($p = 0.095$).

Using hd in the model only 2 trees (instead of 4 trees in Paper II) were falsely classified (Table 4)³⁰. These trees (number 19 and 29) were also misclassified in Paper II. However, in Paper II the misclassified trees show probability values close to the classification threshold³¹ of 0.5. Furthermore, the ratio (hd) of h_{tot} and dbh can have the same value for very small and very big trees, so that the model should also be adjusted to a simple variable (dbh). However, including hd and dbh into the model, the slope of hd was not significant. On the one hand, interpretation of significance was limited owing to the small number of sample trees. On the other hand, the small number of sample trees suggested limiting the number of parameters. Additionally, in the t-test hd was not significant on the 5% level, but only on the 10% level. Thus, the results should be considered as an indication that there may be an effect of hd, but further analyses on a larger sample would be necessary to evaluate this effect. Both in Paper II and in the complementary analysis the same effect of branch scars was found; to quantify the effect of individual branch scars on red heart occurrence was the aim of analysis II.

Table 4. Probability of each tree of group 2 being a white tree (P_{white}); in comparison with Paper II, the probability at the dendrometric level was estimated from the hd-ratio (hd) instead of dbh; threshold probability $P_{\text{white}} = 0.5$ (dashed line).

Tree number	Observation	P_{white}
35	Red heart tree	0.000
39	Red heart tree	0.000
41	Red heart tree	0.000
15	Red heart tree	0.000
45	Red heart tree	0.000
24	Red heart tree	0.000
50	Red heart tree	0.000
2	Red heart tree	0.000
43	Red heart tree	0.000
47	Red heart tree	0.000
22	Red heart tree	0.000
31	Red heart tree	0.000
19	White tree	0.000
42	Red heart tree	0.000
4	Red heart tree	0.000
1	Red heart tree	0.078
21	Red heart tree	0.153
11	White tree	0.788
30	White tree	0.988
52	White tree	0.991
8	White tree	0.992
28	White tree	0.994
44	White tree	0.997
56	White tree	0.998
17	White tree	0.999
25	White tree	0.99953
55	White tree	0.99981
9	White tree	0.99991
7	White tree	0.99993
13	White tree	0.99999
29	Red heart tree	1.00000

³⁰ Parameter estimates, approximate standard errors, significance tests and correlation matrix of parameter estimates of this model are given in Annex section 8.1.2.

³¹ The classification threshold was chosen arbitrarily, and it was set a priori.

In literature, an effect of hd on the probability of occurrence of coloured heartwood was found by von Büren (2002), who discusses relationships to knottiness: more slender trees would have smaller branch scars, i.e. smaller possible entrances for air, since secondary growth would have been reduced and crowns would have received less light. Additionally, an effect of the presence of larger branch scars is reported by this author. Both variables are relatively coarse indicators of knottiness, while the model of the present analysis makes it possible to quantify the effect of individual branch scars on red heart occurrence. The results of von Büren (2002) were obtained for trees from various stands in terms of site characteristics, and dbh and age classes. The present model indicates an effect of hd in the situation of a single stand. Therefore, a possible effect of hd may be taken into account if the model is tested and developed in different silvicultural situations as discussed in Paper II and in section 5 below.

Referring to the research questions of section 1.3, results of analysis II contributed to answer question Q3.

Q3: How can this relationship (between dead branches/branch scars and red heart) be used to estimate the occurrence (initiation) of red heart?

To respond to this question it may be said that geometric relationships between branch scars, knots and red heart were used to develop variables which reflected the hypotheses that red heart initiation changes with the inclination, diameter and/or depth of a dead branch/knot. The variables were based on measurements of branch scars on the outside of the stem, and they were used to estimate the probability of each branch scar of its being an initiation point of red heart formation. Based on probabilities of branch scars, the probability of red heart occurrence was estimated including an effect on the dendrometric level.

3.3 Overall red heart shape (Paper III)

The aim of analysis III was to develop a modelling approach for the overall red heart shape in standing trees between the felling cut and the crown base. This approach should make it possible to take into account factors initiating and influencing red heart formation (Paper III).

To reach this objective, the hypothesis about stages of development of the red heart shape (section 3.1) was used to develop a model based on 16 red heart trees of group 2, as described in Paper III. The red heart shape was defined as the mean red heart radius versus tree height (measured on discs with an inter-disc distance of approximately 2 m, section 2.2) between the felling cut and the crown base. The shape was modelled by sections of bell-shaped curves, given by an exponential function with a fourth order polynomial term. The curves were defined by parameters for the red heart width (in stem-radial direction), length (in stem-axial direction) and height in the stem. First, a descriptive model was developed with parameter estimates of the red heart width, length and height for each tree. Second, an

approach of a predictive model at the standing tree level was developed for estimating these parameters from the diameter at breast height, the relative height of the crown base, and the height of the most recently occluded knot as possible red heart initiation point.

Starting from results of Paper III, the model was tested on an independent sample which was the 4 trees of group 1. Parameters of the descriptive model were estimated based on the data of each tree (mean red heart radius about every 50 cm of tree height, section 2.1)³². Parameters of the predictive model were adopted from Paper III.

Figure 13 shows the observed red heart shape and the results of the descriptive and predictive model for each tree of group 1. The observed red heart shapes of all trees were closely described by the model. With respect to the predictive model, the red heart width was systematically larger than observed for tree B01, and slightly smaller for tree B08 (the red heart below the fork was analysed). Differences between the observed and predicted red heart length and height³³ appeared at the top end (tree C04), or both at the top and bottom ends (tree C06) of the red hearts. Comparing in this way the observed and predicted red heart shape, the best result was obtained for tree B08. Among other things, this may be explained by the explanatory variable dbh of B08 (Table 2) being close to the dbh of the trees of group 2 which were used in Paper III to parameterise the model (Table 3, 16 red heart trees excluding tree number 1), while the dbh of B01, C04 and C06 were larger (Table 2). More generally speaking, parameterising the model based on trees representing different stages of tree growth and red heart development may improve its precision and widen its scope of application.

³² Parameter estimates, approximate standard errors and 95% confidence limits of this model are given in Annex section 8.1.3.

³³ In the predictive model a linear relationship between the red heart height and length was used (Paper III), so that the effect of both parameters cannot be evaluated separately.

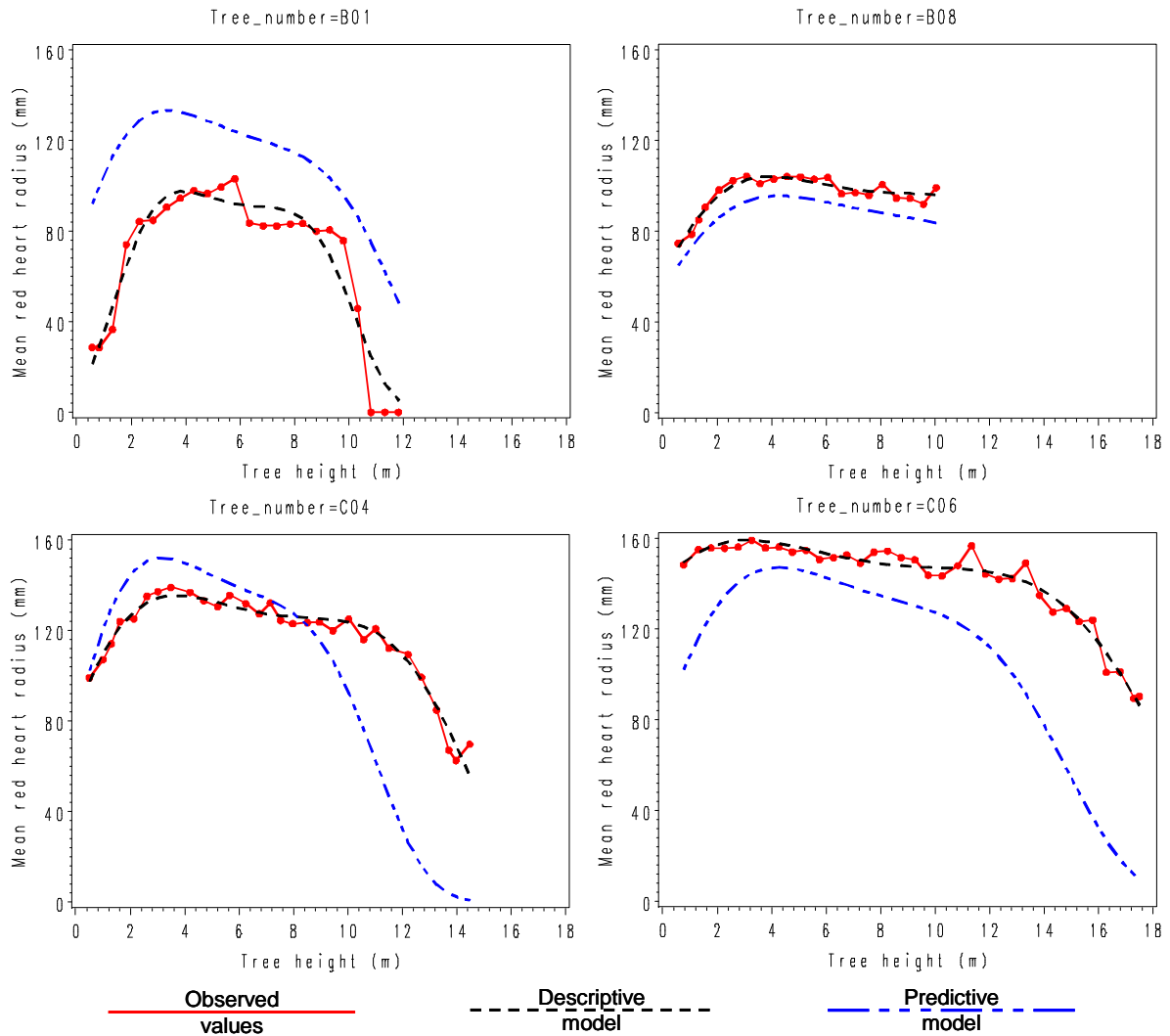


Figure 13. Application to group 1 of the model of the overall red heart shape (mean red heart radius versus tree height) developed in Paper III. Observed (measured) values and results of the descriptive and predictive model are plotted for each tree ($N = 110$ mean radii in total). Parameters of the descriptive model were estimated based on the observed red heart shape (group 1), those of the explicative model adopted from Paper III (group 2). The red heart of tree B08 was analysed below the fork.

The histogram of residuals and the scatter plot of residuals versus predicted values of the descriptive model are given in Figure 14. For small predicted values the variation of the residuals is relatively high. This can be explained by the red heart shape of tree B01 (Figure 13): between 9 m and 11 m of tree height the red heart radius estimated by the descriptive model decreases less sharply than the observed red heart radius.

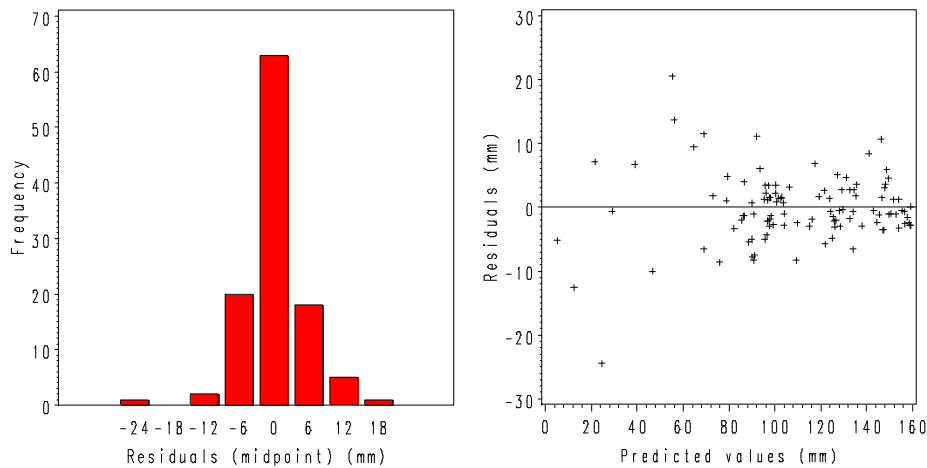


Figure 14. Descriptive model (group 1): histogram of residuals and scatter plot of residuals and predicted values ($N = 110$).

With the chosen modelling approach, promising results were obtained both in Paper III and in the test based on the trees of group 1. The model used the hypothesis that red heart starts at a middle stem height and develops to the stem base and up to the crown base (section 3.1). Keller (1961) assumes that coloured heartwood develops in the stem upwards (for coppice shoots) or downwards (for forks at a relatively low stem height). This may result in coloured heartwood with cone shape tapering towards the stem top and bottom, respectively. The model can also deal with these cases, since it defines the shape of coloured heartwood as a section of a bell-shaped curve which reaches from $-\infty$ to $+\infty$ in abscissa direction; depending on the position of the section within the entire curve, spindle or cone shapes are modelled (Figure 15). The parameter height defines the position of the curve in stem-axial direction relative to the bottom and top end of the stem analysed.

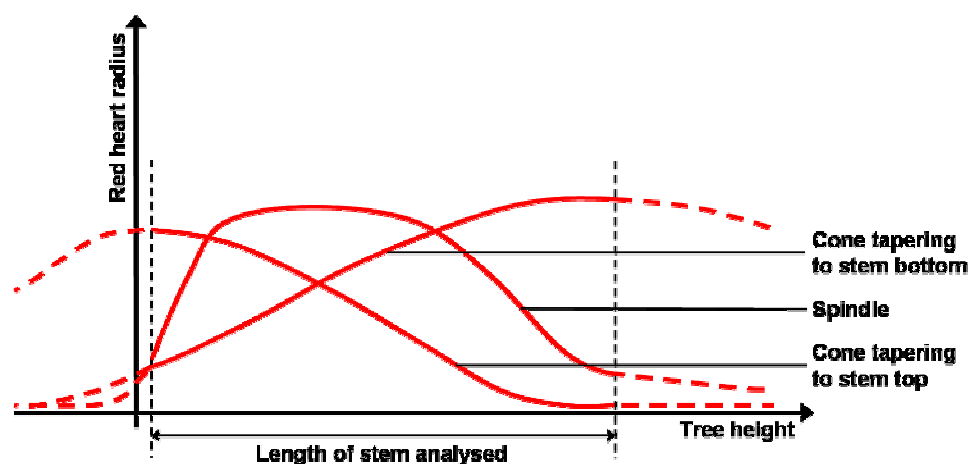


Figure 15. Modelling of coloured heartwood with cone or spindle shape by sections of bell-shaped curves.

Tree B08 of group 1 had a cone-shaped red heart below the fork, which tapered towards the stem bottom. In Paper III the red heart areas occurring at the same height on the branches of a fork were added, and the mean radius was calculated using the formula for circular areas (trees number 4, 15, 24, 35 and 43 of group 2, Table 3). The results showed that the red heart of forked trees can also be spindle shaped, if the red heart in the branches of the fork is taken into account (red heart shapes of group 2 are given in Figure 4 of Paper III).

The shape of a cone tapering towards the stem top seems characteristic for the splashing heartwood. According to Walter and Kucera (1991), splashing heartwood³⁴ has its maximum extent at the stem base and runs through the entire stem axis. Similarly, Höwecke et al. (1991) report that splashing heartwood occurs most frequently at the stem base. Compared with this, red heart³⁵ occurrence increases rapidly within the first meters of stem height, and it is highest at 2–10 m of stem height (Höwecke et al. 1991). The characteristics of splashing heartwood in comparison with red heartwood are given in section 1.2.1. Problems in modelling of splashing (and abnormal) heartwood are discussed in section 4.3 below.

The spindle shape of red heart is modelled by Knoke and Schulz Wenderoth (2001) and Knoke (2003a) by using the height and the height squared of stem cross-sections in multiple regression analyses³⁶. With respect to sampling, a similar approach is used by these authors, and by Rácz (1961) and Höwecke et al. (1991) who describe the shape of coloured heartwood (section 1.2.6): the size of coloured heartwood is measured on bottom and top ends of logs of different length and diameter [butt-logs in the studies by Knoke and Schulz Wenderoth (2001) and Knoke (2003a), butt-logs and also logs from higher stem zones in the studies by Rácz (1961) and Höwecke et al. (1991)]. In this way, observations at various tree heights are obtained from many trees, but the shape of coloured heartwood of each individual tree is only represented by few observations along the stem axis. Rácz (1961) remarks that it would be more exact from the point of view of natural sciences to determine coloured heartwood systematically at constant intervals in all trees. This was done in the present study, and as a consequence fewer trees were analysed. The results showed that the red heart shape in stem-axial direction varies considerably within trees of similar diameter, and a model based on first and second order polynomial terms was found not to be flexible enough to take account of this variability (in Paper III third and fourth order terms were used additionally).

³⁴ Splashing heartwood according to the classification by Walter and Kucera (1991) may include splashing and abnormal heartwood according to the classification by Sachsse (1991).

³⁵ Coloured heartwood with round or cloudy appearance on cross-sections according to the classification by Höwecke et al. (1991), which corresponds most likely to red heart according to the classification by Sachsse (1991). Höwecke et al. (1991) also report analyses of coloured heartwood with irregular appearance: this type would be frequent and relatively even distributed at all stem heights. However, it is difficult to match with the classification by Sachsse (1991).

³⁶ Knoke and Schulz Wenderoth (2001) use the relative height of cross-sections in the zone of the branch-free bole.

Referring to the research questions asked in section 1.3, results of analysis III contributed to answer questions *Q4* and *Q5*.

Q4: How can this relationship (between dead branches/branch scars and red heart) be used to estimate the overall shape of red heart along the stem axis (e.g. spindle shape)?

Q5: How can relationships between dendrometric variables and red heart be used to estimate the overall shape of red heart?

In response to questions *Q4* and *Q5* it may be said that geometric relationships between branch scars, knots and red heart, and the dendrometric variables relative height of the crown base and diameter at breast height, were used to estimate the parameters height, length and width of the overall red heart shape³⁷. This was done by means of a statistic model based on an exponential function with a fourth order polynomial term. The model described the red heart shape in stem-axial direction by a section of a bell shaped curve.

3.4 Local red heart shape (not yet reported in a paper)

In Paper I, local variation (bulging) of red heart shape was observed close to dead branches/branch scars, and geometric relationships were developed to conclude from the stem outside (branch scar) to the inside (knot and red heart). In Paper II, the geometric relationships were used to estimate probabilities of branch scars of their being initiation points of red heart formation. In Paper III the height of a particular branch scar was used to estimate the height of the overall red heart in the stem. Results suggested that the zone of red heart close to dead branches/branch scars is important to estimate red heart occurrence and shape. Thus, this zone was analysed more closely in analysis IV: first, the red heart shape close to dead branches/knots was studied with the aim of quantifying local deviation from the overall red heart shape; second, the geometric relationships between branch scars, knots and red heart were tested and further developed.

3.4.1 Methods

3.4.1.1 Local red heart shape

In section 3.3, the overall red heart shape of 16 trees of group 2 was analysed using discs. Deviation of the local red heart shape around knots from the overall red heart shape was analysed using boards of these trees. The boards were cut from the inter-disc sections (Figure 5 and Figure 6), and they were related to the nearest discs as illustrated in Figure 8. The variables for quantifying the deviation had to be independent of the overall red heart shape as far as possible. Thus, to quantify the deviation, the

³⁷ Questions *Q4* (related to external traits) and *Q5* (related to dendrometric variables) were not answered separately for the following reason: in Paper III a linear relationship between the parameters height and length was used, so that the effect of branch scar height (external trait) and relative height of the crown base (dendrometric variable) could not be evaluated separately.

mean radius of each red heart zone on boards (Figure 7) was related to the mean red heart radius of the nearest discs (Figure 8) as illustrated in Figure 16: the coordinates tree height (abscissa) and mean red heart radius (ordinate) of the disc below the board [A (h_{below} , r_{below})], the lower board zone [B ($h_{\text{lowerZone}}$, $r_{\text{lowerZone}}$)], the knot zone including the red heart in the knot [C (h_{knotZone} , $r_{\text{knotZoneIncl}}$)], the knot zone excluding the red heart in the knot (h_{knotZone} , $r_{\text{knotZoneExcl}}$; not illustrated in Figure 16), the upper board zone [D ($h_{\text{upperZone}}$, $r_{\text{upperZone}}$)] and the disc above the board [E (h_{above} , r_{above})] were used to calculate the deviation of

- the lower zone $d_{\text{lowerZone}}$,
- the knot zone including the red heart in the knot $d_{\text{knotZoneIncl}}$,
- the knot zone excluding the red heart in the knot $d_{\text{knotZoneExcl}}$ (not illustrated in Figure 16) and
- the upper zone $d_{\text{upperZone}}$

from the linear interpolation between the discs below and above the board (dashed line between A and E in Figure 16). Deviation was perpendicular to the interpolation line between A and E. It was positive if the respective zone (B, C or D) was located above the interpolation line, and negative below. (The absolute values of deviation were equal to the mathematic distance of B, C or D to the interpolation line.)³⁸

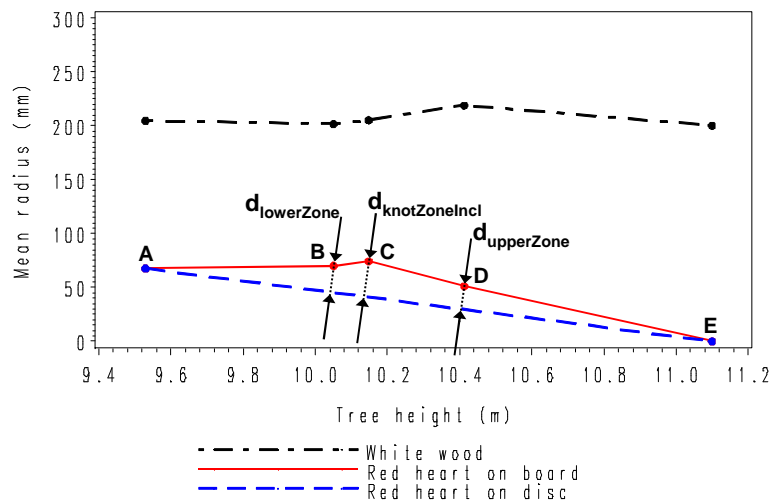


Figure 16. Plot of mean red heart radius versus tree height of the disc below the board [A (h_{below} , r_{below})], the lower board zone [B ($h_{\text{lowerZone}}$, $r_{\text{lowerZone}}$)], the knot zone including the red heart in the knot [C (h_{knotZone} , $r_{\text{knotZoneIncl}}$)], the upper board zone [D ($h_{\text{upperZone}}$, $r_{\text{upperZone}}$)] and the disc above the board [E (h_{above} , r_{above})]; deviations $d_{\text{lowerZone}}$, $d_{\text{knotZoneIncl}}$ and $d_{\text{upperZone}}$ of B, C and D, respectively, to the interpolation line (dashed) between A and E; white wood: mean radii of discs ($r_{\text{discBelow}}$, $r_{\text{discAbove}}$) and board ($r_{\text{boardLowerZone}}$, $r_{\text{boardKnotZone}}$, $r_{\text{boardUpperZone}}$) under bark; example taken from tree 22 (board 220312 between discs 6 and 7).

³⁸ Referring to Figure 16, the perpendicular deviations of B, C and D from the interpolation line between A and E (as presented) were very similar to the corresponding deviations in parallel to the ordinate axis: the maximum difference accounted for less than 1 mm ($N = 174$; 58 boards and 3 zones per board).

If one of the nearest discs showed no red heart, e.g. point E in Figure 16, the slope of the interpolation line between A and E, and the deviations $d_{\text{lowerZone}}$, $d_{\text{knotZoneIncl}}$ and $d_{\text{upperZone}}$ were not known exactly, since the upper red heart end might have been located between D and E. Thus, the following rule was defined: point E was moved to the same height as point D if the ordinate of D was smaller than 15 mm; the corresponding algorithm was: if $r_{\text{upperZone}} \leq 15$ mm then $h_{\text{above}} = h_{\text{upperZone}}$ (valid for 3 out of 58 boards analysed; see below).

The deviation of the local red heart shape in relation to the overall red heart shape was defined as the quotient between the deviation of a board zone ($d_{\text{lowerZone}}$, $d_{\text{knotZoneIncl}}$, $d_{\text{knotZoneExcl}}$ and $d_{\text{upperZone}}$) and the mean red heart radius on discs at the height of the respective board zone (later referred to as relative deviation). Referring to Figure 16, the mean red heart radius on discs at the height of a board zone (B, C or D) was calculated by linear interpolation between A and E (dashed line). The variable abbreviations of the relative deviations were:

- $d_{\text{lowerZoneRel}}$,
- $d_{\text{knotZoneInclRel}}$,
- $d_{\text{knotZoneExclRel}}$ and
- $d_{\text{upperZoneRel}}$.

Differences between deviations of upper zone and lower zone were defined as:

- $\Delta d_{\text{upperZoneLowerZone}} = d_{\text{upperZone}} - d_{\text{lowerZone}}$ and
- $\Delta d_{\text{upperZoneLowerZoneRel}} = d_{\text{upperZoneRel}} - d_{\text{lowerZoneRel}}$.

Furthermore, using plots as given in Figure 16, each board was visually classified by its position

- in the middle between the nearest discs (position = 'middle'; N = 26) or
- close to one of the discs (position = 'close'; N = 32).

Fifty-eight of 60 boards were included in the analysis. One board of tree number 15 was excluded since the upper disc was located in the ramification zone of the fork. Another board taken from tree number 43 was excluded since the red heart boarder on the opposite knot side was not clearly enough visible.

3.4.1.2 Geometric relationships between branch scars, knots and red heart

For testing and further developing the geometric relationships between branch scars, knots and red heart, first, relationships between branch scars and knots were analysed. The second part of the analysis focused on relationships of these branch scars and knots to the red heart.

3.4.1.2.1 Relationships between branch scars and knots

For testing the geometric relationships between branch scars and knots, the knot variables inclination (β), diameter (dk), depth (Δr) and relative depth (kd) were estimated³⁹ from branch scars, and the results were compared to the corresponding knot variables based on measurements on boards (β_m , dk_m , Δr_m and kd_m). The variables β_m and dk_m were measured directly on boards (Figure 9). The knot depth was defined as

$$\Delta r_m = ro_m - rk_m \quad \text{Equation 1}$$

and the relative knot depth as

$$kd_m = \frac{ro_m}{rk_m} - 1, \quad \text{Equation 2}$$

where ro_m was the observed stem radius from pith to bark, and rk_m was the knot radius (the stem radius at the point in time of knot excision) measured on boards (Figure 9).

The geometric relationships to estimate knot variables from branch scars are given in Figure 17. The original geometric relationships as developed in Paper I were specified to take into account bark buckles, which develop in the course of knot occlusion and occur in the case of recently occluded knots.

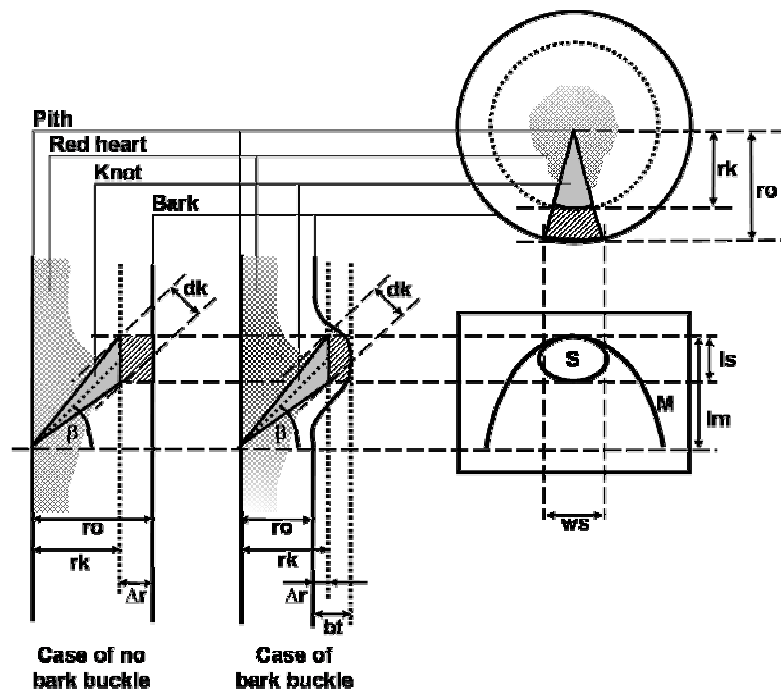


Figure 17. Geometric relationships between branch scars, knots and red heart: case of no bark buckle (as developed in Paper I) and specification in the case of a bark buckle; branch scar consisting of the seal (S) and moustache (M); variables: observed radius (ro), knot radius (rk), seal length (ls), seal width (ws), moustache length (lm), knot inclination (β), knot diameter (dk), knot depth (Δr) and buckle thickness (bt).

³⁹ Geometric relationships (presented below) were used to calculate knot variables from variables of branch scars. The term estimation is applied in this context to reflect that the geometric relationships were based on a simplification of the real stem geometry. However, there was no estimation by a statistic model.

Referring to Figure 17, in the case of a buckle the knot radius (r_k) can be larger than the observed trunk radius (r_o); the knot depth (Δr) is then negative. In the course of radial growth, r_o exceeds r_k and Δr becomes positive, which corresponds to the case of no buckle given in Figure 17. The seal of the branch scar is located on the buckle; since the seal length and width (l_s and w_s) were used to estimate r_k and the knot variables β , dk , Δr and kd , the buckle thickness (bt) was taken into account. In the following, the calculation method in the case of a buckle is described; in case of no buckle bt equalled zero. Based on the estimate function $\frac{r_k}{r_o} \approx \frac{l_s}{w_s}$ of Schulz (1961)⁴⁰, the knot radius was calculated as

$$r_k = \frac{l_s}{w_s} \cdot (r_o + bt) . \quad \text{Equation 3}$$

Using Equation 3 the knot inclination and diameter equalled:

$$\beta = \arctan \frac{lm - \frac{1}{2} \cdot l_s}{r_k} = \arctan \left[\left(\frac{lm}{l_s} - \frac{1}{2} \right) \cdot \frac{w_s}{r_o + bt} \right] \quad \text{Equation 4}$$

and

$$dk = l_s \cdot \cos(\beta) = \frac{l_s}{\sqrt{1 + \left[\left(\frac{lm}{l_s} - \frac{1}{2} \right) \cdot \frac{w_s}{r_o + bt} \right]^2}} , \quad \text{Equation 5}$$

respectively. The knot depth was calculated as

$$\Delta r = r_o - \frac{l_s}{w_s} \cdot (r_o + bt) \quad \text{Equation 6}$$

and the relative knot depth as

$$kd = \frac{w_s}{l_s} \cdot \left(1 - \frac{bt}{r_o + bt} \right) - 1 . \quad \text{Equation 7}$$

The geometric relationships made it possible to estimate knot variables from the outside of the stem:

l_s , w_s and lm were measured on branch scars (Figure 4); r_o was set to $r_o = \frac{do_m}{2}$ and bt was set to

$bt = bt_m$ (Figure 9⁴¹). Possible sources of imprecision in the calculation of β (Equation 4) and dk (Equation 5) may be the already estimated variable values of r_k and β , respectively; imprecision in estimation may accumulate. Furthermore, the calculation of Δr (Equation 6) and kd (Equation 7) used

⁴⁰ The estimate function uses the assumption that w_s is about equal to l_s right after branch occlusion ($r_o \approx r_k$).

⁴¹ Figure 9 shows measurements on boards. At the outside of a tree do_m and bt_m can be measured by callipers: the height and azimuth of the measurement of do_m are given by the lower ends of the moustache and the azimuth of the seal of the branch scar, respectively (Figure 17); measuring the stem diameter x on the buckle, it is $bt_m = x - do_m$.

the approximation $ro = \frac{do_m}{2}$. However, particularly in cases with eccentric course of the pith it is

$ro_m \neq \frac{do_m}{2}$. Considering this, three methods of calculation of β , dk , Δr and kd were tested:

- a. ignoring the thickness of buckles: for all branch scars, bt was set to $bt = 0$; this method corresponded to the original geometric relationships as developed in Paper I and was used as a reference;
- b. taking account of the buckle thickness: for all branch scars, bt was set to $bt = bt_m$ [there were $N = 23$ branch scars with buckles ($bt_m > 0$) and $N = 35$ branch scars with no buckles ($bt_m = 0$)];
- c. using measured variables only: as opposed to a and b, method c was not completely based on measurements on the outside of the stem, but on measurements of branch scars and boards as well. The aim was to identify possible sources of imprecision in methods a and b. Therefore, β was calculated from Equation 4 using the measured variable rk_m , and dk was calculated from Equation 5 using the measured variable β_m (calculation was the same for branch scars with buckles and for branch scars with no buckles). Furthermore, Δr and kd were calculated using the measured variable ro_m in Equation 6 and Equation 7, respectively (calculation was such that the buckle thickness was taken into account, i.e. $bt = bt_m$).

3.4.1.2.2 Relationships of branch scars and knots to the red heart

For testing the relationships of branch scars and knots to the red heart, a visual assessment was carried out to identify knots linked to the red heart. The assessment was based on the assumption that red heart initiation results in a discoloured zone between the knot end and the central red heart. Three classes of knots were distinguished (Figure 18):

1. a knot was considered as being linked to the red heart (link = 'yes'), if the necrosis at the spot of branch excision was located clearly outside the central red heart, and a continuous discoloured zone occurred between the necrosis and the central red heart ($N = 20$);
2. a knot was considered as not being linked to the red heart (link = 'no'), if the necrosis at the spot of branch excision was located clearly outside the central red heart, and non-discoloured, white wood separated the necrosis and the central red heart⁴² ($N = 18$);
3. a possible link between knot and red heart was considered as undetermined (link = 'undetermined'), if the spot of branch excision was located at the red heart margin⁴³ ($N = 20$).

⁴² Bark inclusions and the knot pith (Figure 18, images bottom left and right) were not taken into account, but they are discussed in section 3.4.2.2.2 below.

⁴³ Knots which were completely included in the central red heart were eliminated (section 2.2).

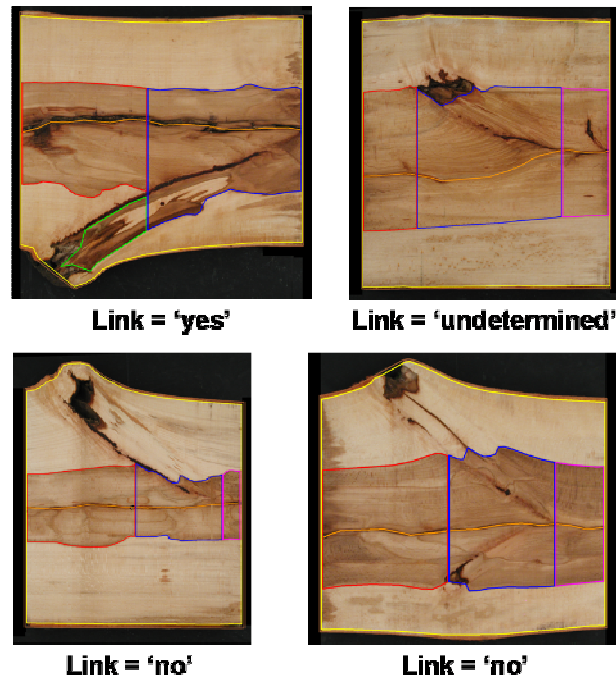


Figure 18. Visual assessment of link knot to red heart as continuous discoloured zone between knot necrosis and central red heart.

Based on the visual assessment, it was analysed if the occurrence of link depended on the dimensions of the corresponding branch scar or knot. The class link = 'undetermined' was excluded from this analysis, as the knots of this class were located deeper in the wood than those with determined link; there might have been additional factors to take into account which did not apply for the knots with determined link (e.g. at the point in time of knot occlusion the trees were considerably younger and smaller). The number of observations was considered to be too small to develop a more complex model which could take account of this issue. Logistic regression was used to analyse the occurrence of link knot to red heart. The probability q_k of each knot k of its being not linked to the red heart was calculated from the inverse of the logit function with the parameters c_0, c_1, c_2, \dots and the explanatory variables s_k, t_k, \dots :

$$q_k = \frac{e^{c_0 + c_1 s_k + c_2 t_k + \dots}}{1 + e^{c_0 + c_1 s_k + c_2 t_k + \dots}}.$$

Equation 8

Two models S (for scar) and K (for knot) were distinguished. In model S, the “mechanistic” variables of branch scars developed in Paper II were tested as explanatory variables (s_k , t_k, \dots). The “mechanistic” variables reflected the hypotheses that red heart initiation changes with inclination, diameter and/or depth of a dead branch/knot (Paper II):

- $mec1 = \left(\frac{lm}{ls} - \frac{1}{2} \right) \cdot \frac{ws}{ro}$,
- $mec2 = ls \cdot \left[\left(\frac{lm}{ls} - \frac{1}{2} \right) \cdot \frac{ws}{ro} \right]^2$,
- $mec3 = ro \cdot \frac{ls}{ws}$,
- ls and
- ro.

In model K, an effect of the knot variables measured on boards was tested:

- knot inclination (β_m),
- knot diameter (dk_m),
- knot depth (Δr_m) and
- relative knot depth (kd_m).

The model parameters were estimated by maximising the logarithm $\ln(L)$ of the likelihood function

$$L = \prod_{k=1}^n \left[q_k^{X_k} \cdot (1 - q_k)^{1 - X_k} \right], \quad \text{Equation 9}$$

using the LOGISTIC procedure in the SAS 8.2 software (SAS institute, Cary, USA). In Equation 9, it was $X_k = 1$ if knot k was not linked to the red heart, otherwise $X_k = 0$.

Fifty-eight of 60 boards were included in the analysis. Two boards with dead branches were excluded since seals were not formed yet (trees number 31 and 47).

3.4.2 Results and discussion

3.4.2.1 Local deviation from the overall red heart shape

3.4.2.1.1 Results

To analyse the local red heart shape around knots (boards) in relation to the overall red heart shape between the felling cut and the crown base (discs), the deviation was calculated of the mean red heart radius of board zones ($d_{lowerZone}$, $d_{knotZoneIncl}$, $d_{knotZoneExcl}$ and $d_{upperZone}$) from the mean red heart radius of the nearest discs (section 3.4.1.1).

First, it was tested by a t-test⁴⁴ if the calculation of deviation was biased by the fact that some boards were situated in the middle between the nearest discs (position = 'middle') and others were situated close to one of the discs (position = 'close'). The test was not significant at the 5% level for any of the variables $d_{\text{lowerZone}}$, $d_{\text{knotZoneIncl}}$, $d_{\text{knotZoneExcl}}$ and $d_{\text{upperZone}}$. The same result was obtained for the relative deviation ($d_{\text{lowerZoneRel}}$, $d_{\text{knotZoneInclRel}}$, $d_{\text{knotZoneExclRel}}$ and $d_{\text{upperZoneRel}}$). Thus, boards were not distinguished by their position in the subsequent analysis.

Figure 19 shows for each board zone the scatter plot of deviation and mean height relative to the upper red heart end (on the left: $d_{\text{lowerZone}}$ vs. $h_{\text{moyZoneRel}}$; in the middle: $d_{\text{knotZoneIncl}}$, $d_{\text{knotZoneExcl}}$ vs. $h_{\text{moyZoneRel}}$; on the right: $d_{\text{upperZone}}$ vs. $h_{\text{moyZoneRel}}$). The deviations of all zones (lower zone, knot zone including/excluding the red heart in the knot and upper zone) increased close to the upper red heart end, where the highest values were found. Only the knot zone including the red heart in the knot showed comparably high values in the middle part of the overall red heart. The size (mean radius) of the overall red heart was taken into account by the relative deviation, which is plotted versus mean height relative to the upper red heart end in Figure 20 (on the left: $d_{\text{lowerZoneRel}}$ vs. $h_{\text{moyZoneRel}}$; in the middle: $d_{\text{knotZoneInclRel}}$, $d_{\text{knotZoneExclRel}}$ vs. $h_{\text{moyZoneRel}}$; on the right: $d_{\text{upperZoneRel}}$ vs. $h_{\text{moyZoneRel}}$). Below about 0.8 of height relative to the upper red heart end, the relative deviation of the lower zone, the knot zone excluding the red heart in the knot and the upper zone scattered about evenly around zero (horizontal line in Figure 20), and few elevated values were observed for the knot zone including the red heart in the knot. Above 0.8 of height relative to the upper red heart end, the increase in deviation observed in Figure 19 was even clearer for the relative deviation (Figure 20), since the overall red heart was small close to the upper red heart end owing to its spindle shape⁴⁵: the relative deviations $d_{\text{lowerZoneRel}}$, $d_{\text{knotZoneInclRel}}$, $d_{\text{knotZoneExclRel}}$ and $d_{\text{upperZoneRel}}$ were calculated as the quotient of $d_{\text{lowerZone}}$, $d_{\text{knotZoneIncl}}$, $d_{\text{knotZoneExcl}}$ and $d_{\text{upperZone}}$, and the mean radius of the overall red heart (discs), respectively.

⁴⁴ A t-test was used even though observations were not normally distributed; according to Saporta (1990) the t-test is robust in case of a sufficient number of observations (several multiples of ten) and stands up well against a change in the distribution of observations.

⁴⁵ The overall red heart shapes of the sample trees are illustrated in Figure 4 of Paper III.

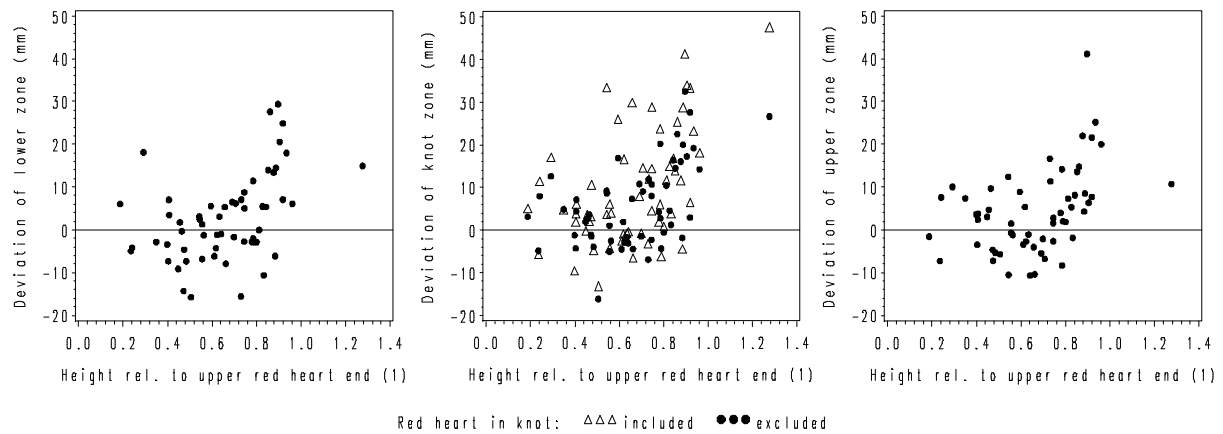


Figure 19. Deviation of the local red shape (board zones) from the overall red heart shape (discs); on the abscissa axes: mean height of board zones related to the height of the upper red heart end (tree number 47 had a second small red heart above the upper red heart end which was represented by one board); on the ordinate axes: deviation of lower zone (left), knot zone including/excluding the red heart in the knot (middle) and upper zone (right); (1) in axis legends stands for no unit; N = 58 boards.

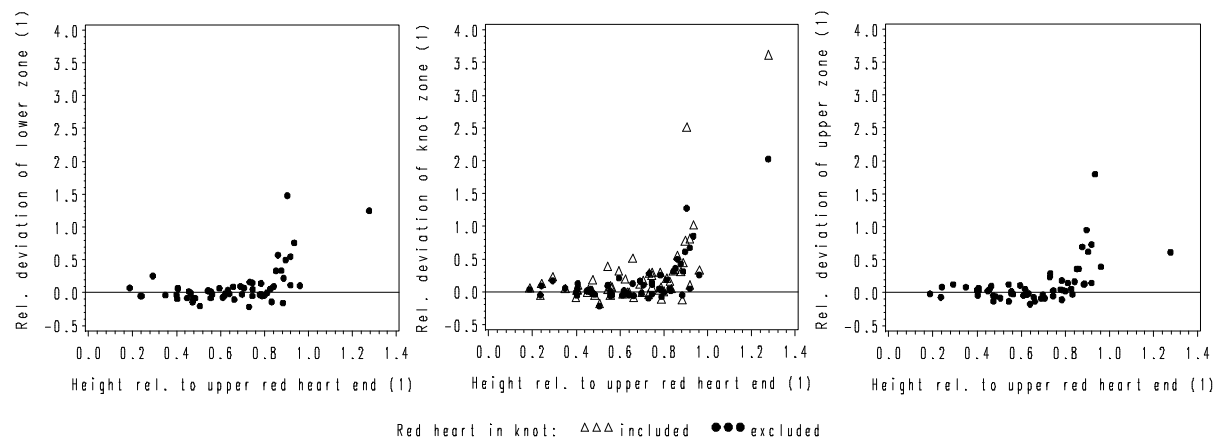


Figure 20. Relative deviation of the local red shape (board zones) from the overall red heart shape (discs); on the abscissa axes: mean height of board zones related to the height of the upper red heart end (tree number 47 had a second small red heart above the upper red heart end which was represented by one board); on the ordinate axes: relative deviation of lower zone (left), knot zone including/excluding the red heart in the knot (middle) and upper zone (right); (1) in axis legends stands for no unit; N = 58 boards.

The more homogenous red heart shape below 0.8 of height relative to the upper red heart end is described in the following (the height limit of 0.8 was determined visually using the plots of Figure 19 and Figure 20). Descriptive statistics of this part of the red heart are given in Table 5.

Table 5. Descriptive statistics of deviation ($d_{\text{lowerZone}}$, $d_{\text{knotZoneIncl}}$, $d_{\text{knotZoneExcl}}$ and $d_{\text{upperZone}}$) and relative deviation ($d_{\text{lowerZoneRel}}$, $d_{\text{knotZoneInclRel}}$, $d_{\text{knotZoneExclRel}}$ and $d_{\text{upperZoneRel}}$) of board zones located below 0.8 of height related to the upper red heart end ($h_{\text{moyZoneRel}} \leq 0.8$).

Variable	N	Mean (mm)	Median (mm)	Std (mm)	CV (%)	Min (mm)	Max (mm)	Prob > t H ₀ : Mean = 0
$d_{\text{lowerZone}}$	41	-0.7	-1.2	7.1	-1071	-15.8	18.2	0.5535
$d_{\text{knotZoneIncl}}$	41	6.0	3.8	10.9	182	-13.1	33.4	0.0011
$d_{\text{knotZoneExcl}}$	41	2.4	2.0	7.2	293	-16.1	20.3	0.0350
$d_{\text{upperZone}}$	41	0.7	-0.7	7.0	1024	-10.6	16.7	0.5352
		(1)	(1)	(1)	(%)	(1)	(1)	
$d_{\text{lowerZoneRel}}$	41	-0.003	-0.023	0.094	-3048	-0.213	0.256	0.8347
$d_{\text{knotZoneInclRel}}$	41	0.084	0.040	0.147	174	-0.175	0.515	0.0007
$d_{\text{knotZoneExclRel}}$	41	0.034	0.020	0.100	297	-0.216	0.282	0.0370
$d_{\text{upperZoneRel}}$	41	0.008	-0.010	0.101	1184	-0.173	0.296	0.5918

N: number of observations

Std: standard deviation

CV: variation coefficient

Min: minimum

Max: maximum

Prob: probability

t: t-value (Student)

H₀: null hypothesis

(1): no unit

Below 0.8 of height relative to the upper red heart end, the deviation of the lower zone, the knot zone excluding the red heart in the knot and the upper zone ($d_{\text{lowerZone}}$, $d_{\text{knotZoneExcl}}$ and $d_{\text{upperZone}}$) varied within a range of about -15 to 20 mm, which corresponded to a proportion of about -0.2 to 0.3 of the mean radius of the overall red heart ($d_{\text{lowerZoneRel}}$, $d_{\text{knotZoneExclRel}}$ and $d_{\text{upperZoneRel}}$; 41 of 58 boards, Table 5). The highest values were found in the knot zone including the red heart in the knot (Figure 19 and Figure 20), where the maximum deviation accounted for 33 mm or 0.5 (Table 5: $d_{\text{knotZoneIncl}}$ and $d_{\text{knotZoneInclRel}}$, respectively). The mean of deviations differed significantly from zero in the knot zone only (t-test⁴⁶, $\alpha = 0.05$; Table 5).

The question if deviation from the overall red heart shape was different below and above the knot was analysed using the difference between the deviation of the upper zone and the deviation of the lower zone; the difference was calculated for each board ($\Delta d_{\text{upperZoneLowerZone}}$; section 3.4.1.1). The scatter plot of this variable versus the mean height relative to the upper red heart end ($h_{\text{moyZoneRel}}$) is given in Figure 21 (on the left). This figure also shows the scatter plot of the deviation of the upper zone versus the deviation of the lower zone (on the right: $d_{\text{upperZone}}$ vs. $d_{\text{lowerZone}}$). The corresponding scatter plots of the relative deviation are given in Figure 22 (on the left: $\Delta d_{\text{upperZoneLowerZoneRel}}$ vs. $h_{\text{moyZoneRel}}$; on the right: $d_{\text{upperZoneRel}}$ vs. $d_{\text{lowerZoneRel}}$). Referring to Figure 21, the difference between upper zone and lower zone ranged between about ± 15 mm (with one exception), and there was no clear tendency with increasing/decreasing height relative to the upper red heart end. Furthermore, the deviations of lower

⁴⁶ See footnote 44.

zone and upper zone were clearly correlated (coefficient according to Pearson: $r = 0.63$, $N = 58$). The relative difference between upper zone and lower zone (Figure 22) scattered between about ± 0.2 below about 0.8 of height relative to the upper red heart end (with one exception). Above this height the relative difference increased in absolute terms (there were higher, positive values and smaller, negative values), since the overall red heart was small close to the upper red heart end (see above). Correlation between the relative deviations of upper zone and lower zone accounted for $r = 0.70$ (Pearson, $N = 58$). Altogether, deviation and relative deviation did not differ distinctly between upper zone and lower zone, apart from few single values of the relative deviation (Figure 22) which rather indicate small overall red heart than difference between upper zone and lower zone. The results of a t-test confirmed this observation for all boards analysed: there was no significant difference between $d_{\text{upperZone}}$ and $d_{\text{lowerZone}}$ ($p = 0.1733$) or between $d_{\text{upperZoneRel}}$ and $d_{\text{lowerZoneRel}}$ ($p = 0.3558$; paired t-test⁴⁷, $\alpha = 0.05$, $N = 58$).

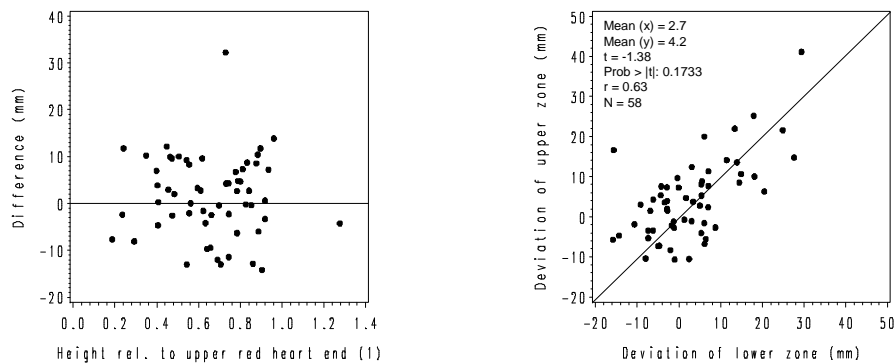


Figure 21. Deviation of the local red heart shape from the overall red heart shape below and above the knot; on the left: scatter plot of the difference between the deviations of upper zone and lower zone, and the height relative to the upper red heart end (tree number 47 had a second small red heart above the upper red heart end which was represented by one board); on the right: scatter plot of the deviations of upper zone and lower zone, the bisector ($y = x$) of the coordinate axes is given as auxiliary line; (1) in axis legend stands for no unit; $N = 58$ boards.

⁴⁷ See footnote 44.

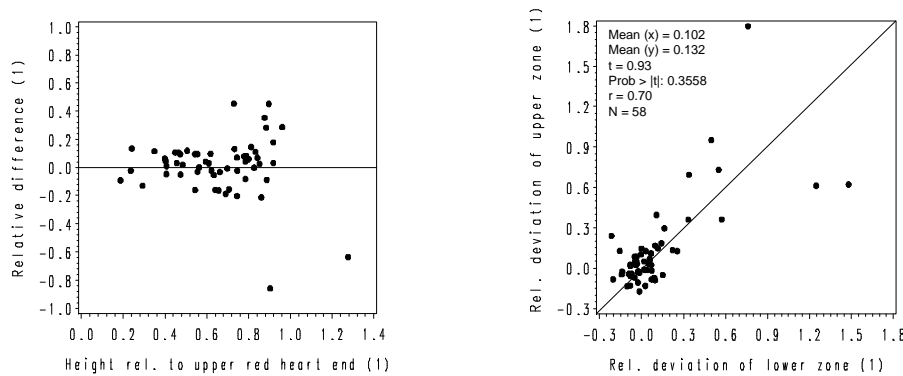


Figure 22. Relative deviation of the local red heart shape from the overall red heart shape below and above the knot; on the left: scatter plot of the difference between the relative deviations of upper zone and lower zone, and the height relative to the upper red heart end (tree number 47 had a second small red heart above the upper red heart end which was represented by one board); on the right: scatter plot of the relative deviations of upper zone and lower zone, the bisector ($y = x$) of the coordinate axes is given as auxiliary line; (1) in axis legends stands for no unit; $N = 58$ boards.

With respect to methodology, possible influences of other knots, having different radial orientation (azimuth) than the knot analysed, may have been limited by determining the local red heart shape in one longitudinal plane (board surface related to angular disc sections, Figure 8)⁴⁸. However, the mean red heart radius of the entire discs (and not of angular disc sections) was used to quantify the overall red heart shape (section 3.3). Thus, it was verified that results about deviation from the overall red heart shape, based on the mean red heart radius of angular disc sections (as presented), did not lead to different conclusions (section 3.4.2.1.3 below) than those based on the mean red heart radius of the entire discs (calculated from 360 radii; presented in Annex section 8.1.4).

3.4.2.1.2 Discussion

Close to the upper red heart end, relatively high deviation and relative deviation from the overall red heart shape was found (Figure 19 and Figure 20, respectively). One reason for this result may be that close to the upper red heart end there may be less interference of the local red heart shape analysed by other red heart formation zones: hypothesising that red heart can develop downwards in the stem (Keller 1961), there were no red heart zones originating from higher stem parts. On the contrary, in the middle parts of the overall red heart, deviation from the overall red heart shape around knots may be overlaid by other red heart formation zones to a larger extent. Additionally, there was a numeric effect which emphasised this result with respect to the relative deviation (Figure 20), as described above (small overall red heart owing to its spindle shape). Similar relationships might have occurred close to the lower red heart end, but boards were not sampled there.

⁴⁸ Furthermore, only one larger knot with a minimum seal length of 50 mm had to occur per board (section 2.2).

In the study by Krempf and Mark (1962) and in Paper I (trees of group 1), local red heart bulges towards branch scars/knots were observed. In the present analysis, which was based on another group of trees (group 2), this observation was confirmed. Additionally, the location of bulges in stem-axial direction was specified: bulges occurred particularly in the knot zone including the red heart in the knot and above 0.8 of height relative to the upper red heart end. Outside these parts of the red heart, the mean deviation and the mean relative deviation between local and overall red heart shape were not significantly different from zero ($d_{\text{upperZone}}$, $d_{\text{lowerZone}}$, $d_{\text{upperZoneRel}}$ and $d_{\text{lowerZoneRel}}$ in Table 5). Furthermore, there was no significant difference between the deviation of upper zone and lower zone. However, these results were only valid for the red heart shape close to the knot (upper zone and lower zone were located just above the zone of branch excision and occlusion, and just below the junction of the piths of knot and stem, respectively; section 2.2). Extended bulges, and differences in stem-axial direction occurring further away from the knot, may not have been detected.

Despite this limitation, one may hypothesise that there is no significant bulging of the overall red heart shape below and above the knot (disregarding the knot zone itself and the upper red heart end). However, standard deviation of the deviations of upper zone and lower zone accounted for about 0.1 of the mean radius of the overall red heart with a range of about -0.2 to 0.3 ($d_{\text{upperZoneRel}}$ and $d_{\text{lowerZoneRel}}$ in Table 5). In the present study, this variability was detected between longitudinal sections (boards) of different stem height and radial orientation; it may be a consequence of variability in stem-radial direction. Thus, further analyses may better explain this variability by analysing the red heart shape on cross-sections: the red heart shape on cross-sections is usually not circular, but appears cloudy and composed of several formation zones. This may lead to variability between the red heart shape of longitudinal sections. The red heart shape in stem-radial direction may be related to knottiness as illustrated in Figure 11, and its course along the stem-axis to spiral grain as reported and illustrated by Zycha (1948), for instance.

3.4.2.1.3 Conclusion

Deviation of the local red heart shape from the overall red heart shape, i.e. local bulging of the red heart towards the bark, was analysed on longitudinal sections (boards) passing through the piths of knot and stem. Results contributed to answering of question *Q6* asked in section 1.3.

Q6: How does the overall red heart shape vary close to external traits?

The results showed that

- deviation around knots was rather low in stem-axial direction, apart from the upper red heart end and the knot zone itself;
- if there is variation in stem-axial direction, it will occur below and above the boards analysed; that is between discs where, however, variation appears mainly in stem-radial direction (apart from discs very close to knots; analysis I);

- beyond the overall red heart shape, variability of red heart shape seems mainly due to variation in stem-radial direction; the latter may be related to the position (height and azimuth) of knots and spiral grain, for instance.

The subsequent section 3.4.2.2 takes account of the red heart in the knot zone. Among other things the occurrence of a link between knot and central red heart is estimated from knot variables and branch scars.

3.4.2.2 Geometric relationships between branch scars, knots and red heart

3.4.2.2.1 Relationships between branch scars and knots

3.4.2.2.1.1 Results

To evaluate the geometric relationships between branch scars and knots, the scatter plots of estimated and measured values of the knot variables inclination, diameter, depth and relative depth are given in Figure 23, Figure 24, Figure 25 and Figure 26, respectively. Referring to section 3.4.1.2, the results of calculation methods a (ignoring the thickness of buckles), b (taking account of the buckle thickness) and c (using only measured variables, but no estimated variables in the calculations in order to identify possible sources of imprecision) are given for each knot variable. Furthermore, branch scars with buckles are identified in the plots to observe differences between calculation methods a and b. Examples of branch scars/knots with very high differences between estimated and measured values were selected in the plots, and their characteristics are illustrated in Figure 27.

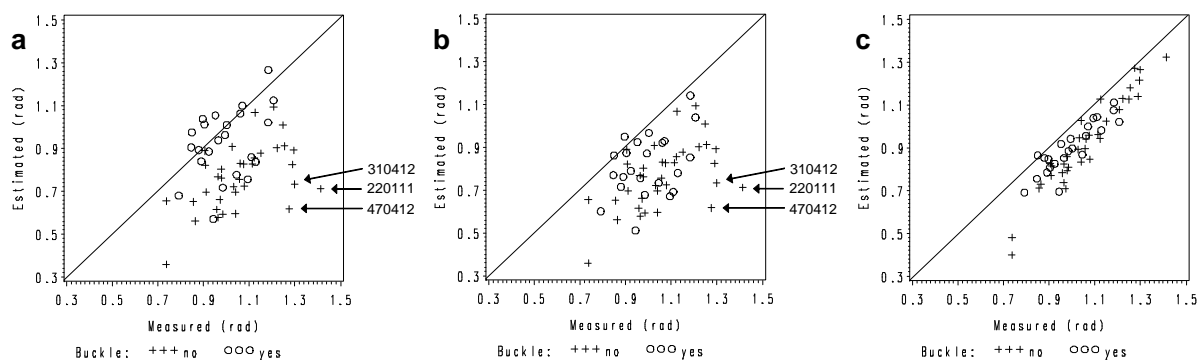


Figure 23. Knot inclination (β): scatter plots of estimated and measured values for calculation methods a (ignoring the thickness of buckles), b (taking account of the buckle thickness) and c (using measured variables only); the bisector ($y = x$) of the coordinate axes is given as auxiliary line; selection of examples (branch scar/knot numbers) with very high differences between estimated and measured values; $N = 58$ knots including partly occluded knots.

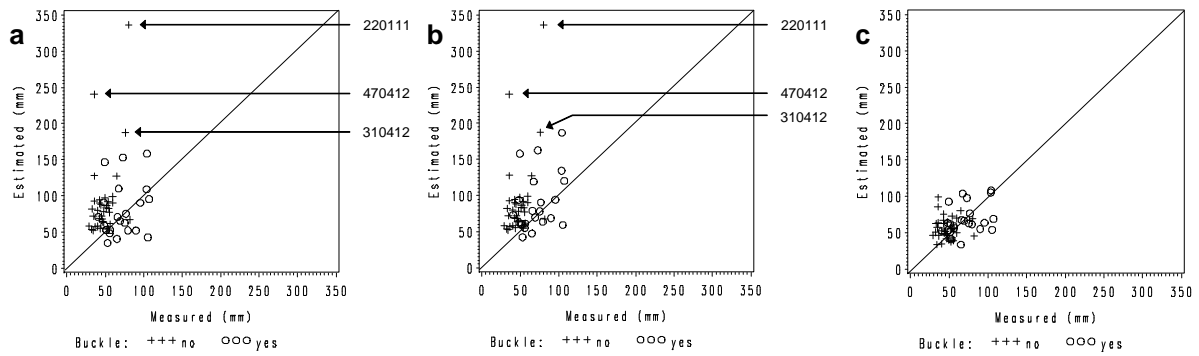


Figure 24. Knot diameter (dk): scatter plots of estimated and measured values for calculation methods a (ignoring the thickness of buckles), b (taking account of the buckle thickness) and c (using measured variables only); the bisector ($y = x$) of the coordinate axes is given as auxiliary line; selection of examples (branch scar/knot numbers) with very high differences between estimated and measured values; $N = 58$ knots including partly occluded knots.

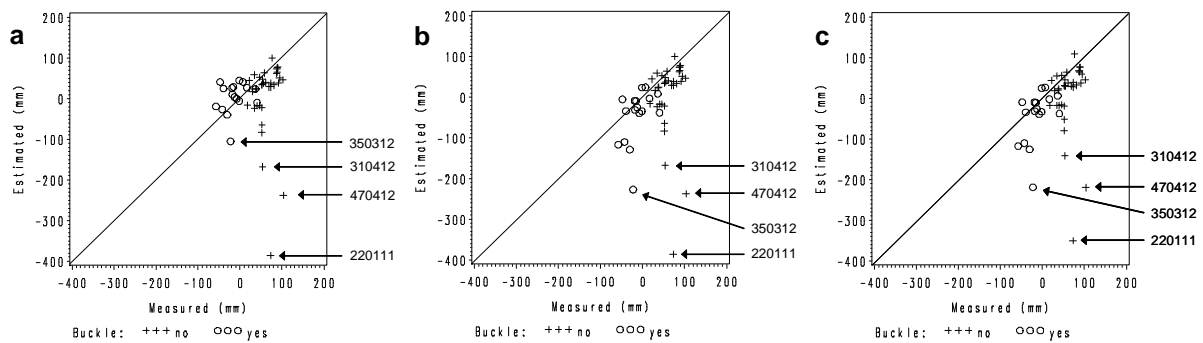


Figure 25. Knot depth (Δr): scatter plots of estimated and measured values for calculation methods a (ignoring the thickness of buckles), b (taking account of the buckle thickness) and c (using measured variables only); the bisector ($y = x$) of the coordinate axes is given as auxiliary line; selection of examples (branch scar/knot numbers) with very high differences between estimated and measured values; $N = 52$ knots excluding partly occluded knots.

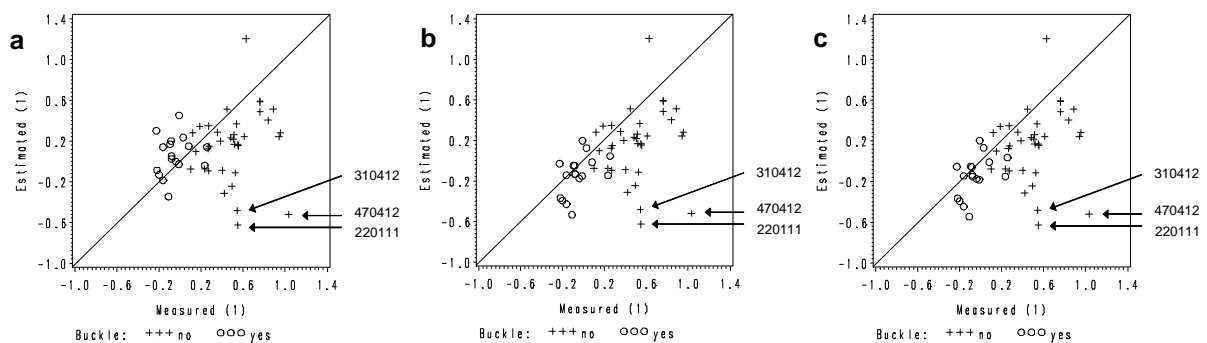


Figure 26. Relative knot depth (kd): scatter plots of estimated and measured values for calculation methods a (ignoring the thickness of buckles), b (taking account of the buckle thickness) and c (using measured variables only); the bisector ($y = x$) of the coordinate axes is given as auxiliary line; selection of examples (branch scar/knot numbers) with very high differences between estimated and measured values; (1) in axis legends stands for no unit; $N = 52$ knots excluding partly occluded knots.

Figure 23 shows that knot inclination was underestimated in most cases (plots a, b and c). Heterogeneity within the point cloud of plot a (calculation method ignoring the thickness of buckles) was reduced by taking the buckle thickness into account (plot b). This can be observed by comparing the positions of branch scars/knots with buckles in the respective point clouds. Correlation between estimated and measured values was clearly stronger if the measured values of knot radius (rk_m) were used in Equation 4 instead of the estimated values (rk ; plot c compared to plots a and b). The results suggest correcting underestimation, e.g. by introducing a correction factor in Equation 4, and improving the estimation method of the knot radius. Estimation of the knot radius was based on the shape of the seal (ratio of ls and ws in Equation 3); the seal shape may vary depending on factors like the real knot shape (curved, etc.) and the way of branch excision, which are difficult to take into account.

With respect to the knot diameter (Figure 24), results of calculation methods a (ignoring the thickness of buckles) and b (taking account of the thickness of buckles) were very similar. Very high differences between estimated and measured values were eliminated by using the measured values of knot inclination (β_m) in Equation 5 instead of the estimated values (β ; plot c compared to plots a and b). Precision may therefore be increased by improving the estimation methods of rk and β as stated above. Figure 25 indicates that differences between estimated and measured values of knot depth were slightly reduced by taking buckles into account (plot b compared to plot a). Compared with this, results given in plots b and c were very similar; using the approximation $ro = \frac{do_m}{2}$ in Equation 6 seemed not to affect the precision of estimation. The latter also applied to the estimation of the relative knot depth (Figure 26): the results given in plots b and c were very similar. Comparing plots a and b (Figure 26), correlation between estimated and measured values was increased by taking the buckle thickness into account (the position of branch scars/knots with buckles changes between the respective point clouds). Furthermore, plot b indicates that the relative knot depth was underestimated in most cases, which may be reduced by introducing a correction factor in Equation 7, for instance.

Examples of branch scars/knots with very high differences between estimated and measured values are illustrated in Figure 27. Knot number 220111 had the highest knot inclination of all knots analysed (Figure 23), and the upper part of the knot run almost in parallel to the bark. Correspondingly, the seal of the branch scar was very extended in stem-axial direction ($ls \gg ws$, Figure 27), which resulted in underestimation of β , Δr and kd (Equation 4/Figure 23, Equation 6/Figure 25 and Equation 7/Figure 26, respectively), and in overestimation of dk (Equation 5/Figure 24). Similarly, extended seals may be the reason for the underestimation of β , Δr and kd , and for the overestimation of dk , of knots number 470412 and 310412. However, in these cases extended seal shapes may result from interference of the occlusion process by bark inclusions (Figure 27). Underestimation of Δr of knot number 350312 may be related to its relatively thick buckle of $bt = 80$ mm (maximum of $bt = 89$ mm, Equation 6), since the difference between estimated and measured values was smaller for calculation

method a (ignoring the thickness of buckles) than for method b (taking account of the buckle thickness; Figure 25).



Figure 27. Examples of knots with very high differences between estimated and measured values, which were identified in Figure 23, Figure 24, Figure 25 and Figure 26; an example of a knot with very good correspondence of estimated and measured values is given as a reference; the length of the black line in each knot image equals 10 cm.

3.4.2.2.1.2 Discussion

In literature, relationships between branch scars and knots of beech trees were analysed by Mayer-Wegelin (1929), Erteld and Achterberg (1954) and Schulz (1961). A calculation method of knot inclination is not given in the studies by these authors. Furthermore, the relationship reported between knot inclination and tree height seems not clear comparing results of Mayer-Wegelin (1929) and Erteld and Achterberg (1954). Mayer-Wegelin (1929) reports knot diameter to be mainly dependent on seal width. However, seal width increases with radial growth while the knot diameter is constant. Correspondingly, Erteld and Achterberg (1954) found a stronger correlation of knot diameter with seal length (which is constant at increasing stem radius as well), than with seal width. The present study showed that this relationship depends on knot inclination [Figure 17; correlation (Pearson) between dk_m and ls : $r = 0.39$, $p = 0.0028$, $N = 58$; correlation between dk_m and dk (calculated from ls and β_m , Equation 5): $r = 0.36$, $p = 0.0056$, $N = 58$]. With respect to knot depth, negative correlation with seal length and moustache length is reported (Mayer-Wegelin 1929; Erteld and Achterberg 1954)⁴⁹. This is

⁴⁹ Erteld and Achterberg (1954) also analysed the relationship between knot depth and angle of the moustache, which was not determined in the present study. Among the variables seal length, moustache length and moustache angle, correlation between moustache length and knot depth was strongest in the study by these authors.

assumed to be related to stretching of the bark and fading of the lower moustache ends, which would lead to a decrease in moustache length (Mayer-Wegelin 1929). However, as a rule the lower moustache ends indicate the height of the junction of the piths of knot and stem (Burschel and Huss 1997), so that constant moustache height after branch excision can be hypothesised. Negative correlation between knot depth and the lengths of seal and moustache (Mayer-Wegelin 1929; Erteld and Achterberg 1954) may be an effect of tree height: knot depth decreases with tree height (Burschel and Huss 1997), and larger branches with longer seals and moustaches are usually more frequent in the upper stem parts. In the present study, the knot depth was calculated independently of tree height, based on the estimate function of Schulz (1961) which could also be deduced from the geometric relationships (Figure 17). The author reports the difference between estimated and measured values of knot depth to be less than 3 cm for 15 out of 19 knots analysed, most of which were located very deep under the stem surface (10 – 20 cm). In the present study, the precision of the estimation of knot depth according to Schulz (1961) was specified with respect to more recently occluded knots, by taking buckles into account in the estimation of knot radius (Equation 3, Equation 6, Figure 17). Since the knot radius was used to calculate other knot variables, further studies should continue to improve the estimation of this variable, by analysing relationships between pith location and stem shape, for instance.

3.4.2.2.2 Relationships of branch scars and knots to the red heart

3.4.2.2.2.1 Results

To evaluate the relationships of branch scars and knots to the red heart, the probability of each knot of its being not linked to the red heart (link = ‘no’) was estimated from “mechanistic” variables of branch scars (model S) and from knot variables measured on boards (model K).

Model S used the “mechanistic” variables *mec1* and *mec2* (with no intercept). The resulting probabilities are given in Figure 28: the two groups of knots with link to the red heart (link = ‘yes’) and with no link to the red heart (link = ‘no’) were distinguished by probabilities below and above about 0.5, respectively. However, there were 4 knots with no link to the red heart, and 5 knots with link to the red heart, both of which were clearly misclassified by the model (probabilities below 0.4 and above 0.6, respectively). Parameters of “mechanistic” variables were strongly correlated (Table 6), since they were based on the same measured variables of branch scars (section 3.4.1.2); using the geometric relationships between branch scars, knots and red heart, the variables *mec1* and *mec2* were developed in Paper II to reflect the hypotheses that red heart initiation changes with the inclination and/or diameter of a dead branch/knot.

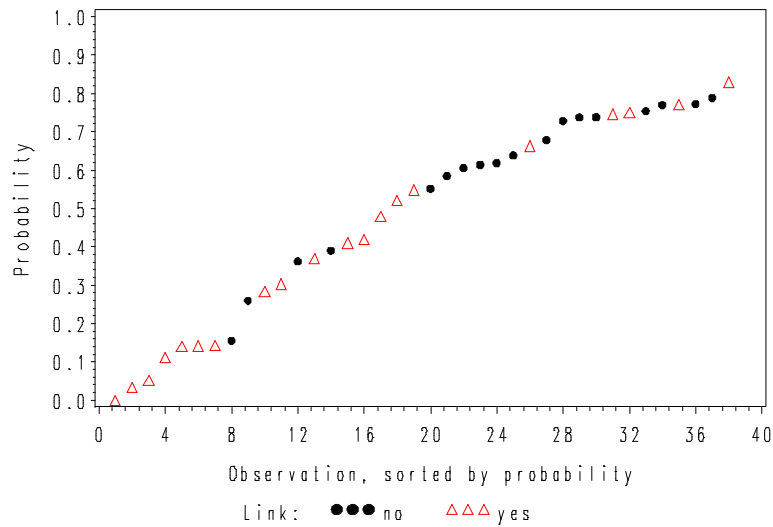


Figure 28. Model S: probability for each knot of its being not linked to red heart, estimated from “mechanistic” variables *mec1* and *mec2* of branch scars (no intercept); $N = 38$ knots including partly occluded knots.

Table 6. Model S: parameter estimates, standard error, significance test and correlation of parameter estimates.

Parameter (Variable)	Estimate	Standard error	Prob > χ^2	Correlation c_1
c_1 (<i>mec1</i>)	2.5383	1.0268	0.0134	1
c_2 (<i>mec2</i>)	-0.0156	0.00599	0.0095	-0.9573

Figure 29 shows the probabilities of no link to the red heart estimated from knot variables (model K). In accordance with model S, a significant effect of knot inclination (β_m) and knot diameter (dk_m) was found. Thirteen knots with a link to the red heart were clearly separated from the other knots by probabilities below 0.3. However, the probabilities of 7 knots with a link to the red heart were about evenly distributed among the probabilities of the knots with no such link. Parameter estimates and correlation matrix of model K are given in Table 7.

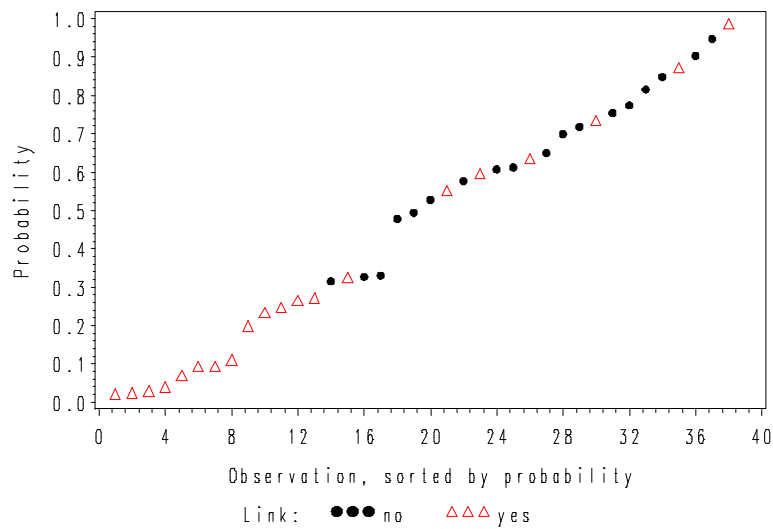


Figure 29. Model K: probability for each knot of its being not linked to red heart, estimated from the knot variables β_m and dk_m measured on boards; $N = 38$ knots including partly occluded knots.

Table 7. Model K: parameter estimates, standard error, significance test and correlation matrix of parameter estimates.

Parameter (Variable)	Estimate	Standard error	Prob > χ^2	Correlation matrix	
				c_0	c_3
c_0	9.1670	3.3827	0.0067	1	
c_3 (β_m)	-5.6221	2.8225	0.0464	-0.8989	1
c_4 (dk_m)	-0.0592	0.0253	0.0193	-0.5139	0.1055

3.4.2.2.2 Discussion

The results about the relationships of branch scars and knots to the red heart were based on a relatively coarse visual assessment (section 3.4.1.2), hypothesising that the penetration of oxygenous air results in a discoloured zone between knot necrosis and central red heart. Other imaginable ways of oxygen penetration were not taken into account, e.g. by necrotised bark inclusions or the knot pith, as illustrated in Figure 18 by the images at the bottom left and right, respectively. Furthermore, possible secondary discolouration caused by fungi (Volkert 1953) could not be identified by visual assessment. However, only one longitudinal plane (board) of each knot was analysed, and information was not easily accessible to perform a more detailed assessment in a systematic manner; the knot pith was not visible on all boards, for instance. Furthermore, more detailed analyses on other than the macroscopic level would not have been in the scope of the overall objective of the present study (section 1.3); in the present study resolution of measurements was high in comparison with existing approaches to quantify red heart occurrence and size (section 1.2.6). Also, statistic results of logistic regression were coarse owing to the small number of samples.

In literature, the probability of occurrence of discolouration in relation to variables of naturally and artificially pruned knots was analysed by Hein (2004) on beech trees aged 24 – 42 years. The author distinguishes discolouration within the stem and within the knot. In comparison with results of the present study it should be considered that the trees of Hein (2004) were probably too young to form a central red heart. For naturally pruned knots having a diameter range of 6 – 42 mm, no significant relationship was found between occurrence of discolouration and knot variables (diameter, duration of occlusion, years since termination of occlusion, height in the stem); the frequency of discolouration within the stem was 2.4%, within the knot 4.8%. Knots analysed in the present study (natural pruning) had larger diameters (range: 29 – 107 mm), and an effect of knot diameter and inclination on the probability of no link between knot and red heart was found for larger and more inclined knots in particular (the slopes of dk_m and β_m were negative, Table 7). For artificially pruned knots (diameter range: 2 – 59 mm), Hein (2004) found a significant effect of knot diameter on the probability of occurrence of discolouration in stem and knot, and knot inclination had such an effect on discolouration in the knot. However, using both knot diameter and inclination in a multiple logistic model, the effect of knot inclination was not significant in the study by this author; the author stresses correlation between knot inclination and diameter ($r = -0.54$, $\alpha \leq 0.0001$, $N = 149$, correlation coefficient according to Pearson), which was weaker in the present study ($r = 0.28$, $\alpha = 0.09$, $N = 38$; correlation between parameters c_3 and c_4 of knot diameter and inclination accounted for 0.11, Table 7)⁵⁰. The result of the present study that particularly larger knots had most likely a discoloured zone between knot and red heart may be explained by the protection zone in the bases of larger branches being incomplete (Aufsess von 1975; Aufsess von 1984). Furthermore, larger and more inclined branches (having a relatively small angle between the axes of branch and stem) seem more susceptible to rot (Mayer-Wegelin 1929; Erteld and Achterberg 1954), which may also facilitate oxygen penetration. Very inclined branches may be oxygen entrances due to cracking by freezing of accumulated water (at the upper side of the junction between branch and stem) and by wind-stress, which was stated similarly by Amann (2003) and by Knoke (2003a) for forks, respectively.

Furthermore, Hein (2004) found no significant relationship between duration of occlusion of artificially pruned knots and frequency of discolouration, but reports increasing frequency of discolouration with increasing time since the termination of knot occlusion. The latter would not have been expected assuming discolouration in Beech to be caused by the penetration of air through dead branches (Zycha 1948). Considering this, further studies on larger and naturally pruned knots may evaluate the effect of duration of occlusion on the probability of red heart initiation and occurrence. In Paper I, relationships between branch scars/knots and outer red heart formation zones were found for recently occluded knots (given by a small relative knot depth). Including interior/earlier formed red

⁵⁰ Signs of correlation coefficients: Hein (2004) measured knot inclination as the angle between the axes of knot and stem, while in the present study knot inclination was defined as the angle between knot axis and a radial (horizontal) axis (Figure 9).

heart zones into the analysis may be a starting point to further analyses about red heart formation over time (discussed in more detail in section 4.3 below).

3.4.2.2.3 Conclusion

In analysis I/Paper I geometric relationships were developed between branch scars, knots and red heart. In the present analysis IV the geometric relationships were tested using the assumption that red heart initiation by dead branches results in a discoloured zone between knot necrosis and central red heart, which was called “the link between knot and red heart”. Results contributed to answer question *Q2* asked in section 1.3.

Q2: How are these external traits (dead branches/branch scars) related to the red heart inside the stem?

The results showed that

- particularly larger and more inclined knots were most likely to be linked to the red heart, which was in accordance with results of Paper I;
- the probability of a link could also be estimated from external tree characteristics by using geometric relationships between branch scars and knots; a significant effect of “mechanistic” variables was found which reflected the effect of knot inclination and diameter as well;
- the choice was supported to use the “mechanistic” variables to conclude from branch scars to the red heart, since they were developed in Paper II for being simple variables which reflect basic “mechanisms” between branch scars, knots and red heart; the evaluation of the geometric relationships revealed the geometric model (Figure 17) being a simplification of the real stem and knot geometry, which is rather complex for tree species like Beech;
- the precision of the geometric relationships could be increased by taking the thickness of bark buckles into account, and other possible sources of imprecision were identified.

Further analyses may use this information to further develop the geometric relationships. They should include a higher number of branch scars/knots, and knots representing a diameter range below that of the knots analysed in the present study (including smaller and younger trees). Besides the assessment of red heart, geometric relationships between branch scars and knots may also be of interest in other applications in forestry to obtain more precise information about knottiness, in the course of quality assessment in standing trees or roundwood, for instance.

4 Synoptic discussion

The starting point of the present study was the problem that red heart occurrence and shape vary considerably within and between trees, so that it appears difficult to estimate and control the quality of beechwood with respect to red heartwood (section 1.1). Research questions, based on the state-of-the-art (section 1.2), were about relationships between external and dendrometric tree characteristics and the occurrence and shape of red heart (section 1.3). Results referring to the research questions were presented and discussed separately in section 3. In the present section, analyses I – IV are put together, and they are discussed in a synoptic manner. Discussion in context of literature includes methodological developments for measuring red heart shape in relation to external tree characteristics, interpretation of results with respect to red heart initiation and development, and new approaches to the modelling of red heart occurrence and shape.

4.1 Methodological developments

Paper I describes an *original method to obtain three-dimensional data about traits on the stem surface and red heart shape inside the stem*. The method was based on Constant et al. (2003); major development in the course of the present study was performed in cooperation with Constant and Mothe who are co-authors of both papers [Constant et al. (2003) and Paper I]. Development included the mapping of link between logs after felling (Figure 1 of Paper I; performed by Constant and Wernsdörfer) as an alternative to the mapping of the spatial position of logs on the standing tree. Development also included the standardised mapping of external traits by specific points (Figure 2 of Paper I; performed by Constant and Wernsdörfer). To visualise external traits and the stem surface, the software Bil3d was specially adapted by Mothe. Using this method, high resolution data for scientific analyses was provided. However, given this aim, measurements may be too time-consuming for application to serial use in forestry or wood industry. Similar to the AMEB device used in the present study (Figure 3), the stem surface can be mapped using terrestrial laser scanning (Thies et al. 2004). However, measurements of terrestrial scanners are not specific; thus far it appears difficult to extract information about dimensions of relatively small traits like branch scars from the outputted point clouds. (May be high resolution scans of single branch scars could provide this information. But compared with this, it seems easier to measure branch scars by few specific points, as it was done in Paper I.) For scientific analyses, the suitability of photogrammetry (Fürst and Nepveu 2005) may be analysed as an alternative to measure branch scars on standing trees.

The red heart shape inside logs was measured and visualised in three dimensions by Seeling and Becker (2002), using several cross-sections per log and eight red heart radii (oriented in cardinal directions) per cross-section. In the present study, methods of digital image analysis (Badia 2003;

Wernsdörfer et al. 2004) were further developed and applied to increase measurement resolution in stem-radial direction (inter-measurement angle of 1°; analyses I and IV). Development also included red heart measurement on longitudinal sections (inter-measurement step of 4 mm in stem-axial direction; analysis IV). However, image analysis was semi-automatic. Developing an automatic method to detect the outer red heart border may reduce time of image processing.

In the present study, the measurements of red heart were destructive, so that the limiting factor of resolution was the number of wood samples which had to be handled. Non-destructive methods like computer tomography do not have this limitation⁵¹. Studies on red heart detection in trees by computer tomography (Schwartz-Spornberger 1990; Isenmann 1999; Seeling et al. 1999) report that mainly differences in water (moisture) content between red heartwood and sapwood are detected. Compared with this, there are only small differences in density (Bauch and Koch 2001). The problem with red heart detection is that there seems an indirect relationship rather than a direct relationship (determinism) between water content and red heart occurrence (Sachsse 1967). However, information from computer tomography may be used in a modelling approach. An important aim of such approach would be to deduce information about red heart development over time, using repeated measurements in standing trees, for instance.

4.2 Interpretation of results with respect to red heart initiation and development

According to Zycha (1948), red heart formation is initiated by the penetration of oxygenous air into the stem core of older trees, where water content usually is low (gas content is high) compared to the sapwood. Torelli (1985) distinguishes an initial dehydration phase and a subsequent discolouration phase, dehydration in cross-section being more important for trees with shorter crowns and larger stems. Relationship with reduction of water content may be an interpretation of the effect of diameter at breast height at the dendrometric level in the model of red heart occurrence (the probability of red heart occurrence increased with diameter at breast height; Paper II). However, the condition of red heart formation with respect to water content in cross-section may have been similar for white trees and red heart trees of group 2: ranges of diameter at breast height of white trees and red heart trees were relatively small and they were largely overlapping (Table 3). Furthermore, crown variables (h_{cb} , h_{cbrel} , cl and cl_{rel}) had no clear effect on the probability at the dendrometric level in the model of red heart occurrence (analysis II). Also, there was no significant difference between crown variables of white trees and red heart trees (t-test; analysis II). However, between red heart trees, there may have been relationship between water content variation and red heart extent in stem-axial direction: in

⁵¹ Using computer tomography, slices (cross-section images) can be obtained with an inter-slice distance of 10 mm, for instance.

Paper III, the length of the overall red heart was related to the relative height of the crown base, where water content within stems is reported to be highest (Seeling and Sachsse 1992). Furthermore, in stem-radial direction, the width of the overall red heart shape was related to the diameter at breast height (Paper III). In this respect, it may be interesting to include the stem-axial and stem-radial distribution of water content into further analyses of red heart occurrence and shape.

Results of Paper II supported the assumption that red heart formation in trees of group 2 depended on the *possibility of penetration of oxygenous air by dead branches*; their effect on red heart initiation was estimated after occlusion based on branch scars. Keeping in mind the small number of sample trees, but the relatively high number of measurements per tree, results of Paper II and of analysis IV suggested the probability of red heart initiation being higher for larger and more inclined branches. Such branches may be particularly susceptible to oxygen penetration owing to incomplete protection zone (Aufsess von 1975; Aufsess von 1984), rot (Mayer-Wegelin 1929; Erteld and Achterberg 1954) and/or cracking at the ramification zone of branch and stem, the latter being assumed similarly for forks (Amann 2003; Knoke 2003a). The effect of knot depth on red heart initiation (Paper II) may reflect the conditions of red heart formation (section 1.2) changing with tree age and diameter: deeper knots had been possible oxygen entrances on younger and smaller trees, and recently occluded knots had been possible oxygen entrances on older and larger trees.

In Paper I, local red heart bulges towards some dead branches/branch scars were observed. Analysis IV suggested that bulging in stem-axial direction mainly occurs in the zone of the knot, and no significant difference in deviation (relative deviation) below and above the knot was found. Hypothesising that red heart formation started from traits with red heart bulges, the *direction of red heart development along the stem axis* may be upwards and downwards as well. In literature, discoloration is reported to form below and above artificial wounds (Dujesiefken and Liese 1990; Torelli et al. 1994), while it seems not clear whether the larger extent occurs below or above a wound. Altogether, these results supported the hypothesis that red heart can start at a middle stem height and develop to the stem base and up to the crown base (Zycha 1948), which was used in Paper III to estimate the overall red heart shape.

4.3 New approaches to the modelling of red heart occurrence and shape

Relationships between external traits and red heart were taken into account in the models by Knoke and Schulz Wenderoth (2001), von Büren (2002) and Knoke (2003a; 2003b). The authors report an effect of the presence of larger branch scars and damage areas (Büren von 2002), and of the number of dead branches and knobs/scars with minimum sizes of 6 cm and 9 cm, respectively (Knoke and Schulz Wenderoth 2001; Knoke 2003a; Knoke 2003b). Furthermore, an effect of the occurrence of forks

related to tree age is reported by Knoke (2003a; 2003b). In comparison, there was no clear effect of the trait “fork” in the model of Paper II. However, only a small number of trees was analysed, so that a possible effect of this trait should be kept in mind for further analysis. This is also suggested by Paper I, where a relationship between the ramification zone of a fork and red heart was observed in the particular case of tree B08. Based on results of Paper I, wounds and cracks to the bark were not taken into account in the models of the present study. On the one hand, an effect of wounds or cracks could not be excluded in general, since only 4 trees were analysed in Paper I, and taking account of results by von Büren (2002). On the other hand, the choice of focusing on dead branches/branch scars in modelling was based on a visual assessment of link between these traits and red heart (Paper I), while other models are not based on such an explorative analysis⁵². Results of the explorative analysis and those of the models of Paper II and analysis IV suggested an effect of larger dead branches/knots on red heart initiation. This was in accordance with results by Knoke and Schulz Wenderoth (2001), von Büren (2002) and Knoke (Knoke 2003a; Knoke 2003b). However, in the present study, this effect was specified: the model of Paper II made it possible to quantify the effect of individual branch scars on the probability of red heart occurrence. Moreover, estimation of this effect was based on hypothesised, basic “mechanisms” of red heart initiation (the probability of red heart initiation was hypothesised to change with inclination, diameter and/or depth of a dead branch/knot; Paper II). Also, relationships between the stem outside and inside were quantified using geometric relationships between branch scars, knots and red heart as developed in Paper I, which may reflect red heart initiation being related to the outside of the stem (penetration of oxygenous air).

The model of red heart occurrence was based on sample trees with a relatively small range of age and diameter at breast height, in order to focus on the effect of external traits (Paper II, section 2.2). However, there was an effect on the dendrometric level in this model. Similar to Paper II, an effect of diameter at breast height on the probability of occurrence of coloured heartwood is included in other models (Knoke and Schulz Wenderoth 2001; Börner 2002; Büren von 2002; Zell 2002; Mavric 2003; Knoke 2003a; Knoke 2003b; Schmidt 2004; Zell et al. 2004)⁵³; an effect of hd-ratio (analysis II) is included in the model by von Büren (2002). Keeping in mind the small number of sample trees, it may be interesting for further analyses that results of the present study about effects on the dendrometric level were found in the single stand situation presented.

Models to estimate the shape of the outer red heart boarder in continuity along the stem axis are reported by Knoke and Schulz Wenderoth (2001) and Knoke (2003a). The models are based on two observations of red heart diameter per tree, which are measured at the bottom and top ends of butt-logs

⁵² Larger damage areas did not occur on the trees of group 2, which were used to develop the models of Papers II and III.

⁵³ In the models by Knoke (2003a; 2003b), the ratio of diameter at breast height and tree age is included.

of different lengths. The authors use a second order parabola to describe the diameter and diameter percentage of red heart along the stem axis, so that the overall shape of a spindle is modelled. In the present study, the mean red heart radius was measured systematically about every 2 m of tree height between the felling cut and the crown base. Thus, more detailed information about variation of the overall red heart shape within individual trees was obtained. The overall red heart shape could be described closely, using an exponential function with a fourth order polynomial term (Paper III). Description included an extended middle section and a sharp decrease in mean red heart radius at the lower and upper red heart ends. These characteristics of the overall red heart shape were not taken into account in modelling thus far. However, another model structure using a more robust (but less flexible) function (e.g. arctangent function) was not already tested, since the model was difficult to adjust owing to the small number of sample trees. As a further new aspect, the model structure presented in Paper III reflected a hypothesis of red heart initiation and development in stem-axial and stem-radial direction (analysis I). The corresponding parameters height, length and width of the overall red heart shape could be estimated from tree traits and dendrometric variables, using the height of a possible red heart initiation point (branch scar), the relative height of the crown base and the diameter at breast height (Paper III). The explanatory variables diameter at breast height and relative height of the crown base are discussed in comparison with literature in Paper III. In this paper, the height of a particular branch scar (one per tree) as possible red heart initiation point was identified using a simple rule. To improve this, branch scars which are most likely red heart initiation points may be identified by the model of Paper II. However, thus far results of this model were coarse (“caricatured”) with respect to the effect of individual branch scars (as explained in Paper II). Furthermore, a possible effect of the trait “fork” may be included into the models (this effect was not clear thus far; see above): in the model of red heart occurrence (Paper II), a fork may be included as special case of a branch. In the model of overall red heart shape (Paper III), the fork height may contribute to estimate the parameter height of the overall red heart in the stem (a fork may be located about in the middle of spindle-shaped red heart, if the red heart in the branches of the fork is taken into account; section 3.3). This way, the models of Papers II and III may be linked to estimate red heart occurrence and, based on the results, to estimate the overall red heart shape. Starting from these reflections, perspectives of model validation and development are given in section 5 below.

In the chain of models by Schmidt (2004), the occurrence of red heartwood or splashing heartwood is estimated at the ends of butt-logs, using the diameter at breast height as independent variable. Based on this, the diameters of red heartwood and splashing heartwood are modelled. The author stresses correlation between the occurrences of coloured heartwood on cross-sections of the same tree. Compared with this, in the present study red heart occurrence was analysed between trees: white trees and red heart trees were distinguished (Paper II). Differentiation between heartwood types within trees (i.e. differentiation by stem height) may be taken into account, if other types of coloured heartwood

(splashing or abnormal heartwood) shall be included into the model; since splashing and abnormal heartwood can develop around (parts of) a central red heart. However, not only for this reason the formation processes of splashing and abnormal heartwood seem more complex, and related factors seem lesser known than those of red heartwood (Sachsse 1991; Seeling and Sachsse 1992). Thus, further research should be performed in this respect, before other types of coloured heartwood may be included into the model of Paper II.

Especially the formations of splashing and abnormal heartwood (Walter and Kucera 1991)⁵⁴, but also red heart formation may be related to the tree roots (Raunecker 1953). The trait “dead root” was not analysed in the present study, and it was not included into other approaches to the modelling of coloured heartwood in Beech (section 1.2.6). Thus, an explorative analysis, similar to Paper I, may reveal quantitative information about possible relationships between dead roots and red heart. However, there is the difficulty to access the root system for data acquisition, regarding both model development, and model application in particular.

In the present study, the outer red heart surface was focused, which is also the case for the other approaches to the modelling of coloured heartwood in Beech (section 1.2.6). However, based on results of Paper I, another approach might have been envisaged: knots located close to the bark were found to be linked to outer red heart formation zones, and there was indication that interior red heart formation zones were related to knots located deeper in the wood (Figure 3 of Paper I). This might have been a starting point to further analyses of red heart development in stem-radial direction/over time. Hypothesising that red heart formation zones are linked to dead branches/knots, development and successive overlaying of red heart zones might have been estimated based on individual probabilities of branch scars to initiate red heart formation (Paper II). This way, both red heart development and the outer red heart surface at a given stage of development might have been modelled. However, there were several difficulties which made this approach appearing too ambitious, so that it was not chosen in the present study: first, it has proven difficult to clearly distinguish red heart zones on longitudinal sections or cross-sections (an attempt was made in the course of analysis I), in order to measure their extent and position in the stem. Second, little is known about the dynamic of red heart formation, the progress of the discolouration and related factors which can be used in statistical modelling. Third, an adopted mathematical approach would have to be developed. Maybe a multidisciplinary project (physiology, botany, wood quality modelling) could come back to this approach.

⁵⁴ Coloured heartwood with splashing appearance according to Walter and Kucera (1991) corresponds most likely to splashing or abnormal heartwood according to Sachsse (1991).

In summary, the advantage and the original characteristics of the models of the present study were their level of detail with respect to red heart initiation and description of red heart shape. Furthermore, the models were well adapted to the observed variability of red heart occurrence and shape. The main limitation of the models was the small number of sample trees, so that results were only valid in the situation presented. In contrast, models reported in literature (section 1.2.6) are based on a high number of trees from various stands, but on few observations of coloured heartwood per trees. Thus, they have a much wider scope of application. However, they seem less adapted to account for the variability of occurrence and intra-tree shape of red heart.

5 Conclusions and perspectives

5.1 Conclusions

Based on results of the present study, the following conclusions can be drawn about relationships between external and dendrometric tree characteristics and the occurrence and shape of red heart in beech trees:

- (1) an ***original method based on log laser scanning and digital image analysis***, was developed and applied to 4 sample trees. The method, based on Constant et al. (2003), made it possible ***to obtain three dimensional data about traits on the stem surface and red heart shape inside the stem*** (Paper I). While the method was time consuming and destructive, its advantage was the close link between measurements on the stem outside and inside. The data measured was suitable to visualisation and geometric/statistic analysis. Using this method, relationships between tree external traits and red heart could be observed and characterised;
- (2) geometric relationships were developed between branch scars, knots and red heart (Paper I). Using these relationships, ***a simple hypothesis was deduced about basic “mechanisms” of red heart initiation depending on dead branch/knot dimensions*** (inclination, diameter and depth);
- (3) based on the hypothesis of red heart initiation, a type logistic regression model was developed which made it possible ***to quantify the effect of individual external traits (branch scars) on the probability of red heart occurrence*** (Paper II). Red heart initiation being related to the outside of the stem (penetration of oxygenous air), relationships between the stem outside and inside were quantified using geometric relationships. Using this model, a good discrimination of red heart trees and white trees was obtained (only 4 out of 31 trees were misclassified). However, the scope of the results was restricted owing to the small number of sample trees and the single stand situation presented;
- (4) the ***overall red heart shape in stem-axial direction*** between the felling cut and the crown base (mean red heart radius versus tree height) was closely described using an exponential function with a fourth order polynomial term (Paper III). Model structure was such that ***a simple hypothesis of red heart initiation and development in stem-axial and stem-radial direction was reflected***, using the parameters height, length and width of the red heart shape. Results indicated that, at a given stage of red heart development, these parameters could be estimated from external tree characteristics. Estimation was based on branch scars, the relative height of the crown base and the diameter at breast height. Remaining issues concerning the model structure (model function, local problems for predicted values close to zero; Paper III) could not be analysed owing to the small number of 16 sample trees. Application to an independent sample of 4 trees showed promising results;

- (5) *deviation of the local red heart shape around knots from the overall red heart shape* was limited to the zone of the knot and to the upper red heart end (analysis IV). Further analyses, aiming at modelling local variations of the overall red heart shape, should focus on variations in different stem-radial directions;
- (6) results of the *test of the geometric relationships* [point (2)] were coarse, but they basically supported the hypothesised relationships between branch scars, knots and red heart (analysis IV).

5.2 Perspectives

There are **two complementary analyses which can be envisaged in the short term**, based on data and results of the present study:

- (7) referring to point (4) in section 5.1, the model of the overall red heart shape could be developed for *estimating the number of annual rings with red heart at a given height in the stem*. Therefore, the number of annual rings containing red heart and white wood, respectively, was counted on discs of 16 red heart trees (group 2)⁵⁵. Using the number of annual rings containing red heart as target variable in the model of red heart shape (Paper III), promising results were already obtained in preliminary analyses;
- (8) referring to point (5) in section 5.1, the *red heart shape in different stem-radial directions could be analysed*. As examples, the red heart shapes of two trees (number 31 and 35, group 2) are illustrated in Figure 30 using matrices of grey values. In the matrices, each row represents one disc. Within a row, the grey value of a square represents the median length of the red heart radii (r_a ; section 2.2) within an angular disc section of 10° (36 angular section per disc), where black is the minimum length (zero) and white is the maximum length⁵⁶.

⁵⁵ Counting was in two directions per disc, which were the directions of the red heart radii with the median and maximum lengths.

⁵⁶ Calibration of grey values was based on the minimum and maximum of all median radii ($N = 684$) of the two trees displayed, so that grey values can be compared within and between trees. Calibration and visualisation was done using ImageJ 1.34s (Wayne Rasband, National Institutes of Health, USA).

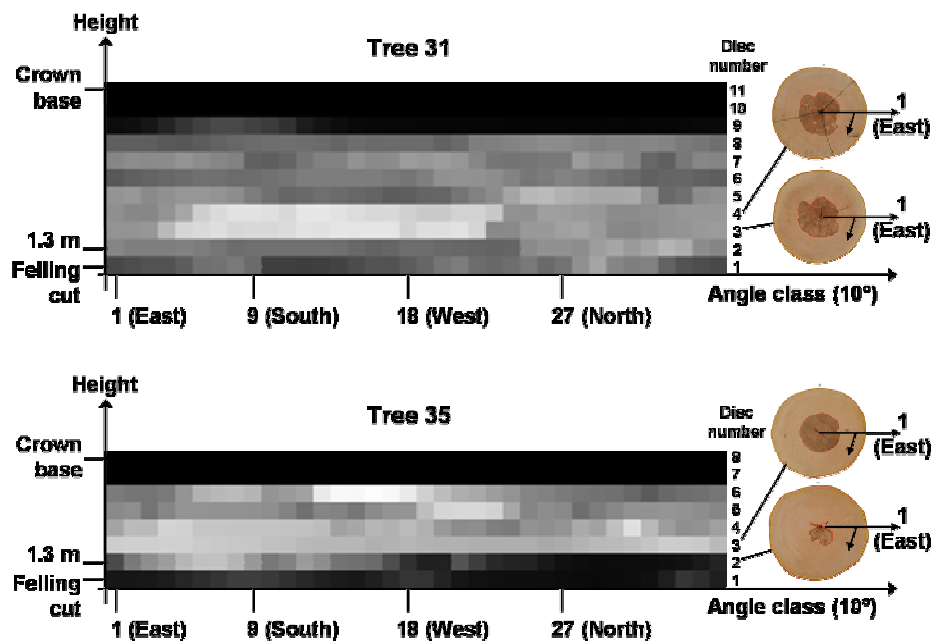


Figure 30. Examples (trees 31 and 35 of group 2) of variability of red heart shape illustrated as matrices of grey values: each row represents one disc, and each square represents the median length of the red heart radii within an angular disc section of 10° (36 angular sections per disc), where black is the minimum length (zero) and white is the maximum length; distance between matrix rows (discs) was approximately 2 m starting from 1.3 m of tree height towards the crown base.

Figure 30 suggests that the red heart shape in stem-radial direction can be similar within 2 m of tree height (discs 3 and 4 of tree 31; Figure 30), and more variable in other stem parts. There could also be very low variation in stem-radial direction at a given stem height (round red heart shape on disc 3 of tree 35), adjacent to higher variation in stem parts below and above.

The red heart shape in different stem-radial directions was measured for 20 red heart trees (4 trees of group 1 and 16 trees of group 2; section 2). In a first step, characteristic red heart shapes could be described geometrically in cross-section, including variation of these shapes along the stem axis. Subsequently, possible relationships to external and dendrometric tree characteristics may be analysed, using the position (height and azimuth) of branch scars, for instance (a complete map of branch scars on the stem surface is only available for the 4 trees of group 1).

Referring to points (3) and (4) in section 5.1, two statistic models were developed in the present study: the model to estimate red heart occurrence (Paper II) and the model to estimate the overall red heart shape (Paper III). The models were parameterised based on few sample trees (31 and 16 trees, respectively), since in the present study an approach of more detailed analyses on a smaller number of trees was chosen in comparison with existing approaches to the modelling of coloured heartwood in Beech (section 1.3; existing approaches focus on a high number of trees, but on few observations of coloured heartwood per tree). Consequently, model validation and development should be **the next**

step to continue the present study in the short term [this step and the analyses of points (7) and (8) can be performed independently]:

- (9) *the aim of model validation should be to provide robust models*, which are suitable to estimate red heart occurrence and shape in different silvicultural situations. In this respect, important considerations of sampling would be:
- to represent red heart trees of different stages of red heart development, and white reference trees;
 - to widen the range of tree age and diameter;
 - to represent different levels of spacing;
 - to test an effect of site characteristics (starting with basic site characteristics given in forest inventory data);
- (10) *development of the model of red heart occurrence* (Paper II) should focus on the effect on the dendrometric level and a possible effect of forks. With respect to the *model of red heart shape* (Paper III), remaining issues concerning the model structure (section 4.3, Paper III) should be taken into account. Development of both models should aim at linking the models, so that the output of the model of red heart occurrence can be used as input for the model of red heart shape.

Assuming successful validation and development of the models of the present study, **perspectives in the medium and long term** may include linking of the models to a growth model for Beech. As an example, linking to the growth model *Fagacées* (Dhôte 1998; Dhôte and Le Moguédec 2005) is discussed in the following. *Fagacées* is developed and used in the LERFoB-laboratory in Nancy.

Fagacées is a distance-independent tree model for Beech (*Fagus sylvatica* L.) in Northern France. In the framework of pure even-aged stands, various thinning regimes can be simulated. For given stand fertility, initial stand age and density, *Fagacées* simulates height and diameter growth of individual trees, using age-steps of 3 years⁵⁷. At each step, trees are described by their age, height, diameter and status (living, felled, dead or disappeared). Additional models for description of individual trees can be linked to *Fagacées* such that model output is provided a posteriori for a group of trees, which is

⁵⁷ From a statistical point of view it is realistic to simulate tree growth up to an age of about 200 years.

generated by *Fagacées* and which corresponds to specified criteria. For example, an estimation of stem profile was introduced (Vallet 2005) based on Trincado and von Gadow (1996)⁵⁸.

Similar to the stem profile, ***an estimation of red heart occurrence and shape at different steps of tree growth may be provided*** using the models of the present study (after model validation). However, an additional model of natural pruning would have to be developed and linked to *Fagacées* as well. The pruning model should provide dead branch/knot inclination, diameter, depth and status (dead branch or knot) to estimate red heart occurrence (Paper II). It should additionally provide dead branch/knot height to estimate the overall red heart shape (Paper III)⁵⁹. An estimation of red heart percentage at a given stem height may be provided using the models of overall red heart shape and stem taper.

Fagacées is developed under the platform of Computer-Aided Projection for Strategies In Silviculture (CAPSIS), which “aims at integrating several types of forest growth and dynamics models (...) and providing forest management tools to establish and compare different silvicultural scenarios” (De Coligny et al. 2002). Linking red heart models to *Fagacées* would come within this aim. Referring to the scope given in section 1.1, ***different silvicultural concepts may be tested and evaluated for optimising the yield (volume percentage) of white beechwood*** and other criteria (e.g. wood quality, monetary) of virtual logs, which may be defined by a rule of bucking. Downstream the forest-wood chain, using the red heart shape in virtual logs, the yield of white and red heart beechwood in simulated manufacturing of sliced or peeled veneer may be analysed using the model SidGeo (Mothe et al. 2002). Sawing simulation by Ohnesorge (2004) hypothesises cylindrical red heart shape and may be further developed using an approximation of the “real” red heart shape.

For forestry practice it seems important that the input variables of the models of red heart occurrence and shape [dead branch/knot dimensions and height, diameter at breast height (hd-ratio), relative height of the crown base] can be controlled (to a certain extent) by silvicultural treatment: for given site conditions, natural pruning and crown base height at a given stage of tree growth depend on how concurrence by neighbouring trees is managed in tending and thinning. The related live crown size controls diameter growth, and thus hd-ratio and duration of knot occlusion/knot depth. In this respect, beech trees growing under very wide spacing, which is suggested by recent silvicultural concepts (Bastien 1997; Wilhelm et al. 1999), are reported to contain relatively small red hearts up to target

⁵⁸ The model is also developed for Oak (*Quercus petraea* [Matt.] Liebl.). For this tree species, the stem profile (Dhôte et al. 2000) (crown base height, relative crown length and stem taper) and several tree compartments (bark thickness, sapwood/heartwood limit, knotty core and wood volume) can be reconstructed. Reconstruction is based on tree growth description (age, height, diameter and status) generated by the growth model, using an allometric procedure.

⁵⁹ The models of Papers II and III also used the diameter at breast height, which is generated by *Fagacées*. The model of Paper III used the relative height of the crown base, which may be estimated by the model of stem profile or the pruning model.

diameters of 60 cm [Klädtker (2002), Seeling and Becker (2002)]. ***An instrument to analyse possibilities of controlling red heart occurrence and shape by silvicultural treatment*** may be provided by linking the respective models to growth models. Coming back to the example of *Fagacées*, strategic decisions about silvicultural concepts (thinning sequence and intensity, number of crop trees, etc.) may be derived from simulations rather than decision tools to select trees to be cut in thinning and felling operations. Therefore, growth prediction of individual trees should be closely linked to estimation of red heart occurrence and shape, so that information about red heart development can be deduced (Knoke 2002; Knoke 2003a). The development of decision tools may take advantage of the models of the present study (after model validation), which provide complementary knowledge about relationships between external and dendrometric tree characteristics and the occurrence and shape of red heart.

In view of an application of the models of the present study in forestry, further development may also reveal if the effect of branch scars can be assessed by a simpler rule. Based on this, ***an assessment of red heart occurrence and shape in forestry inventory*** may be analysed, for instance. For this purpose, methods like terrestrial laser scanning are under development (Thies et al. 2003; Schütt et al. 2004). Among other things, development aims at detecting external traits like branch scars on standing trees to conclude on the inner wood quality. The possibility to use laser scanner measurements as input for the models of the present study would depend on the precision of scanner measurements (section 4.1) and the possible simplification of assessment of the effect of branch scars. Measurement of the input variables diameter at breast height (Papers II and III) and relative height of the crown base (Paper III) seems less difficult (Thies et al. 2004).

Developing an instrument to assess red heart occurrence and shape in standing trees may also be of interest for foresters and wood buyers to negotiate stumpage prices when beechwood is sold before felling. Most of the French beechwood is sold this way, while in Germany roundwood quality is usually assessed after felling and bucking. According to European Standards EN 1316-1 (CEN 1997c), the diameter percentage⁶⁰ of red heart on log cross-sections is used ***to determine roundwood quality with respect to the size of red heartwood*** (or splashing heartwood). However, to assess the volume percentage of red heartwood, the red heart shape between the ends of logs would have to be taken into account. Providing this information would also be useful in wood industry ***to determine patterns of sawing and veneering for optimising the yield of white beechwood***. In this respect, the model of red heart shape may be developed to using explicitly the red heart size on cross-sections of logs as an explanatory variable. In wood industry, red heart detection and measurement of red heart size on wood

⁶⁰ Ratio (%) of the diameter of the circle enclosing the red heart and the diameter of the cross-section, according to EN 1310 (CEN 1997b).

surfaces may be based on optoelectronic methods. The development of such methods is part of an applied research project under participation and coordination of the Fobawi-institute⁶¹.

⁶¹ CRAFT project “Innovation for Beech”, refer to <http://www.innobeech.uni-freiburg.de/objectives.htm> (visited 20 October 2005).

6 Summary

6.1 English summary

Beech (*Fagus sylvatica* L.) is a tree species that is capable of forming coloured heartwood (facultative formation of coloured heartwood), which is most frequently developed as red heart. The occurrence of large red hearts reduces the value of Beech roundwood considerably, since industrial processing, which aims at high added value, focuses on appearance products of light-coloured, “white” beechwood. Consequently, foresters are interested in estimating red heart occurrence and controlling its formation in standing trees. To approach this aim, statistical models are developed.

However, variability of red heart occurrence between trees and of red heart shape between and within trees is high. In stem-axial direction, red heart is often spindle-shaped. The spindle can reach from the felling cut to the crown base, but it can be located somewhere in between as well. In stem-radial direction, red heart does usually not coincide with the annual rings, but appears cloudy and composed of several formation zones. In contrast to existing models, the present study proposes a closer examination of this variability within trees. Therefore, a special focus was set on possible relationships between tree external traits and red heart occurrence and shape; external traits like dead branches are assumed to be possible initiation points of red heart formation. Furthermore, there is relationship between dendrometric variables like the diameter at breast height and red heart formation. In this context, the overall objective of the present study was to quantify relationships between external and dendrometric tree characteristics and the occurrence and shape of red heart in stem-axial and stem-radial direction. To reach this objective, four analyses were performed.

The study started with an explorative analysis (analysis I) of four trees with the aim of identifying and characterising possible relationships between tree external traits and red heart within the tree. Therefore, complete mapping of traits (dead branches, branch scars, wounds, cracks and fork) on the stem surface was performed as well as detailed description of the red heart shape. For the mapping of traits and the description of red heart shape, an original method of log laser scanning and digital image analysis was developed and applied. The method made it possible to reconstruct and visualise the external traits on the stem surface and the red heart shape inside the stem. Based on results of a visual assessment of link between external traits and red heart, a simple hypothesis of red heart initiation depending on the dimensions of dead branches/branch scars was developed, using geometric relationships between branch scars, knots and red heart. Furthermore, a simple hypothesis was developed of red heart development in stem-axial and stem-radial direction. The hypotheses were used in subsequent analyses to develop models of red heart occurrence and shape.

Using the hypothesis of red heart initiation, a type logistic regression model was developed (analysis II). The model made it possible to quantify the effect of individual external traits (branch scars) on the probability of red heart occurrence. Also, it included an effect on the dendrometric level

(diameter at breast height). Using this model, 15 out of 17 red heart trees and 12 out of 14 trees with no coloured heartwood (“white trees”) were correctly classified.

Based on the hypothesis of red heart development, the overall red heart shape was modelled at a given stage of development (analysis III). Therefore, the overall red heart shape was measured on 16 trees as the mean red heart radius versus tree height between the felling cut and the crown base (the inter-measurement distance was approximately 2 m). Using a non-linear model, the observed red heart shapes were closely described. Results of a predictive model at the standing tree level suggested that model parameters could be estimated from external traits and dendrometric variables (branch scars, relative height of the crown base and diameter at breast height). Application of the model to an independent sample of four trees (analysis I) showed promising results.

Finally, local deviations from the overall red heart shapes of the 16 trees were studied using boards cut from these trees (N = 58; analysis IV). The analysis focused on the local red heart shape in stem-axial direction below and above branch scars/knots. Results showed that deviation was limited to the zone of the knot and to the upper red heart end. Furthermore, the geometric relationships between branch scars, knots and red heart (developed in analysis I) were tested and further developed. Results were rather coarse, but they basically supported the hypothesis of red heart initiation developed in analysis I.

Perspectives were about further analyses in the short term, based on data and results of the present study: modelling of the overall red heart shape based on the number of annual rings containing red heart in about every 2 m of stem height; and analysing of the local red heart shape in different stem-radial directions. Furthermore, the importance of model validation was stressed. As perspectives in the medium and long term, linking of the models of red heart occurrence and shape (analyses II and III) to models of Beech growth and roundwood processing is discussed as well as application of the models in practice of forestry and wood industry.

6.2 French summary (Résumé)

Le Hêtre (*Fagus sylvatica* L.) est une essence qui forme facultativement un cœur coloré. Dans la plupart des cas, le cœur développé est un cœur rouge. La transformation industrielle favorise le bois clair du Hêtre, notamment pour les produits pour lesquels l’aspect est important. L’occurrence de cœurs rouges de tailles élevées diminue ainsi considérablement la valeur des bois ronds. Pour cette raison, les forestiers aimeraient pouvoir estimer l’occurrence du cœur rouge et contrôler sa formation dans l’arbre sur pied. En vue d’atteindre cet objectif, des modèles statistiques sont développés.

Cependant, la variabilité de l’occurrence du cœur rouge au niveau inter-arbre, et de sa forme au niveau inter- et intra-arbre est importante. Dans la direction longitudinale, le cœur rouge a souvent une forme de noyau, qui peut s’étendre de la coupe d’abattage jusqu’à la base du houppier, ou alors se trouver complètement inclus entre ces deux extrémités. Dans la direction radiale, souvent, le cœur rouge ne

suit pas les limites de cerne, mais il a une apparence « nuageuse », composée de plusieurs vagues de formation. Par rapport aux travaux existants dans la littérature, cette étude se propose de décrire de façon très précise la variabilité intra-arbre du cœur rouge (échantillonnage de haute résolution). Pour cela, un point important était les relations possibles entre les défauts apparents sur le tronc et l'occurrence et la forme du cœur rouge à l'intérieur de celui-ci ; des défauts tels que des branches mortes sont supposés être des points d'initiation possible de la formation du cœur rouge. De plus, un effet des variables dendrométriques telles que le diamètre à 1.3 m sur la présence du phénomène est reconnu. Dans ce contexte, l'objectif principal de cette étude était de quantifier des relations entre les défauts externes de l'arbre, des caractéristiques dendrométriques et l'occurrence et la forme du cœur rouge dans les directions longitudinale et radiale. Pour atteindre cet objectif, quatre analyses ont été menées.

Dans un premier temps, une analyse exploratoire (analyse I) réalisée de façon intensive à partir de quatre arbres avait pour objectif d'identifier et de caractériser des relations possibles entre les défauts externes et le cœur rouge au niveau intra-arbre. Pour ce faire, les défauts (branches mortes, cicatrices de branche, blessures, fentes et fourche) visibles sur l'écorce ont été cartographiés, et la forme locale du cœur rouge au voisinage des défauts a été décrite en détail ainsi que sa forme globale dans la direction longitudinale. La carte des défauts a été établie par un scanner optique à billon et la description du cœur rouge par analyse d'image sur des rondelles. A partir des résultats obtenus, une hypothèse simple sur l'initiation du cœur rouge a été développée basée sur des dimensions des branches mortes/cicatrices de branche, en utilisant des relations géométriques entre des cicatrices de branche, les nœuds correspondants et le cœur rouge. Une autre hypothèse simple portait sur le développement du cœur rouge dans les directions longitudinale et radiale. Ces hypothèses ont été utilisées dans les analyses suivantes pour développer des modèles d'occurrence et de forme du cœur rouge.

A partir de l'hypothèse portant sur l'initiation du cœur rouge, un modèle de type logistique a été développé (analyse II). Le modèle permettait de quantifier individuellement l'effet des défauts (cicatrices de branche) sur la probabilité d'occurrence du cœur rouge ; il incluait aussi un effet au niveau dendrométrique (diamètre à 1.3 m). En utilisant ce modèle, 15 parmi 17 hêtres avec un cœur rouge et 12 parmi 14 hêtres « blancs » (sans cœur coloré) ont été classés correctement.

La forme globale du cœur rouge à un stade de développement donné a été modélisée à partir de l'hypothèse sur le développement du cœur rouge (analyse III). Pour cela, le rayon moyen du cœur rouge a été mesuré sur 16 arbres, environ tous les deux mètres entre la coupe d'abattage et la base du houppier. Par un modèle non linéaire, la forme globale des cœurs rouges observés a pu être décrite avec une précision jugée plutôt satisfaisante. Les résultats d'une approche de modèle prédictif au niveau de l'arbre sur pied indiquaient que les paramètres du modèle pourraient être estimés à partir des défauts et des variables dendrométriques (cicatrices de branche, hauteur relative de la base du

houppier et diamètre à 1.3 m). L'application du modèle à l'échantillon indépendant portant sur les 4 arbres de l'analyse I donnait des résultats encourageants.

Enfin, l'analyse IV portait sur des déviations locales de la forme globale de 16 cœurs rouges. Plus particulièrement, la forme longitudinale du cœur rouge en dessous et au dessus des cicatrices de branche/nœuds a été analysée. Les résultats obtenus indiquaient que les déviations sont limitées à la zone du nœud et à l'extrémité du cœur rouge coté apical. De plus, les relations géométriques entre les cicatrices de branche, les nœuds et le cœur rouge (mises en place dans l'analyse I) ont été testées et développées. Les résultats étant assez grossiers, ils soulignaient cependant l'hypothèse sur l'initiation du cœur rouge développée dans l'analyse I.

En perspectives à court terme, les analyses suivantes peuvent être envisagées à partir des résultats de cette étude : la modélisation de la forme globale du cœur rouge à partir du nombre de cernes contenant du cœur rouge environ tous les deux mètres le long du tronc, et une analyse de la forme locale du cœur rouge dans des différentes directions radiales. En perspectives à plus long terme, les possibilités de lier les modèles de l'occurrence et de la forme du cœur rouge à des modèles de croissance ou de la transformation des bois ronds sont discutées, ainsi que l'application des modèles dans la pratique forestière et dans l'industrie du bois.

6.3 German summary (Zusammenfassung)

Die Buche (*Fagus sylvatica* L.) gehört zu den Baumarten, die fakultativ farbiges Kernholz ausbilden. Meist ist der Farbkern als so genannter Rotkern ausgeprägt. Das Vorkommen größerer Rotkerne führt bei dem Rundholz zu deutlichen Preisabschlägen, da im Hinblick auf eine industrielle Verarbeitung zu hochwertigen Produkten für den sichtbaren Bereich vor allem das helle, „weiße“ Buchenholz nachgefragt wird. Daher besteht in der Forstwirtschaft großes Interesse an Verfahren zur Abschätzung des Rotkernvorkommens und zur Steuerung der Rotkernentstehung im stehenden Baum. Um sich diesem Ziel anzunähern werden statistische Modelle entwickelt.

Jedoch variiert das Vorkommen des Rotkerns stark zwischen den Bäumen. Weiterhin weißt die Form des Rotkerns eine große Variabilität zwischen den Bäumen und innerhalb von Einzelbäumen auf. In stammaxialer Richtung verläuft der Rotkern häufig spindelförmig. Dabei kann er sich vom Fallschnitt bis zum Kronenansatz erstrecken, oder aber sich zwischen diesen Grenzen befinden. In stammradialer Richtung folgt der Rotkern in der Regel nicht dem Jahrringverlauf, sondern er besitzt häufig eine wolkige Form, die sich aus mehreren Bildungszonen zusammensetzt. Im Gegensatz zu bestehenden statistischen Modellen soll in der vorliegenden Untersuchung diese Variabilität des Rotkerns innerhalb von Einzelbäumen genauer analysiert und quantifiziert werden. Dabei wird besonderes Augenmerk auf mögliche Zusammenhänge zwischen äußeren Stammmerkmalen und dem Vorkommen und der Form des Rotkerns gelegt; denn es wird angenommen, dass äußere Stammmerkmale wie z.B. Totäste Ausgangspunkte der Rotkernbildung sein könnten. Des Weiteren stehen dendrometrische Variablen

wie z.B. der Brusthöhendurchmesser in Zusammenhang mit der Rotkernbildung. Vor diesem Hintergrund ist es das übergeordnete Ziel dieser Arbeit, Zusammenhänge zwischen äußeren Stammmerkmalen und dendrometrischen Variablen einerseits, und dem Vorkommen und der Form des Rotkerns andererseits, zu quantifizieren. Um dieses Ziel zu erreichen wurden vier Untersuchungen durchgeführt.

Das Ziel der ersten Untersuchung ist es, mögliche Zusammenhänge zwischen äußeren Stammmerkmalen und dem Rotkern zu identifizieren und zu charakterisieren. Im Rahmen dieser Zielsetzung wurde eine originäre Methode entwickelt und an vier Buchen getestet: Die Stammmerkmale (Totäste, Astnarben, Wunden, Risse und Zwiesel) sowie der Stammmantel wurden mittels Laser-scanning vermessen. Die Erfassung der Form des Rotkerns erfolgte an Stammscheiben mittels digitaler Bildanalyse. Anhand der gemessenen Daten konnten die Versuchsbäume dreidimensional rekonstruiert und visualisiert werden. Ausgehend von den Ergebnissen dieser Untersuchung wurden einfache Hypothesen abgeleitet, die in dem Folgenden für die Entwicklung von statistischen Modellen zur Abschätzung des Vorkommens und der Form des Rotkerns im stehenden Baum verwendet wurden: Es konnte eine einfache Hypothese über die Auslösung der Rotkernbildung in Zusammenhang mit Variablen von Totästen und Astnarben abgeleitet werden. Des Weiteren wurde eine einfache Hypothese hinsichtlich des Ausgangspunkts und der Entwicklung des Rotkerns in stamm-axialer und stamm-radialer Richtung aufgestellt.

Ausgehend von der Hypothese über die Auslösung der Rotkernbildung wurde ein logistisches Regressionsmodell entwickelt (Untersuchung II). Das Modell ermöglicht es, den Einfluss von äußeren Stammmerkmalen (Astnarben) auf das Vorkommen des Rotkerns einzeln zu schätzen. Des Weiteren wurde der Einfluss des Brusthöhendurchmessers auf die Rotkernwahrscheinlichkeit in dem Modell berücksichtigt. Unter Anwendung des Modells konnten 15 von 17 rotkernigen Buchen und 12 von 14 „weißen“ Buchen ohne Farbkernholz richtig klassifiziert werden.

Das Modell für die so genannte Grundform des Rotkerns (Untersuchung III) fußt auf der Hypothese über die Rotkernentwicklung in stammaxialer und stammradialer Richtung. Für die Parametrisierung des Modells wurde der mittlere Rotkernradius an 16 Bäumen gemessen, und zwar in Abständen von ungefähr 2 m vom Fällschnitt bis zum Kronenansatz. Der auf diese Weise ermittelte Verlauf des Rotkerns entlang der Stammachse konnte mittels eines nichtlinearen Modells genau beschrieben werden. Im Hinblick auf eine Prognose am stehenden Baum wurden die Modellparameter anhand von Stammmerkmalen und dendrometrischen Variablen (Astnarben, relative Kronenansatzhöhe und Brusthöhendurchmesser) geschätzt. Bei dieser Schätzung und bei der Anwendung des Modells auf einen unabhängigen Datensatz (vier Bäume aus der ersten Untersuchung) konnten viel versprechende Ergebnisse erzielt werden.

In der vierten Untersuchung wurden schließlich anhand von Längsschnitten lokale Abweichungen von der Rotkerngrundform im Bereich von Ästen quantitativ beschrieben. Aus den Ergebnissen geht hervor, dass die Abweichungen vor allem in unmittelbarem Bereich des untersuchten Astes und am

oberen Ende des Rotkerns auftreten. In dem zweiten Teil dieser Untersuchung wurden geometrische Zusammenhänge zwischen Astnarben, den entsprechenden Ästen und dem Rotkern (Untersuchung I) geprüft und weiterentwickelt. Auch wenn zum Teil grobe Ergebnisse erzielt wurden, so stützten sie doch die Hypothese über die Auslösung der Rotkernbildung.

Als kurzfristig mögliche Folgeuntersuchungen werden die Modellierung der Rotkerngrundform innerhalb des Jahrringprofils (Anzahl der Jahrringe mit Rotkern in verschiedenen Schafthöhen) und die Beschreibung und Modellierung der lokalen Rotkernform in stammradialer Richtung diskutiert. Weiterhin wird die Bedeutung der Modellvalidierung betont. Als mittel- bis langfristige Perspektiven werden eine Verbindung der vorgestellten, statistischen Rotkernmodelle mit einem Wachstumssimulator für Buche ebenso diskutiert wie die Anwendung der Modelle in der forst- und holzwirtschaftlichen Praxis.

7 References

- Albert L, Hofmann T, Németh ZI, Rétfalvi T, Koloszár J, Varga S and Csepregi I (2003) Radial variation of total phenol content in beech (*Fagus sylvatica* L.) wood with and without red heartwood. *Holz als Roh- und Werkstoff* 61:227-230
- Amann M (2003) Untersuchungen über Beziehungen zwischen dem Auftreten und der Ausprägung des Farbkerns bei der Buche (*Fagus sylvatica* L.) und verschiedenen baumindividuellen und bestandesbezogenen Merkmalen [Investigations about relationships between the occurrence and extent of coloured heartwood in beech (*Fagus sylvatica* L.) and different tree individual and stand related characteristics]. Diploma thesis, *Fachhochschule Rottenburg*, 167 pp
- Aufsess von H (1975) Über die Bildung einer Schutzsperre an der Astbasis von Laub- und Nadelbäumen und ihre Wirksamkeit gegen das Eindringen von Pilzen in das Kernholz lebender Bäume [The formation of a protection zone on the base of hardwood and softwood branches and its efficiency against fungi penetrating the heartwood of living trees]. *Forstwissenschaftliches Centralblatt* 94:140-152
- Aufsess von H (1984) Some examples of wood discolourations related to mechanisms for potential protection of living trees against fungal attack. *IAWA Bulletin* 5:133-138
- Badia MA (2003) Modélisation de la distribution du bois de tension dans une grume de peuplier à partir de l'empilement tridimensionnel des cernes [Modelling the distribution of tension wood in trunks of poplar trees based on the three-dimensional stack of annual rings]. Doctoral thesis, *Ecole Nationale du Génie Rural des Eaux et des Forêts ENGREF*, Nancy, 329 pp
- Bastien Y (1997) Pour l'éducation du Hêtre en futaie claire et mélangée [About the management of beech in open and mixed high-forest stands]. *Revue Forestière Française* 49:49-68
- Bauch J and Koch G (2001) Biologische und chemische Untersuchungen über Holzverfärbungen der Rotbuche (*Fagus sylvatica* [L.]) und Möglichkeiten vorbeugender Maßnahmen [Biological and chemical analyses about wood discolourations of Common beech (*Fagus sylvatica* [L.]) and possibilities of preventing measures]. Final Report, *Bundesforschungsanstalt für Forst- und Holzwirtschaft, Universität Hamburg*, 66 pp
- Baum S (2000) Abbau- und Ausbreitungsstrategien holzzeretzender und endophytischer Pilze in Buche und anderen Laubbäumen [Degradation and spreading strategies of wood decomposing and entophytic fungi in beech and other hardwoods]. Doctoral thesis, *Albert-Ludwigs-Universität Freiburg*, 147 pp
- Baum S and Bariska M (2002) Der falsche Kern: Buchenrotkern [The false heart: beech red heart]. *Holz-Zentralblatt* 128:633
- Baum S, Schwarze FWMR and Fink S (2000) Persistence of the gelatinous layer within altered tension-wood fibers of beech degraded by *Ustilina deusta*. *New Phytologist* 147:347-355
- Becker G, Seeling U and Wernsdörfer H (2005) Relations entre la sylviculture et la qualité du bois de Hêtre : l'expérience allemande [Relationship between silvicultural methods and Beech wood quality - the German experience]. *Revue Forestière Française* 57:227-238
- Börner M (1998) Zu Wachstum und Wachstumsreaktion der Rotbuche (*Fagus sylvatica* L.) nach Freistellung im fortgeschrittenen Alter [About growth and growth reaction of Common beech (*Fagus sylvatica* L.) after release at an advanced age]. *LINCOM Studien zur Forstwissenschaft* 03, München, 197 pp
- Börner M (2002) Zieldurchmesser und Rotkern bei der Buche [Target Diameter and Red Heart of European Beech]. *Forst und Holz* 57:123-128
- Bosshard HH (1967) Über die fakultative Farbkernbildung [On the Facultative Formation of Stained Heartwood]. *Holz als Roh- und Werkstoff* 25:409-416
- Bosshard HH (1974) Holzkunde [Wood science], Volume 2. *Birkhäuser*, Basel Stuttgart, 312 pp
- Buchholz E (1958) Kernbildung und Astreinigung [Heartwood formation and pruning]. *Holz-Zentralblatt* 84:372
- Büren von S (1998) Buchenrotkern: Erkennung, Verbreitung und wirtschaftliche Bedeutung [Red Heartwood Formation in Beech: Identification, Occurrence and Economic Importance]. *Schweizerische Zeitschrift für Forstwesen* 149:955-970

- Büren von S (2002) Der Farbkern der Buche (*Fagus sylvatica* L.) in der Schweiz nördlich der Alpen [Red Heartwood Formation in Beech: Identification, Occurrence and Economic Importance]. *Schweizerische Zeitschrift für Forstwesen, Supplement 86*, Zürich, 137 pp
- Burschel P and Huss J (1997) Grundriß des Waldbaus: ein Leitfaden für Studium und Praxis [Outline of silviculture: a guide for study and practice]. *Pareys Studentexte 49*, Berlin, 487 pp
- CEN (1997a) European Standard EN 844, Round and sawn timber, Terminology - Part 8: Terms relating to features of round timber. *European Committee for Standardization*, Brussels, 12 pp
- CEN (1997b) European Standard EN 1310, Round and sawn timber - Method of measurement of features. *European Committee for Standardization*, Brussels, 13 pp
- CEN (1997c) European standard EN 1316, Hardwood round timber, Qualitative classification - Part 1: Oak and beech. *European Committee for Standardization*, Brussels, 6 pp
- Constant T, Mothe F, Badia MA and Saint-André L (2003) How to relate the standing tree shape to internal wood characteristics: Proposal of an experimental method applied to poplar trees. *Annals of Forest Science* 60:371-378
- De Coligny F, Ancelin P, Cornu G, Courbaud B, Dreyfus P, Goreaud F, Gourlet-Fleury S, Meredieu C, Orazio C and Saint-André L (2002) CAPSIS: Computer-aided projection for strategies in silviculture: Open architecture for a shared forest-modelling platform. In: Nepveu G (Ed) Fourth Workshop IUFRO WP 5.01.04, Harrison Hot Springs, BC, Canada, *LERFoB/2004 INRA-ENGREF Nancy-France*, 371-380
- Denstorf H-O (2004) Der Einfluss von Standort und Bestand auf den Buchenfarbkern sowie seine Bedeutung für den Holzverkauf [The influence of site and stand on the coloured heartwood of beech as well as its importance for wood selling]. Doctoral thesis, *Albert-Ludwigs-Universität Freiburg*, 371 pp
- Dhôte J-F (1998) Fagacées©, simulateur "arbre indépendant des distances" de la croissance du Hêtre et du Chêne. [Fagacées©, distance independent tree simulator of the growth of Beech and Oak.]. *LERFoB (INRA-ENGREF)*, Nancy
- Dhôte J-F, Hatsch E and Rittié D (2000) Forme de la tige, tarifs de cubage et ventilation de la production en volume chez le Chêne sessile [Stem taper curves, volume tables and volume yield compartments in Sessile Oak]. *Annals of Forest Science* 57:121-142
- Dhôte J-F and Le Moguédec G (2005) Présentation du modèle Fagacées [Presentation of the model Fagacées]. *Document of LERFoB (INRA-ENGREF)*, 2 February 2005, Nancy, 35 pp
- Dietrichs HH (1964) Das Verhalten von Kohlenhydraten bei der Holzverkernung [The Behaviour of Carbohydrates during Formation of Heartwood]. *Holzforschung* 18:14-24
- Dujesiefken D and Liese W (1990) Einfluß der Verletzungszeit auf die Wundheilung bei Buche (*Fagus sylvatica* L.) [Time of wounding and wound healing in beech (*Fagus sylvatica* L.)]. *Holz als Roh- und Werkstoff* 48:95-99
- Ebert H-P and Amann M (2004) Buche: Ist am Baum zu sehen, ob der Stamm einen Farbkern aufweist? [Beech: Does it appear on the tree if the stem has coloured heartwood?]. *Allgemeine Forst Zeitschrift/DerWald* 59:61-65
- Erteld W and Achterberg W (1954) Narbenbildung, Qualitätsdiagnose und Ausformung bei der Rotbuche [Scar formation, quality diagnosis and shaping of Common beech]. *Archiv für Forstwesen* 3:577-619
- Frommhold E (2001) Buchen-Rotkern in Brandenburg [Beech red heart in Brandenburg]. *Allgemeine Forst Zeitschrift/Der Wald* 56:200-202
- Fürst C and Nepveu G (2005) Assessment of the assortment potential of the growing stock - a photogrammetry based approach for an automatized grading of sample trees. *Annals of Forest Science*, accepted
- Gäumann E (1946) Über die Pilzwiderstandsfähigkeit des roten Buchenkerns [About the fungi resistance of the red heart of beech]. *Schweizerische Zeitschrift für Forstwesen* 97:24-32
- Groß HG (1992) Untersuchungen über das Auftreten des Buchenrotkerns in den Buchenplenterwäldern des Hainichs (Thüringen) [Investigations about the occurrence of red heart of beech in the beech selection forests of Hainich (Thuringia)]. Diploma thesis, *Fachhochschule Hildesheim/Holzminden/Göttingen*, 59 pp

- Günsche F (2000) Verwendungsrelevante Qualitätsparameter von Buchenholz [Quality parameters of beechwood relevant for its utilisation]. Diploma thesis, *Technische Universität München*, 102 pp
- Hein S (2004) Ästungsqualität und Wachstumsreaktion bei Buche (*Fagus sylvatica* L.) [Quality of pruning and growth reaction of beech (*Fagus sylvatica* L.)]. In: Nagel J (Ed) Deutscher Verband Forstlicher Forschungsanstalten, Sektion Ertragskunde, Jahrestagung, Stift Schlägl, Austria, 69-76
- Höwecke B, Mahler G, Voss A and Brandl H (1991) Untersuchungen zur Farbverkernung bei der Rotbuche (*Fagus sylvatica* L.) in Baden-Württemberg (Teil I und II) [Investigations about the formation of coloured heartwood of Common beech (*Fagus sylvatica* L.) in Baden-Württemberg (Part I and II)]. *Mitteilungen der Forstlichen Versuchs- und Forschungsanstalt Baden-Württemberg* 158, Freiburg, 106+57 pp
- Hupfeld M, Berendes G and Lehnhardt F (1997) Buchenrotkern und Zielstärkennutzung [Red heart in beech and target diameter harvest]. *Allgemeine Forst Zeitschrift/DerWald* 52:1024-1027
- Isemann W (1999) Zerstörungsfreie Erfassung von Rotkern an Buchenstämmen mittels Computer-Tomographie unter Berücksichtigung jahreszeitlicher Einflüsse [Nondestructive detection of red heart in beech stems by the means of Computer-Tomography considering seasonal effects]. Diploma thesis, *Albert-Ludwigs-Universität Freiburg*, 47 pp
- Jaroschenko (1935) Der Einfluß der natürlichen Reinigung des Stammes von Ästen auf die Bildung des falschen Kerns bei der Buche und einiger ähnlicher Bildungen bei anderen Holzarten [The influence of natural pruning on the formation of false heartwood of beech and some similar formations of other wood species]. *Forstwissenschaftliches Centralblatt* 57:375-379
- Keller H (1961) Vom Rotkern der Buche [About red heart in beech]. *Schweizerische Zeitschrift für Forstwesen* 8:498-502
- Klädtker J (2001) Konzepte zur Buchen-Lichtwuchsdurchforstung [Concepts of thinning by open stand felling for beech]. *Allgemeine Forst Zeitschrift/Der Wald* 56:1047-1050
- Klädtker J (2002) Wachstum großkroniger Buchen und waldbauliche Konsequenzen [Growth of beech trees with large crowns and silvicultural consequences]. *Berichte Freiburger Forstliche Forschung* 44:19-31
- Klemmt H-J (1996) Untersuchungen zum Auftreten des Buchenfarbkerns in unterfränkischen Beständen [Investigations about the occurrence of coloured heartwood of beech in stands of Lower Franconia]. Diploma thesis, *Ludwig-Maximilian-Universität München*, 84 pp
- Knoke T (2002) Value of complete information on red heartwood formation in beech (*Fagus sylvatica*). *Silva Fennica* 36:841-851
- Knoke T (2003a) Eine Bewertung von Nutzungsstrategien für Buchenbestände (*Fagus sylvatica* L.) vor dem Hintergrund des Risikos der Farbkernbildung [An evaluation of harvesting strategies for beech stands (*Fagus sylvatica* L.) considering the risk of coloured heartwood formation]. *Forstliche Forschungsberichte München* 193, 200 pp
- Knoke T (2003b) Predicting red heartwood formation in beech trees (*Fagus sylvatica* L.). *Ecological Modelling* 169:295-312
- Knoke T and Schulz Wenderoth S (2001) Ein Ansatz zur Beschreibung von Wahrscheinlichkeit und Ausmaß der Farbkernbildung bei Buche (*Fagus sylvatica* L.) [An approach to predict probability and extent of red coloured heartwood in beech (*Fagus sylvatica* L.)]. *Forstwissenschaftliches Centralblatt* 120:154-172
- Koch G, Puls J and Bauch J (2003) Topochemical Characterisation of Phenolic Extractives in Discoloured Beechwood (*Fagus sylvatica* L.). *Holzforschung* 57:339-345
- Kotar M (1994) Gesetzmäßigkeiten der Verbreitung des Rotkerns bei der Buche [Conformity to natural laws of the spread of the red heart of beech]. In: Kotar M and Quednau HD (Ed) Deutscher Verband Forstlicher Forschungsanstalten, Sektion Forstliche Biometrie und Informatik, 7. Tagung, Ljubljana, Slovenia, 197-224
- Krempl H and Mark E (1962) Untersuchungen über den Kern der Rotbuche [Investigations about the heartwood of beech]. *Allgemeine Forstzeitung Wien*:186-191
- Kügler O (1999) Modelling red heart probabilities in European Beech (*Fagus Sylvatica* L.). *Working paper*, *Albert-Ludwigs-Universität Freiburg, Institut für Forstökonomie*, unpublished, cited according to Zell (2002) and Zell et al. (2004)

- Lanier L and Le Tacon F (1981) Coeur rouge [Red heart]. In: Teissier du Cros E, Le Tacon F, Nepveu G, Pardé J, Perrin R and Timbal J (Ed) Le Hêtre [The beech]. *Institut National de la Recherche Agronomique INRA*, Paris, 505-507
- Liu S, Loup C, Gril J, Dumonceaud O, Thibaut A and Thibaut B (2005) Studies on European beech (*Fagus sylvatica* L.). Part 1: Variations of wood colour parameters. *Annals of Forest Science* 62:625-632
- Lux M (2001) Untersuchungen zu Vorkommen und Ausbreitung des Rotkerns der Buche (*Fagus sylvatica* L.) in Abhängigkeit von ausgewählten Einflussfaktoren im Großraum Eberswalde [Investigations about the occurrence and extent of red heart of beech (*Fagus sylvatica* L.) depending on selected influencing factors in the region of Eberswalde]. Diploma thesis, *Fachhochschule Eberswalde*, 55 pp
- Magel EA and Höll W (1993) Storage Carbohydrates and Adenine Nucleotides in Trunks of *Fagus sylvatica* L. in Relation to Discolored Wood. *Holzforschung* 47:19-24
- Mahler G and Höwecke B (1991) Verkernungserscheinungen bei der Buche in Baden-Württemberg in Abhängigkeit von Alter, Standort und Durchmesser [Occurrence of heartwood of beech in Baden-Württemberg depending on age, site and diameter]. *Schweizerische Zeitschrift für Forstwesen* 142:375-390
- Mavric L (2003) Untersuchungen zur Rotkernbildung in Buchenbeständen [Investigations about red heart formation in beech stands]. Master thesis, *Georg-August-Universität Göttingen*, 66 pp
- Mayer-Wegelin H (1929) Ästigkeit und Aushaltung des Buchenholzes [Branchiness and bucking of beechwood]. *Forstarchiv* 20:413-418
- Mayer-Wegelin H (1930) Grünästung der Rotbuche [Green pruning of Common beech]. *Forstarchiv* 6:493-498
- Mothe F, Constant T and Leban J-M (2002) Simulating veneering and plywood manufacturing of virtual trees described by a growth and wood quality simulation software. In: Nepveu G (Ed) Fourth Workshop IUFRO WP 5.01.04, Harrison Hot Springs, BC, Canada, *LERFoB/2004 INRA-ENGREF Nancy-France*, 519-527
- Necesany V (1960) Der Buchenkern - Struktur, Entstehung und Entwicklung [The heart of beech - structure, origin and development], *Vydavatelstvo Slovenskej Akedemie Vied Bratislava*, 206-222
- Necesany V (1966) Die Vitalitätsänderung der Parenchymzellen als physiologische Grundlage der Kernholzbildung [The change in vitality of the parenchyma cells as physiological basis of the heartwood formation]. *Holzforschung und Holzverwertung* 18:61-65
- Necesany V (1969) Forstliche Aspekte bei der Entstehung des Falschkerns der Rotbuche [Forestry aspects of the formation of false heart of Common beech]. *Holz-Zentralblatt* 95:563-564
- Nepveu G, Constant T and Wernsdörfer H (2005) La qualité du bois de Hêtre : vingt ans après, quoi de neuf depuis la monographie INRA [Wood quality criteria for Beech - new developments since the INRA monograph published twenty years ago]. *Revue Forestière Française* 57:239-248
- Ohnesorge D (2004) Modellierung der Schnittholzausbeute von Buchenstammholz unter Berücksichtigung der Dimension und des Verkernungsgrades [Modelling of the yield of sawn timber from beech stemwood considering dimension and red heart proportion]. Master thesis, *Georg-August-Universität Göttingen*, 78 pp
- Paclt J (1953) Kernbildung der Buche (*Fagus sylvatica* L.) [Heartwood formation of beech (*Fagus sylvatica* L.)]. *Phytopathologische Zeitung* 20:255-259
- Pichery C (2000) Coeur rouge du hêtre : peut-on trouver des indicateurs externes de la coloration rouge du bois de hêtre ? [Red heart in beech: are there indicators of the red colouration of the wood of beech?]. Report, *Ecole Nationale du Génie Rural des Eaux et des Forêts ENGREF, Office National des Forêts ONF*, Nancy, 23 pp
- Rác J (1961) Untersuchungen über das Auftreten des Buchenrotkerns in Niedersachsen [Investigations about the occurrence of beech red heart in Lower Saxony]. Doctoral thesis, *Georg-August-Universität Göttingen*, 153 pp
- Rác J, Schulz H and Knigge W (1961) Untersuchungen über das Auftreten des Buchenkerns [Investigations about the occurrence of beech heartwood]. *Der Forst- und Holzwirt* 16:413-417

- Rathke K-H (1996) Zu: Rotkern bei Buche [About: Red heart of beech]. *Allgemeine Forst Zeitschrift/Der Wald* 51:1312
- Raunecker H (1953) Die Entstehung des Buchenrotkerns [The formation of red heart in beech]. *Holz-Zentralblatt* 79:1343
- Redde N (1998) Fakultative Farbkernbildung an wertholzhaltigen Starkbuchen [Facultative formation of coloured heartwood on large-dimensioned beech trees containing high value wood]. Diploma thesis, *Georg-August-Universität Göttingen*, 104 pp
- Sachsse H (1967) Über das Wasser/Gas-Verhältnis im Holzporenraum lebender Bäume im Hinblick auf die Kernbildung [On the Water/Gas-Proportion within the Pore-Capacity of the Stemwood of Living Trees with Regard to the Heartwood Formation]. *Holz als Roh- und Werkstoff* 25:291-303
- Sachsse H (1991) Kerntypen der Rotbuche [Heartwood Types of Common Beech]. *Forstarchiv* 62:238-242
- Sachsse H and Simonsen D (1981) Untersuchung über mögliche Zusammenhänge zwischen mechanischen Stammverletzungen und Kernbildung bei *Fagus sylvatica* L. [Investigation on eventual relations between artificial stem wounds and heart wood formation in *Fagus sylvatica* L.]. *Forstarchiv* 52:179-183
- Saporta G (1990) Probabilités, analyse des données et statistique [Probabilities, data analysis and statistics]. *Editions Technip*, Paris, 493 pp
- Schleier D (1999) Untersuchungen über den Einfluß von ultraviolettem Licht auf die Farbe von rotkernigem Buchenholz - Versuche eines Oberflächenschutzes durch die Verwendung von drei Lacken, einem Öl und UV-absorbierenden Additiven - [Investigations about the influence of ultraviolet light on the colour of red heart beechwood - Experiments of surface coatings by the utilisation of three lacquers, one oil and UV-absorbing additives]. Diploma thesis, *Albert-Ludwigs-Universität Freiburg*, 106 pp
- Schmidt M (2004) Vorkommen und Ausprägung von fakultativen Kerntypen bei Rotbuche auf südniedersächsischen Kalk- und Rötstandorten [Occurrence and extent of facultative core types of beech on lime and "Röt" sites in southern Lower Saxony]. In: Nagel J (Ed) Deutscher Verband Forstlicher Forschungsanstalten, Sektion Ertragskunde, Jahrestagung, Stift Schlägl, Austria, 51-68
- Schulz H (1961) Die Beurteilung der Qualitätsentwicklung junger Bäume [The assessment of the quality development of young trees]. *Forstarchiv* 32:89-99
- Schüpbach H and Ruf J (2000) Akzeptanz und Wertschätzung von Rotkern in Buchenholz bei Herstellern, Händlern und Endkunden [Acceptance and esteem of red heart in beechwood by producers, traders and customers]. Final report, short version, *Albert-Ludwigs-Universität Freiburg, Psychologisches Institut, Arbeits- und Organisationspsychologie*
- Schütt C, Spiecker H and Thies M (2004) Qualitätsbestimmung von Wertholzstämmen [Quality assessment of high-value stems]. *Holz-Zentralblatt* 130:595
- Schwartz-Spornberger V (1990) Untersuchungen an Bäumen mit Hilfe eines Computer-Tomographen [Investigations on trees using computer-tomography]. Doctoral thesis, *Philipps-Universität Marburg/Lahn*, 107 pp
- Seeling U (1991) Abnorme Kernbildung bei Rotbuche und ihr Einfluß auf holzbiologische und holztechnologische Kenngrößen [Abnormal heartwood formation of Common beech and its influence on biological and technological wood parameters]. Doctoral thesis, 2nd issue 1998, *Georg-August-Universität Göttingen*, 167 pp
- Seeling U (1998) Kerntypen im Holz - Konsequenzen für die Verwertung am Beispiel der Buche (*Fagus sylvatica* L.) [Heartwood types - consequences for timber utilisation in the case of beech (*Fagus sylvatica* L.)]. *Schweizerische Zeitschrift für Forstwesen* 149:991-1004
- Seeling U and Becker G (2002) Holzqualität großkroniger Buchen unter besonderer Berücksichtigung des Rotkerns [Wood quality of beech trees with large crowns taking especially account of the red heart]. *Berichte Freiburger Forstliche Forschung* 44:45-60
- Seeling U and Becker G (2002) Red heart in beech (*Fagus sylvatica* L.). Is it related to tree architecture and silviculture? Occurrence and relevance for wood quality. In: Nepveu G (Ed) Fourth Workshop IUFRO WP 5.01.04, Harrison Hot Springs, BC, Canada, *LERFoB/2004 INRA-ENGREF Nancy-France*, 210-218

- Seeling U, Becker G and Schwarz C (1999) Stand der Buchenrotkernforschung und zerstörungsfreie Erfassung des Rotkerns bei Buche (*Fagus sylvatica* L.) [State of the research on beech red heart and nondestructive detection of red heart of beech (*Fagus sylvatica* L.)]. Internal final report, *Albert-Ludwigs-Universität Freiburg, Institut für Forstbenutzung und Forstliche Arbeitswissenschaft*, 62 pp
- Seeling U and Sachsse H (1992) Abnorme Kernbildung bei Rotbuche und ihr Einfluß auf holzbiologische und holztechnologische Kenngrößen [Abnormal heartwood formation in beech and its influence on the biological and technological features of the wood]. *Forst und Holz* 47:210-217
- Stuber B, Militz H, Weihs U and Krummheuer F (2002) Nomenklatur und Physiologie der fakultativen Kernbildung von Rotbuche (*Fagus sylvatica* L.) - Eine Literaturrecherche [Nomenclature and Physiology of the Red Heart Development of Beech (*Fagus sylvatica* L.) - A Literature Review]. *Forst und Holz* 57:129-133
- Thies M, Aschoff T and Spiecker H (2003) Terrestrische Laserscanner im Forst [Terrestrial laser scanners in the forest]. *Allgemeine Forst Zeitschrift/Der Wald* 58:1126-1129
- Thies M, Pfeifer N, Winterhalder D and Gorte BGH (2004) Three-dimensional reconstruction of stems for assessment of taper, sweep and lean based on laser scanning of standing trees. *Scandinavian Journal of Forest Research* 19:571-581
- Tomaševski S (1958) Učešće i raspored neprave srži kod bukovich stabala u gospodarskoj jedinici ravna gora [Proportion and distribution of heartwood in beech stems in the management unit "Ravna Gora"]. *Sumarski list* 82:407-410
- Torelli N (1979) Beitrag zur Ökologie und Physiologie der fakultativen Farbkernbildung bei der Rotbuche (*Fagus sylvatica* L.) [Contribution about the ecology and physiology of the facultative formation of coloured heartwood of Common beech (*Fagus sylvatica* L.)]. Doctoral thesis, *Humboldt-Universität Berlin*, 118 pp
- Torelli N (1984) The ecology of discoloured wood as illustrated by beech (*Fagus sylvatica* L.). *IAWA Bulletin* 5:121-127
- Torelli N (1985) Ökologische und waldbauliche Aspekte der fakultativen Farbkernbildung (Rotkern, "Discolored Wood") bei der Buche. Prognostizierung des Ausmasses des Rotkerns an stehenden Bäumen [Ecological and Silvicultural Aspects of the Facultatively Colored Heartwood (Red Heart, "Discolored Wood") Formation in Beech - Prognosticating the Red Heart Extent in Living (Standing) Trees]. *Mitteilungen Bundesforschungsanstalt für Forst- und Holzwirtschaft* 150:182-204
- Torelli N, Križaj B and Oven P (1994) Barrier zone (Codit) and wound-associated wood in beech (*Fagus sylvatica* L.). *Holzforschung und Holzverwertung* 46:49-51
- Trendelenburg R and Mayer-Wegelin H (1955) Das Holz als Rohstoff [The wood as raw material]. *Carl Hanser, München*, 541 pp
- Trincado G and Gadov von K (1996) Zur Sortimentschätzung stehender Laubbäume [Estimating merchantable volume for deciduous trees]. *Centralblatt für das Gesamte Forstwesen* 113:27-38
- Vallet P (2005) Impact de différentes stratégies sylvicoles sur la fonction "puits de carbone" des peuplements forestiers. Modélisation et simulation à l'échelle de la parcelle [Impact of different forest management strategies on the forests' carbon budget. Modelling and simulation at the stand scale]. Doctoral thesis, *Ecole Nationale du Génie Rural des Eaux et des Forêts ENGREF, Nancy*, 190 pp
- Vasiljevic J (1974) Održavanje bukve na području zrinjske gore [Beech heartwood formation in the region of the Zrinjska Gora Mountain (Croatia)]. *Sumarsky list* 98:505-520
- Verhoff S and Wurster M (2002) Projekt: Buchen-Rotkern-Marketing, Vermarktungsmöglichkeiten und Marketing für Verkerntes Buchenholz [Project: Marketing of red heart in Beech, market possibilities and marketing for Beech heartwood]. Summarising final report, *Forstliche Versuchs- und Forschungsanstalt Baden-Württemberg, Abteilung Waldnutzung, Freiburg*, 3.1-3.32
- Volkert E (1953) Untersuchungen über das Verhalten von Astwunden nach Grünästung und natürlichem Astabfall bei Rotbuche [Investigations about the behaviour of branch wounds

- after green pruning and natural branch excision of Common beech]. *Forstwissenschaftliches Centralblatt* 75:110-124
- Wagemann M (2001) Vermarktungsoffensive Rotkernbuche [Marketing offensive red heart beech]. *Allgemeine Forst Zeitschrift/Der Wald* 56:1406-1407
- Walter M and Kucera LJ (1991) Vorkommen und Bedeutung verschiedener Kernformen bei der Buche (*Fagus sylvatica* L.) [Occurrence and importance of different heartwood types of beech (*Fagus sylvatica* L.)]. *Schweizerische Zeitschrift für Forstwesen* 142:391-406
- Wernsdörfer H, Reck P, Seeling U, Becker G and Seifert T (2004) Erkennung und Messung des Reaktionsholzes bei Fichte (*Picea abies* (L.) Karst.) mittels Verfahren der digitalen Bildanalyse [Identifying and measuring compression wood of Norway Spruce (*Picea abies* (L.) Karst.) by using methods of digital image analysis]. *Holz als Roh- und Werkstoff* 62:243-252
- Wilhelm GJ, Letter H-A and Eder W (1999) Konzeption einer naturnahen Erzeugung von starkem Wertholz [Concept for close to nature production of large, high value wood]. *Allgemeine Forst Zeitschrift/DerWald* 54:232-240
- Zell J (2002) Ökonomische Optimierung der Zieldurchmesserernte bei der Buche unter Berücksichtigung des Risikos rotkernbedingter Entwertung - ein Anwendungsbeispiel der linearen Programmierung - [Economic optimisation of target diameter harvest of beech taking into account the risk of devaluation by red heartwood - an example of application of linear programming -]. Work report, *Albert-Ludwigs-Universität Freiburg, Institut für Forstökonomie*, 63 pp
- Zell J, Hanewinkel M and Seeling U (2004) Financial optimisation of target diameter harvest of European beech (*Fagus sylvatica*) considering the risk of decrease of timber quality due to red heartwood. *Forest Policy and Economics* 6:579-593
- Ziegler H (1968) Biologische Aspekte der Kernholzbildung [Biological Aspects of the Heartwood Formation]. *Holz als Roh- und Werkstoff* 26:61-68
- Zycha H (1948) Über die Kernbildung und verwandte Vorgänge im Holz der Rotbuche [About the heartwood formation and similar processes in the wood of Common beech]. *Forstwissenschaftliches Centralblatt* 67:80-109

8 Annex

8.1 Complementary information

8.1.1 Explorative analysis (analysis I)

8.1.2 Red heart occurrence (analysis II)

Referring to section 3.2, Table 8 gives the parameter estimates, approximate standard errors and significance tests of the model of red heart occurrence which used hd as explanatory variable at the dendrometric level. The correlation matrix of parameter estimates of this model is given in Table 9.

Table 8. Model of red heart occurrence using hd as explanatory variable at the dendrometric level. Parameter estimates, approximate standard errors and significance tests.

Parameter (variable)	Estimate	Approximate standard error	Approximate Prob > t
a_0'	-27.32	9.04	0.006
a_1' (hd)	49.02	15.91	0.005
b_0'	6036.62	231.14	$1.2 \cdot 10^{-19}$
b_1' (mec2)	-13.90	0.53	$1.1 \cdot 10^{-19}$
b_2' (mec3)	97.72	3.74	$1.1 \cdot 10^{-19}$
b_3' (ro)	-63.46	2.43	$1.1 \cdot 10^{-19}$

Table 9. Model of red heart occurrence using hd as explanatory variable at the dendrometric level. Approximate correlation matrix of parameter estimates.

	a_0'	a_1'	b_0'	b_1'	b_2'
a_0'	1				
a_1'	-0.98833	1			
b_0'	-0.04399	0.04636	1		
b_1'	0.04367	-0.04602	-0.99992	1	
b_2'	-0.04360	0.04595	0.99990	-0.99999	1
b_3'	0.04373	-0.04609	-0.99996	0.99997	-0.99998

Determinant = $1.5 \cdot 10^{-16}$

Matrix has 6 positive eigenvalue(s)

8.1.3 Overall red heart shape (analysis III)

Referring to section 3.3, Table 10 gives the parameter estimates, approximate standard errors and 95% confidence limits of the descriptive model of the overall red heart shape for the trees of group 1.

Table 10. Descriptive model of the overall red heart shape for the trees of group 1: parameter estimates, approximate standard errors and 95% confidence limits.

Tree number	Parameter	Estimate	Approximate standard error	Approximate 95% confidence limits	
all	k^*_1 (1)	-0.0399	0.00540	-0.0506	-0.0292
	k^*_2 (1)	0.0365	0.0149	0.00691	0.0662
	k^*_3 (1)	0.1579	-	-	-
	k^*_4 (1)	-0.3135	-	-	-
B01	w_{B01} (1)	-4.5412	0.0195	-4.5799	-4.5026
B01	l_{B01} (m)	4.8897	0.1013	4.6886	5.0907
B01	h_{B01} (m)	5.2363	0.0665	5.1042	5.3684
B08	w_{B08} (1)	-4.6061	0.0182	-4.6421	-4.5700
B08	l_{B08} (m)	8.3699	1.6786	5.0379	11.7020
B08	h_{B08} (m)	6.2107	1.0071	4.2117	8.2097
C04	w_{C04} (1)	-4.8683	0.0121	-4.8923	-4.8443
C04	l_{C04} (m)	8.3709	0.2252	7.9239	8.8178
C04	h_{C04} (m)	5.9626	0.1216	5.7213	6.2039
C06	w_{C06} (1)	-5.0274	0.00981	-5.0468	-5.0079
C06	l_{C06} (m)	12.0019	0.5216	10.9665	13.0373
C06	h_{C06} (m)	6.3430	0.3480	5.6523	7.0338

(1): no unit

8.1.4 Local red heart shape (analysis IV)

This section gives results about deviation and relative deviation of the local red heart shape on boards from the overall red heart shape on the nearest discs. The results refer to section 3.4.2.1.1. In section 3.4.2.1.1, results were based on one longitudinal plane, which was the board surface related to angular disc sections (Figure 8). At the end of section 3.4.2.1.1 it is discussed that, however, the mean red heart radius of the entire discs (and not of angular disc sections) was used to quantify the overall red heart shape (section 3.3). To evaluate if this makes a difference, deviation and relative deviation were also calculated using the mean red heart radius of the entire discs: referring to methods given in section 3.4.1.1, deviation and relative deviation were calculated using r'_{below} and r'_{above} instead of r_{below} and r_{above} , where r'_{below} and r'_{above} were the mean of 360 red heart radii [$\text{mean}(r_a)$ with $a = 1$ to 360; section 2.2] of the disc below and above the board, respectively. Results are given in the following: Figure 31, Figure 32, Figure 33 and Figure 34 refer to Figure 19, Figure 20, Figure 21 and Figure 22 of section 3.4.2.1.1, respectively; Table 11 refers to Table 5.

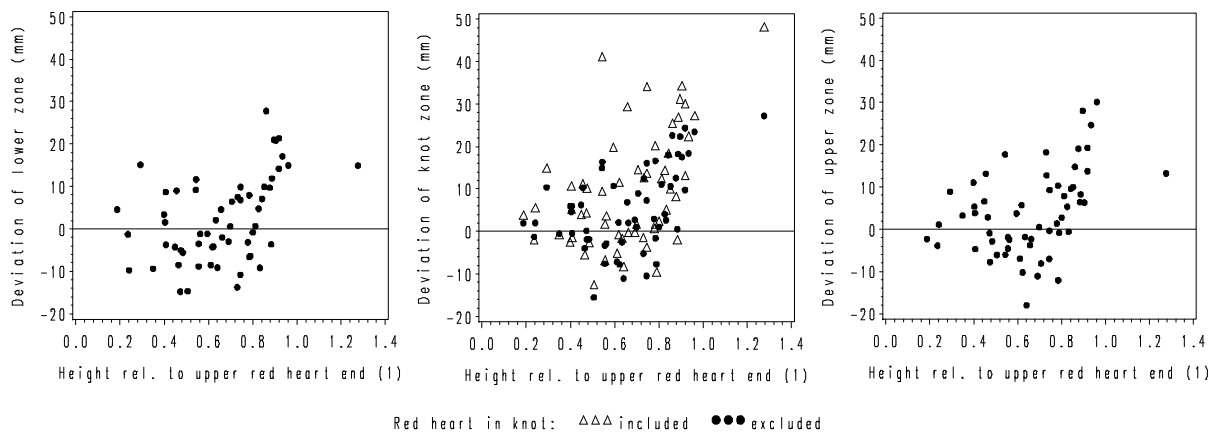


Figure 31. Deviation of the local red shape (board zones) from the overall red heart shape (discs); on the abscissa axes: mean height of board zones related to the height of the upper red heart end (tree number 47 had a second small red heart above the upper red heart end which was represented by one board); on the ordinate axes: deviation of lower zone (left), knot zone including/excluding the red heart in the knot (middle) and upper zone (right); (1) in axis legends stands for no unit; N = 58 boards.

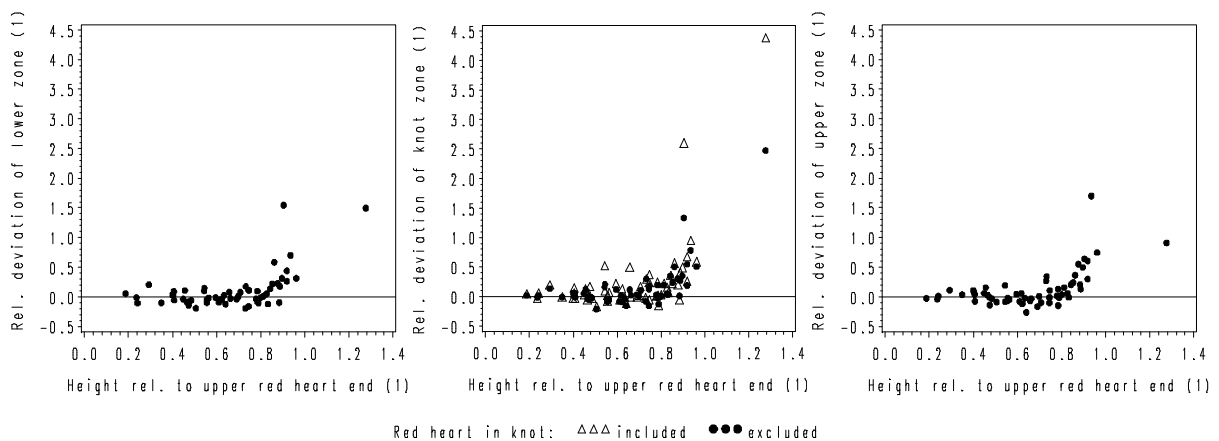


Figure 32. Relative deviation of the local red shape (board zones) from the overall red heart shape (discs); on the abscissa axes: mean height of board zones related to the height of the upper red heart end (tree number 47 had a second small red heart above the upper red heart end which was represented by one board); on the ordinate axes: relative deviation of lower zone (left), knot zone including/excluding the red heart in the knot (middle) and upper zone (right); (1) in axis legends stands for no unit; N = 58 boards.

Table 11. Descriptive statistics of deviation ($d_{\text{lowerZone}}$, $d_{\text{knotZoneIncl}}$, $d_{\text{knotZoneExcl}}$ and $d_{\text{upperZone}}$) and relative deviation ($d_{\text{lowerZoneRel}}$, $d_{\text{knotZoneInclRel}}$, $d_{\text{knotZoneExclRel}}$ and $d_{\text{upperZoneRel}}$) of board zones located below 0.8 of height related to the upper red heart end ($h_{\text{moyZoneRel}} \leq 0.8$).

Variable	N	Mean (mm)	Median (mm)	Std (mm)	CV (%)	Min (mm)	Max (mm)	Prob > t ; H ₀ : Mean = 0
$d_{\text{lowerZone}}$	41	-1.3	-2.9	7.7	-594	-14.8	15.2	0.2878
$d_{\text{knotZoneIncl}}$	41	5.4	1.8	11.5	211	-12.5	41.2	0.0042
$d_{\text{knotZoneExcl}}$	41	1.9	2.0	7.9	421	-15.5	16.7	0.1362
$d_{\text{upperZone}}$	41	0.3	-0.9	8.1	3195	-18.0	18.2	0.8422
		(1)	(1)	(1)	(%)	(1)	(1)	
$d_{\text{lowerZoneRel}}$	41	-0.014	-0.036	0.099	-722	-0.193	0.205	0.3806
$d_{\text{knotZoneInclRel}}$	41	0.074	0.025	0.157	211	-0.168	0.529	0.0041
$d_{\text{knotZoneExclRel}}$	41	0.024	0.022	0.108	448	-0.209	0.301	0.1611
$d_{\text{upperZoneRel}}$	41	0.002	-0.013	0.116	6235	-0.262	0.346	0.9187

N: number of observations

Std: standard deviation

CV: variation coefficient

Min: minimum

Max: maximum

Prob: probability

t: t-value (Student)

H₀: null hypothesis

(1): no unit

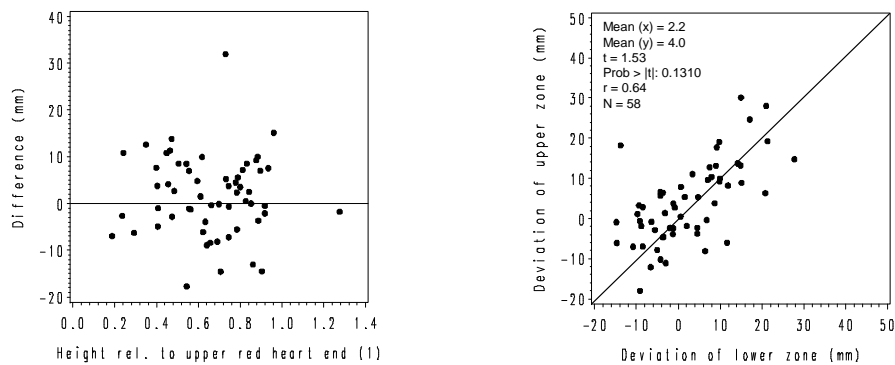


Figure 33. Deviation of the local red heart shape from the overall red heart shape below and above the knot; on the left: scatter plot of the difference between the deviations of upper zone and lower zone, and the height relative to the upper red heart end (tree number 47 had a second small red heart above the upper red heart end which was represented by one board); on the right: scatter plot of the deviations of upper zone and lower zone, the bisector ($y = x$) of the coordinate axes is given as auxiliary line; (1) in axis legend stands for no unit; $N = 58$ boards.

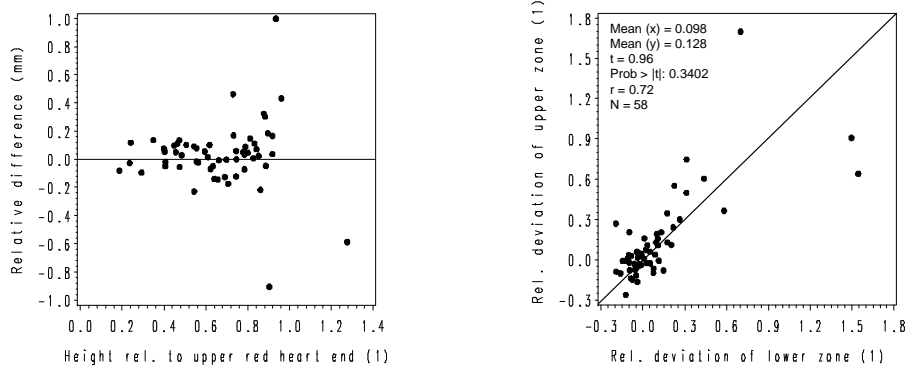


Figure 34. Relative deviation of the local red heart shape from the overall red heart shape below and above the knot; on the left: scatter plot of the difference between the relative deviations of upper zone and lower zone, and the height relative to the upper red heart end (tree number 47 had a second small red heart above the upper red heart end which was represented by one board); on the right: scatter plot of the relative deviations of upper zone and lower zone, the bisector ($y = x$) of the coordinate axes is given as auxiliary line; (1) in axis legends stands for no unit; $N = 58$ boards.

Abstract

In this work, quantitative relationships were studied between external and dendrometric characteristics of beech trees on the one hand, and red heartwood occurrence and shape in stem-axial and stem-radial direction on the other hand. Four analyses were performed:

- I. Explorative analysis – Tree external traits (dead branches, branch scars, wounds, cracks and fork) and the red heart shape were described three-dimensionally and in detail on four trees. Based on visual and geometric relationships, hypotheses were deduced about red heart initiation depending on branch scar/knot dimensions, and about stages of development of the red heart shape.
- II. Red heart occurrence – Using the hypotheses of red heart initiation, a type logistic regression model was developed. It allowed quantifying the effect of individual branch scars on the probability of red heart occurrence. It included an effect on the dendrometric level. Using this model, 27 out of 31 trees were correctly classified.
- III. Overall red heart shape – This shape (mean red heart radius versus height in the tree) was modelled at a given stage of red heart development based on the hypothesis of the explorative analysis. The red heart width, length and height in the tree were controlled by model parameters. The parameters could be estimated from external traits and dendrometric variables. The model was parameterised based on 16 trees and applied to an independent sample which consisted of the four trees of analysis I.
- IV. Local red heart shape – Deviation from the overall red heart shape in stem-axial direction below and above knots was analysed on boards (N=58) taken from the 16 trees of analysis III. Deviation was limited to the zone of the knot and to the upper red heart end. Furthermore, geometric relationships between branch scars, knots and red heart, as developed in the explorative analysis, were tested and further developed.

Perspectives in the short term include modelling of the number of annual rings containing red heart, and quantifying the local red heart shape in different stem-radial directions. Furthermore, the importance of model validation is stressed. Perspectives in the medium and long term include linking of red heart models to models of tree growth and roundwood processing.

Keywords: *Fagus sylvatica*, beech, red heart, model, initiation, occurrence, shape, development, branch scar, geometric relationship, mechanism, probability, standing tree

Résumé

Dans le cadre de ce travail, des relations quantitatives ont été étudiées, chez le Hêtre, entre les singularités externes de l'arbre, des caractéristiques dendrométriques et l'occurrence et la forme du cœur rouge dans les directions longitudinale et radiale. Quatre analyses ont été menées :

- I. Analyse exploratoire – Des singularités externes (branches mortes, cicatrices de branche, blessures, fentes et fourche) et la forme du cœur rouge ont été décrites de façon tridimensionnelle détaillée pour quatre arbres. En se basant sur des relations visuelles et géométriques, des hypothèses ont été développées d'une part sur l'initiation du cœur rouge basées sur des dimensions des cicatrices de branche/nœuds et d'autre part sur des stades de développement de la forme du cœur rouge.
- II. Occurrence du cœur rouge – En utilisant les hypothèses sur l'initiation du cœur rouge, un modèle de type logistique a été développé. Il permettait de quantifier individuellement l'effet des cicatrices de branche sur la probabilité d'occurrence du cœur rouge ; il incluait également un effet dendrométrique. À l'aide de ce modèle, 27 parmi 31 hêtres ont été classés correctement.
- III. Forme globale du cœur rouge – Cette forme (rayon moyen du cœur rouge le long de l'axe du tronc) a été modélisée à un stade de développement donné en se basant sur l'hypothèse de l'analyse exploratoire. La largeur, la longueur et la hauteur du cœur rouge dans l'arbre étaient contrôlées par les paramètres du modèle. Ces derniers ont pu être estimés à partir des singularités externes et des variables dendrométriques. Le modèle a été paramétré en utilisant 16 hêtres ; il a été appliqué à l'échantillon indépendant constitué des quatre arbres de l'analyse I.
- IV. Forme locale du cœur rouge – Des déviations locales de la forme globale du cœur rouge et plus particulièrement la forme longitudinale en dessous et au dessus des nœuds ont été analysées sur des planches (N=58) provenant des 16 arbres de l'analyse III. Les déviations étaient limitées à la zone du nœud et à l'extrémité du cœur rouge côté apical. De plus, des relations géométriques entre les cicatrices de branche, les nœuds et le cœur rouge, mises en place dans l'analyse exploratoire, ont été testées et développées.

Des perspectives à court terme incluent de modéliser le nombre de cerne de cœur rouge et de quantifier la forme locale du cœur rouge dans les différentes directions radiales. De plus, l'importance de la validation des modèles de cœur rouge est soulignée. À plus long terme, ces modèles pourraient ainsi être couplés à des modèles de croissance ou de transformation des bois ronds.

Mots clés : *Fagus sylvatica*, hêtre, cœur rouge, modèle, initiation, occurrence, forme, développement, cicatrice de branche, relation géométrique, mécanisme, probabilité, arbre sur pied

Zusammenfassung

In der vorliegenden Arbeit werden im Rahmen von vier Teiluntersuchungen quantitative Zusammenhänge zwischen äußeren Stammmerkmalen und dendrometrischen Variablen von Buchen einerseits, und dem Vorkommen und der Form des Rotkerns andererseits, analysiert:

- I. „Pilotstudie“ – Äußere Stammmerkmale (Totäste, Astnarben, Wunden, Risse und Zwiesel) sowie die Form des Rotkerns wurden anhand von vier Bäumen im Detail dreidimensional beschrieben. Ausgehend von visuellen und geometrischen Zusammenhängen zwischen Stammmerkmalen und Rotkern wurden Hypothesen abgeleitet, und zwar zum einen über die Auslösung der Rotkernbildung in Abhängigkeit von den Dimensionen von Totästen/Astnarben und zum anderen über Entwicklungsstadien der Rotkernform.
- II. Vorkommen des Rotkerns – Ausgehend von den Hypothesen über die Auslösung der Rotkernbildung wurde ein logistisches Regressionsmodell entwickelt. Mit diesem Modell konnte der Einfluss von Astnarben auf die Rotkernwahrscheinlichkeit einzeln quantifiziert werden, und es wird der Einfluss von dendrometrischen Variablen berücksichtigt. Unter Anwendung des Modells wurden 27 von 31 analysierten Buchen richtig klassifiziert.
- III. Grundform des Rotkerns – Darunter wird der mittlere Rotkernradius in verschiedenen Höhen entlang der Stammachse verstanden. Die Modellierung eines bestimmten Entwicklungsstadiums der Rotkerngrundform erfolgte ausgehend von der in der „Pilotstudie“ aufgestellten Hypothese. Dabei wurden die Breite, Länge und Höhe des Rotkerns im Stamm durch entsprechende Modellparameter gesteuert. Die Parameter konnten anhand von äußeren Stammmerkmalen und dendrometrischen Variablen geschätzt werden. Das Modell wurde für 16 Buchen parametrisiert und mittels eines unabhängigen Datensatzes überprüft, der die vier Bäume aus Untersuchung I umfasste.
- IV. Lokale Abweichungen von der Rotkerngrundform – Es wurden Abweichungen in stammaxialer Richtung unter- und oberhalb von Ästen analysiert. Dies erfolgte anhand von Längsschnitten (N=58), die den 16 Buchen aus Untersuchung III entnommen wurden. Wesentliche Abweichungen traten im unmittelbaren Bereich von Ästen und am oberen Ende des Rotkerns auf. Des Weiteren wurden die in der „Pilotstudie“ aufgestellten geometrischen Zusammenhänge zwischen Astnarbe, Ast und Rotkern getestet und weiterentwickelt.

Kurzfristig mögliche Folgeuntersuchungen könnten sich mit der Modellierung der Rotkerngrundform innerhalb des Jahrringprofils oder mit lokalen Abweichungen von der Grundform in verschiedenen stammradialen Richtungen befassen. Des Weiteren wird betont, dass die entwickelten Rotkernmodelle noch validiert werden sollten. Davon ausgehend wäre längerfristig eine Verknüpfung der Rotkernmodelle mit Modellen für das Baumwachstum und den Rundholzeinschnitt denkbar.

Schlagwörter: *Fagus sylvatica*, Buche, Rotkern, Modell, Auslösung, Vorkommen, Form, Entwicklung, Astnarbe, geometrischer Zusammenhang, Mechanismus, Wahrscheinlichkeit, stehender Baum